

Gravitational wave memory and its effects on particles and fields

Abraham I. Harte,^{1,♣} Thomas B. Mieling,^{2,♦} Marius A. Oancea,^{3,♥} and Florian Steininger^{4,♣}

¹*Centre for Astrophysics and Relativity (CfAR), School of Mathematical Sciences,
Dublin City University, Glasnevin, Dublin 9, Ireland*

²*University of Vienna, Faculty of Physics and Research Network TURIS, Boltzmannngasse 5, 1090 Vienna, Austria*

³*University of Vienna, Faculty of Physics, Boltzmannngasse 5, 1090 Vienna, Austria*

⁴*University of Vienna, Faculty of Physics, Vienna Doctoral School in Physics
(VDSP) and Research Network TURIS, Boltzmannngasse 5, 1090 Vienna, Austria*

Gravitational wave memory is said to arise when a gravitational wave burst produces changes in a physical system that persist even after that wave has passed. This paper analyzes gravitational wave bursts in plane wave spacetimes, deriving memory effects on timelike and null geodesics, massless scalar fields, and massless spinning particles whose motion is described by the spin Hall equations. All associated memory effects are found to be characterized by four “memory tensors,” three of which are independent. These tensors form a scattering matrix for the transverse components of geodesics. However, unlike for the “classical” memory effect involving initially comoving pairs of timelike geodesics, one of our results is that memory effects for null geodesics can have strong longitudinal components. When considering massless particles with spin, we solve the spin Hall equations analytically by showing that there exists a conservation law associated with each conformal Killing vector field. These solutions depend only on the same four memory tensors that control geodesic scattering. For massless scalar fields, we show that given any solution in flat spacetime, a weak-field solution in a plane wave spacetime can be generated just by differentiation. Precisely which derivatives are involved depend on the same four memory tensors. These effects are illustrated for scalar plane waves and higher-order Gaussian beams. Furthermore, we also present a numerical comparison between the dynamics of localized wave packets carrying angular momentum and the spin Hall equations.

I. INTRODUCTION

Gravitational waves provide a novel probe of astrophysical phenomena. By encoding information about their sources, they provide access to highly dynamical systems with strong gravitational fields. However, gravitational waves can also be lensed or otherwise affected by the spacetime through which they propagate, providing information also about mass distributions between a source and its observer. Regardless, gravitational waves are measured by observing their interactions with different physical systems. As gravity affects almost every conceivable observation, a wide variety of physical systems can, in principle, be used as gravitational wave detectors. While the state of a detector typically varies throughout its interaction with any passing gravitational wave, there are cases in which a detector’s state before a wave arrives differs from its state after that wave has left. Such differences are referred to as gravitational wave memory.

The first prediction of a gravitational memory effect is typically attributed to Zel’dovich and Polnarev in 1974 [1] (although see also Ref. [2]), who examined gravitational-wave bursts generated by the flyby of two massive objects in linearized general relativity. They found that the initial and the final separations of pairs of freely falling test par-

ticles can differ due to the resulting gravitational waves. Going beyond the weak-field approximation, a nonlinear memory effect was later obtained by Christodoulou [3] based on mathematical methods used in the proof of the stability of Minkowski spacetime [4, 5]. This has as its physical origin the flux of effective stress-energy which is associated with the gravitational waves emitted by a compact system [6, 7]. Motivated in part by observational prospects [8–10], gravitational wave memory has since been studied in a wide variety of contexts, primarily using linearized gravity [11–13], the post-Newtonian approximation [14–17], or as a device to better understand the structure of null infinity [13, 18–23]. Memory effects have also been discussed on black hole horizons [24, 25].

Much of this work has focused on studying aspects of the spacetime geometry that may be interpreted as producing permanent changes in the separations of freely falling test particles. However, gravitational waves can produce a variety of other persistent changes in the physical systems through which they pass [26–31]. It is these changes that we investigate here. Since we are interested in how gravitational waves affect spatially compact physical systems—and not on, e.g., the large-scale structure of those waves or on their sources—we focus on the effects of gravitational *plane waves*. More precisely, we work with plane wave spacetimes, which are exact solutions to the Einstein field equations. These are a subclass of the more general family of pp-wave spacetimes, and pp-waves are, in turn, a subclass of the Kundt family of spacetimes [32–35]. Regardless, plane wave spacetimes represent a gravitational-wave analog of the scalar or electromagnetic plane waves which are well-known in flat spacetime.

♣ abraham.harte@dcu.ie
♦ thomas.mieling@univie.ac.at
♥ marius.oancea@univie.ac.at
♣ f.steiner@univie.ac.at

From a global perspective, plane wave spacetimes do not provide a physically reasonable model of gravitational radiation: They are not asymptotically flat, or even globally hyperbolic [36], they carry an infinite amount of energy, and they do not have sources. Nevertheless, it is still reasonable to consider these spacetimes as models of gravitational radiation when considering their effects on systems with small spatial extent. At large enough distances, the gravitational waves emitted by compact sources are expected to be well approximated by the plane wave geometry. Separately, plane wave spacetimes also arise as Penrose limits [37–39], and might therefore be viewed as describing the ultra-relativistic geometries near arbitrary null geodesics in arbitrary background spacetimes. Regardless, plane waves provide particularly clean models for the effects of gravitational radiation, as it is possible to consider waves whose curvature is nonzero only for a finite time. Any system which is affected by such a wave therefore evolves from one locally flat spacetime to another, allowing its initial and final states to be easily compared.

This paper studies gravitational memory effects on test particles and test fields in plane wave spacetimes. Unlike in much of the previous work on memory in plane wave spacetimes [40–50], we allow for gravitational wave bursts with arbitrary waveforms (see, however, Refs. [26, 27, 29, 51]). One of our main results is that a large class of physical observables can be completely expressed in terms of the so-called Jacobi propagators. These propagators are typically introduced to characterize solutions to the geodesic deviation equation. However, we show that they also characterize the behavior of all geodesics, of massless test particles with longitudinal angular momentum, and of massless scalar fields. For sandwich wave spacetimes where the curvature is nonzero only for a finite time, the Jacobi propagators can be expressed in terms of four “memory tensors,” three of which are independent. These tensors are constant, and they fully determine all scattering processes and observables we consider.

The first memory effects we discuss are those associated with timelike and null geodesics, which are found to depend on all four of the aforementioned memory tensors. The physical character of these effects can, in general, be considerably more complicated than for the classical memory effect associated with initially comoving pairs of timelike geodesics. Null geodesics, for example, exhibit memory effects that are not only transverse, but also longitudinal.

Moving beyond the geodesic approximation, we also consider the scattering of massless particles with longitudinal angular momentum. Such particles move along *non-geodesic* null trajectories determined by the gravitational spin Hall equations [52, 53]. These equations are a special case of the Mathisson-Papapetrou equations [54]. Physically, they describe the trajectories of high-frequency localized (electromagnetic [53, 55–59], linearized gravitational [60–64], massless Dirac [65], or even some scalar) wave packets that carry longitudinal angular momentum.

Memory effects for *massive* spinning particles have instead been discussed in, e.g., Refs. [28, 29, 66, 67].

The spin Hall description of wave packets is only approximate, and is restricted to describing the bulk motion of compact, high-frequency wave packets. However, memory effects can also be considered for fully generic test fields¹, which we consider from several perspectives. We obtain a general integral formula for the scattering of scalar test fields, and also derive a result which allows fields in flat spacetimes to be easily mapped into solutions in weakly curved sandwich wave spacetimes. Examples are considered as well, including the exact scattering of ingoing plane waves, and of scalar fields constructed from counter-propagating Hermite–Gauss and Laguerre–Gauss beams. Lastly, we use a numerical implementation of the Kirchhoff integral to compare exact solutions of the wave equation with predictions provided by the spin Hall equations.

This paper is structured as follows. We start in Section II with a presentation of the theoretical tools used for our study of memory effects. We review the main properties of plane wave spacetimes and introduce the Jacobi propagators that solve the geodesic deviation equation. For sandwich wave spacetimes, we show that the Jacobi propagators can be entirely expressed in terms of four memory tensors that completely characterize all scattering processes discussed in this paper. Section III discusses geodesic motion. Solutions of the geodesic equations are written in terms of Jacobi propagators, and in the case of sandwich wave spacetimes, the transverse scattering of geodesics is expressed very simply in terms of the memory tensors. We also discuss longitudinal memory effects, focusing mainly on null geodesics. Section IV examines the non-geodesic motion of massless spinning particles, solving the spin Hall equations in terms of the Jacobi propagators. Memory effects for massless spinning particles are then expressed using the memory tensors, similar to the geodesic case. In Section V, we analyze the dynamics of massless scalar fields in plane wave spacetimes. Finally, we present our conclusions in Section VI.

There are five appendices. Appendix A summarizes our notation. Appendix B describes example plane waves and their memory tensors. Appendix C reviews Ward’s [72] progressing-wave solutions for test scalar fields on plane wave backgrounds, and shows that our Kirchhoff-like formula Eq. (5.7) is a special case. Appendix D describes memory effects for charged particles in electromagnetic plane waves in flat spacetime, which contrasts with the gravitational memory effects considered elsewhere in this paper. Finally, Appendix E collects certain technical results on Hermite–Gauss and Laguerre–Gauss beams.

¹ Although we focus here on scalar fields, spin-raising procedures can be used to map scalar fields into, e.g., electromagnetic vector potentials or metric perturbations [68–71].

II. PLANE WAVE SPACETIMES AND MEMORY TENSORS

This section reviews basic properties of plane wave spacetimes and then introduces a set of four memory tensors which can be used to describe all observables discussed in this paper. Section II A begins by reviewing the basic physical and geometric properties of plane wave spacetimes. Section II B then reviews the Jacobi propagators and their properties in a plane wave context. Next, Section II C specializes to sandwich wave spacetimes and introduces the memory tensors. Lastly, Section II D shows that for weak gravitational waves, all four memory tensors are determined by the zeroth, the first, and the second moments of the gravitational waveform.

A. Review of plane wave spacetimes

Exact plane wave spacetimes are commonly specified in one of two classes of coordinate systems: Brinkmann or Rosen. Each of these coordinate systems has its advantages and disadvantages. For example, the Einstein field equations are trivial in Brinkmann coordinates, but not in Rosen. In contrast, many geodesics look trivial in Rosen coordinates but not in Brinkmann. Rosen coordinates are also directly related to the transverse-traceless gauge which is commonly used in first-order perturbation theory, so the waveforms that are natural in that context are somewhat more familiar than the waveforms which appear in Brinkmann coordinates. A detailed discussion of these and other differences can be found in Refs. [27, 39]. Further properties of plane wave spacetimes are reviewed in, e.g., Refs. [26, 32, 34, 35, 73, 74].

Except in Section V C and Appendix C below, we focus mainly on using Brinkmann coordinates (u, v, x, y) to describe gravitational plane waves. The line element is then given by

$$ds^2 = -2du dv + dx^2 + dy^2 + H_{ij}(u)x^i x^j du^2, \quad (2.1)$$

where the indices i, j, \dots are associated with the two “transverse” and spacelike coordinates $x = x^1$ and $y = x^2$. The “phase” coordinate u is null, and constant- u hypersurfaces may be viewed as the wavefronts of the gravitational wave. The waveform here is described by $H_{ij} = H_{(ij)}(u)$, and the exact Einstein field equations require only that this be trace-free in vacuum. Therefore, any 2×2 symmetric, trace-free, matrix function of one variable may be used to describe the waveform of a vacuum gravitational wave. The two free scalar functions that make up that matrix may be viewed as waveforms associated with the two polarization states of the gravitational wave. Unlike gravitational waveforms which might be familiar from flat-spacetime perturbation theory in transverse-traceless gauge, H_{ij} has units of curvature. In fact, all nontrivial Riemann components follow from

$$R_{iuju} = -H_{ij}. \quad (2.2)$$

If H_{ij} vanishes on a particular $u = \text{constant}$ wavefront, the spacetime there is at least locally flat. If H_{ij} is nonzero in a region but can be diagonalized using a *constant* (i.e., u -independent) rotation, the wave is said to be linearly polarized in that region.

Geometrically, Brinkmann coordinates are a type of Fermi normal coordinate system whose origin is the null geodesic $v = x^i = 0$. As is typical in Fermi coordinates, the presence of curvature results in the metric components growing quadratically as one moves away from the origin. In plane wave spacetimes, this quadratic growth rate is, in fact, exact; it is given by the $H_{ij}x^i x^j du^2$ term in the Brinkmann line element. In a generic spacetime, quadratic growth in the metric components would instead appear only as a leading-order approximation near the origin.

This suggests that plane wave metrics can describe the leading-order terms in an expansion of the metric around *generic* null geodesics in *generic* spacetimes. Indeed, it was shown in Ref. [38] that if Fermi coordinates are applied to an arbitrary null geodesic in an arbitrary spacetime, there is a sense in which the leading-order metric near that geodesic is always a gravitational plane wave in Brinkmann coordinates. The particular plane wave that results from this process is called the Penrose limit [37, 39] of the reference null geodesic, and the relevant H_{ij} is determined by certain components of the Riemann tensor along the reference geodesic. The Penrose limit thus provides a sense in which plane wave geometries generically encode local aspects of arbitrary spacetimes as seen by ultra-relativistic observers. Of course, plane waves also model local aspects of the far-field gravitational radiation emitted by compact sources, even for observers which are not in any sense relativistic.

Given a particular plane wave spacetime, the Brinkmann coordinates are not unique. Different frame vectors can be used to construct the relevant Fermi coordinates, and the origins of those coordinates can also be translated. The net effect of these choices is that any Brinkmann coordinate system (u, v, x, y) can be related to any other Brinkmann coordinate system $(\hat{u}, \hat{v}, \hat{x}, \hat{y})$ via the transformations [32]

$$\hat{u} \equiv \frac{1}{\gamma}(u - u_0), \quad \hat{x}^i \equiv r^i_j [x^j - x_0^j(u)], \quad (2.3a)$$

$$\hat{v} \equiv \gamma \{v + \delta_{ij} [\frac{1}{2}x_0^i(u) - x^i] \dot{x}_0^j(u) - v_0\}, \quad (2.3b)$$

where $\gamma > 0$, u_0 , and v_0 are arbitrary constants, r^i_j is a constant orthogonal matrix, and $x_0^i(u)$ is any 2-vector which satisfies the differential equation

$$\ddot{x}_0^i = H^i_j x_0^j. \quad (2.4)$$

Here and below, dots denote derivatives with respect to the phase coordinate u . The matrix r^i_j can be used to effect rotations or reflections in the transverse coordinates, while γ is a Lorentz factor associated with longitudinal boosts. Varying u_0 and v_0 instead allows one to rigidly translate the coordinates u and v . As elaborated in Section III A below, the 2-vector $x_0^i(u)$ can be

used to recenter the origin around any desired geodesic. Regardless, a comparison with Eq. (2.1) shows that the coordinate transformation (2.3) preserves the Brinkmann line element while transforming the waveform into

$$\hat{H}_{ij}(\hat{u}) = \gamma^2 r^k{}_i r^l{}_j H_{kl}(\gamma\hat{u} + u_0). \quad (2.5)$$

Any given Brinkmann waveform is, therefore, unique up to a small number of simple transformations.

All vacuum plane waves are Petrov type N spacetimes wherever they are not flat, and the associated principal null direction is tangent to

$$\ell^\alpha \equiv -g^{\alpha\beta} \nabla_\beta u. \quad (2.6)$$

This can be interpreted as describing the direction in which the gravitational wave propagates. A calculation shows that

$$\nabla_\alpha \ell^\beta = 0, \quad (2.7)$$

so ℓ^α is also a Killing vector field which generates null translations within each wavefront. In fact, plane wave spacetimes admit at least four Killing vector fields in addition to ℓ^α , which may be viewed as generators for the transformations which are associated with the $x_0^i(u)$ in Eq. (2.3). These Killing fields may be shown to have the form

$$[x^i \dot{\Xi}^i(u)] \partial_v + \Xi^i(u) \partial_i, \quad (2.8)$$

where the 2-vector $\Xi^i(u)$ is any solution to the differential equation

$$\ddot{\Xi}^i = H^i{}_j \Xi^j. \quad (2.9)$$

It has been shown in Ref. [75] that the symmetry structure of plane wave spacetimes is related to the Carroll group that arises as the $c \rightarrow 0$ contraction of the Poincaré group [76].

The Killing vectors of plane wave spacetimes can be understood more intuitively by considering the globally flat case in which H_{ij} vanishes. In that context, all five Killing vectors reduce to

$$\partial_v, \quad \partial_i, \quad x^i \partial_v + u \partial_i. \quad (2.10)$$

The first three of these vector fields clearly generate translations. The final two can be more easily interpreted if inertial coordinates

$$t \equiv \frac{1}{\sqrt{2}}(v + u), \quad z \equiv \frac{1}{\sqrt{2}}(v - u) \quad (2.11)$$

are introduced to supplement x and y , in which case

$$x^i \partial_v + u \partial_i = \frac{1}{\sqrt{2}} [(x^i \partial_t + t \partial_i) - (z \partial_i - x^i \partial_z)]. \quad (2.12)$$

The two bracketed terms here generate a transverse boost in the x^i direction and a rotation in the z - x^i plane. Gravitational plane waves may thus be viewed as being preserved by the composition of these two operations (suitably generalized), but not by either operation on its own.

Said differently, applying a transverse boost to a gravitational plane wave is equivalent to rotating its propagation direction. The vector fields in Eq. (2.12) can alternatively be interpreted as “null rotations” whose action preserves the null vector ℓ^α .

One justification for describing gravitational plane wave spacetimes as “plane waves” is that the five Killing fields (2.10) are exactly those Killing fields that preserve electromagnetic plane waves in flat spacetime [77]. More precisely, consider any field strength

$$F_{\alpha\beta} = \ell_{[\alpha} \mathcal{A}_{\beta]}(u) \quad (2.13)$$

in flat spacetime, where \mathcal{A}_α is restricted only to be orthogonal to ℓ^α . Then $\mathcal{L}_\xi F_{\alpha\beta} = 0$ for all ξ^α in Eq. (2.10). Except in Appendix D, we nevertheless focus only on vacuum *gravitational* plane waves.

Plane wave spacetimes admit many types of symmetries in addition to the Killing fields described above [78, 79]. An example which is useful in the following is the homothety

$$\lambda^\alpha \partial_\alpha = 2v \partial_v + x^i \partial_i, \quad (2.14)$$

which satisfies $\mathcal{L}_\lambda g_{\alpha\beta} = 2g_{\alpha\beta}$. This is a special type of conformal Killing vector field which describes a kind of self-similarity in plane wave spacetimes. Indeed, λ^α generates the 1-parameter family of finite dilations $(u, v, x^i) \mapsto (u, e^{2\epsilon} v, e^\epsilon x^i)$, which rescale the metric by $e^{2\epsilon}$ while leaving invariant the null geodesic $v = x^i = 0$. An analogous self-similarity is also present in flat-spacetime electromagnetic plane waves, in the sense that $\mathcal{L}_\lambda F_{\alpha\beta} = F_{\alpha\beta}$ when $F_{\alpha\beta}$ is given by Eq. (2.13). In the gravitational case, λ^α is useful because, just like ordinary Killing vector fields, homotheties generate conservation laws for geodesics [80]. We find below that homotheties—and more generally, all conformal Killing vector fields—also generate conservation laws for the spin Hall equations.

B. Jacobi propagators

One of the main conclusions of prior work on plane wave spacetimes is that essentially all interesting observables can be written in terms of solutions to the geodesic deviation (or Jacobi) equation [26, 27, 29, 31, 74, 81]. Moreover, the many symmetries of these spacetimes allow us to focus only on geodesic deviation in the two-dimensional space which is transverse to the wave’s propagation direction. The Jacobi equation then reduces to Eq. (2.4), or equivalently to Eq. (2.9). Solutions to these equations describe not only coordinate freedoms and the symmetries of the spacetime, but also its complete geodesic structure, including gravitational wave memory effects and all standard observables in gravitational lensing. Even effects involving low-frequency wave propagation can be extracted from solutions of the geodesic deviation equation [82]. We show below that such solutions also describe the motion of massless spinning particles—models for localized massless wave packets which carry angular momentum.

The Jacobi equation is linear, so all of its solutions can be written in terms of two particular solutions to its matrix generalization

$$\partial_u^2 E_{ij} = H_{ik} E^k{}_j. \quad (2.15)$$

It is often convenient to choose these particular solutions to be the two two-point functions $A_{ij}(u, u')$ and $B_{ij}(u, u')$ that satisfy the matrix Jacobi equation together with the initial conditions

$$[A_{ij}] = [\partial_u B_{ij}] = \delta_{ij}, \quad [\partial_u A_{ij}] = [B_{ij}] = 0. \quad (2.16)$$

Here and below, $[\dots]$ denotes the ‘‘coincidence limit’’ in which $u \rightarrow u'$. We refer to A_{ij} and B_{ij} as the ‘‘Jacobi propagators’’ for the given plane wave spacetime. In terms of them, any solution to the differential equation (2.9) has the form

$$\Xi_i(u) = A_{ij}(u, u') \Xi^j(u') + B_{ij}(u, u') \dot{\Xi}^j(u'), \quad (2.17)$$

where $\Xi^i(u')$ and $\dot{\Xi}^i(u')$ are initial data for that equation. Under the coordinate transformations in Eq. (2.3), the Jacobi propagators transform via

$$\hat{A}_{ij} = r^k{}_i r^l{}_j A_{kl}, \quad \hat{B}_{ij} = \gamma^{-1} r^k{}_i r^l{}_j B_{kl}. \quad (2.18)$$

In addition to their use in plane wave spacetimes [26, 29, 74, 82], Jacobi propagators or similar structures have also been applied in more general spacetimes. They have, for example, been essential to understanding the motion of extended bodies [83, 84], particularly because they can be used to construct generalized Killing vectors [85]. Closely related ideas have also been used to understand gravitational lensing in generic spacetimes [86–92]. Although this paper focuses only on plane wave spacetimes, many of the properties of the Jacobi propagators that we discuss remain valid also in more general spacetimes [31, 86, 90, 92].

Given a particular waveform H_{ij} , it is at least conceptually straightforward to compute the corresponding Jacobi propagators. Although exact analytic calculations are rarely practical², approximations in powers of the curvature are easily obtained; see Section IID below and also Ref. [27]. Numerical calculations which place no restrictions on H_{ij} are straightforward as well. Regardless, the problem of computing A_{ij} and B_{ij} for a particular H_{ij} can be considered separately from the problem of describing observables in terms of A_{ij} and B_{ij} . It is only this latter problem with which most of this paper is concerned. Once the Jacobi propagators associated with a particular plane wave are known, essentially all interesting observables can be straightforwardly determined in terms of them.

Before we turn to this, it is useful to first recall some general identities that are satisfied by all Jacobi propagators. Our starting point is to note that given any two solutions $E_{ij}(u)$ and $\tilde{E}_{ij}(u)$ to the matrix Jacobi equation (2.15), their Wronskian is necessarily conserved:

$$E^k{}_i \partial_u \tilde{E}_{kj} - \tilde{E}_{kj} \partial_u E^k{}_i = \text{constant}. \quad (2.19)$$

This can be used to derive a number of useful identities [26, 29, 31, 74, 92]. First, using Eq. (2.19) with $E_{ij} = A_{ij}$ and $\tilde{E}_{ij} = B_{ij}$ results in the constraint

$$A^k{}_i \partial_u B_{kj} - B_{kj} \partial_u A^k{}_i = \delta_{ij}, \quad (2.20)$$

which implies that there is some overlap in the information which is encoded in A_{ij} and in B_{ij} .

In fact, considerably more can be said about this overlap. Noting that $\partial_{u'} B_{ij}$ satisfies the same matrix Jacobi equation as A_{ij} and B_{ij} , the coincidence limits

$$[\partial_{u'} B_{ij}] = -\delta_{ij}, \quad [\partial_u \partial_{u'} B_{ij}] = 0 \quad (2.21)$$

imply that

$$A_{ij}(u, u') = -\partial_{u'} B_{ij}(u, u'). \quad (2.22)$$

Knowledge of B_{ij} alone is therefore sufficient to obtain A_{ij} . Applying a similar argument for $\partial_{u'} A_{ij}$ instead of $\partial_{u'} B_{ij}$ results in

$$B_{ik}(u, u') H^k{}_j(u') = -\partial_{u'} A_{ij}(u, u'). \quad (2.23)$$

Although this could be used to derive B_{ij} from A_{ij} when $H_{ij}(u')$ is invertible, this is often not the case. Eq. (2.22) is therefore more useful than Eq. (2.23); it implies that we can write everything of interest purely in terms of B_{ij} .

In general, neither A_{ij} nor B_{ij} is symmetric. However, appropriate substitutions into Eq. (2.19) can be used to show that the matrices

$$A_{ki} \partial_u A^k{}_j, \quad B_{ki} \partial_u B^k{}_j, \quad B_{ik} A_j{}^k \quad (2.24)$$

are necessarily symmetric [26]. Lastly, we note that if the arguments of A_{ij} and B_{ij} are swapped, conserved Wronskians can be used to show that

$$B_{ij}(u, u') = -B_{ji}(u', u), \quad (2.25a)$$

$$\partial_u A_{ij}(u, u') = -\partial_{u'} A_{ji}(u', u). \quad (2.25b)$$

The first of these identities is a version of Etherington’s reciprocity relation [93, 94] as applied to plane wave spacetimes (although more general versions of that relation can be obtained using an essentially identical argument).

C. Sandwich waves and memory tensors

A particularly clean model for a gravitational wave burst—or perhaps the Penrose limit of a null geodesic

² One analytic example is nevertheless discussed in Appendix B1 below, where the Jacobi propagators are computed for a finite-width square wave.

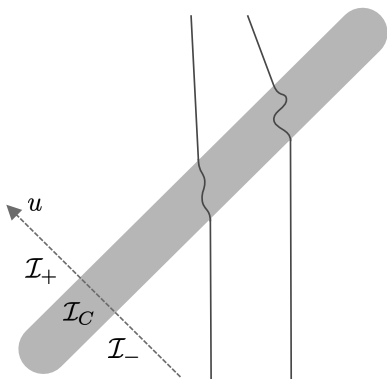


FIG. 1. Schematic diagram of a sandwich wave. The geometry is curved only when the phase coordinate u lies in the region \mathcal{I}_C . The locally flat regions to the future or to the past of the gravitational wave are characterized by u coordinates in \mathcal{I}_+ or in \mathcal{I}_- , respectively. A memory effect is also illustrated using the worldlines of two freely falling objects: Interaction with the gravitational wave is seen to change their relative velocity.

which has been scattered by a compact system—is provided by a plane wave in which $H_{ij}(u)$ vanishes for all u outside some finite interval $\mathcal{I}_C \subset \mathbb{R}$. All points whose u coordinates lie outside that interval are locally flat, so observers will experience a curved gravitational wave region “sandwiched” between two flat regions, as illustrated in Fig. 1. We refer to the u coordinates associated with the flat region to the future of the gravitational wave by $\mathcal{I}_+ \subset \mathbb{R}$ and the flat region to its past by $\mathcal{I}_- \subset \mathbb{R}$. Almost all further discussion in this paper is confined to “sandwich waves” such as these (or occasionally to waves whose curvature decays very rapidly outside some finite u interval). Since both the initial and the final geometries are flat in a sandwich wave, it is straightforward to understand different types of scattering processes.

As remarked above, many observables in plane wave spacetimes can be written in terms of the Jacobi propagators A_{ij} and B_{ij} . Since it follows from Eq. (2.22) that A_{ij} can be easily computed from B_{ij} , our first step is to determine the properties of B_{ij} in sandwich wave spacetimes. To do so, first note that in any region where H_{ij} vanishes, it follows from Eq. (2.15) that

$$B_{ij}(u, u') = C_{ij}(u') + uD_{ij}(u'), \quad (2.26)$$

for some $C_{ij}(u')$ and some $D_{ij}(u')$. If the waveform vanishes *throughout* the region between the wavefronts parameterized by u and by u' , the initial data in Eq. (2.16) implies that $C_{ij}(u') = -u'\delta_{ij}$ and $D_{ij}(u') = \delta_{ij}$, so

$$A_{ij}(u, u') = \delta_{ij}, \quad B_{ij}(u, u') = (u - u')\delta_{ij}. \quad (2.27)$$

This is globally valid in Minkowski spacetime. In nontrivial sandwich wave spacetimes, it is valid whenever u and u' are either both in \mathcal{I}_+ or both in \mathcal{I}_- .

The Jacobi propagators are more interesting when, for example, u' lies in \mathcal{I}_- while u lies in \mathcal{I}_+ . In that case,

$B_{ij}(u, u')$ is given by Eq. (2.26) and

$$B_{ij}(u', u) = \tilde{C}_{ij}(u) + u'\tilde{D}_{ij}(u) \quad (2.28)$$

for some $\tilde{C}_{ij}(u)$ and some $\tilde{D}_{ij}(u)$. Using Eq. (2.25a) to relate both of these expressions shows that

$$C_{ij}(u') + uD_{ij}(u') = -\tilde{C}_{ji}(u) - u'\tilde{D}_{ji}(u), \quad (2.29)$$

which can be true only when $C_{ij}(u')$, $\tilde{C}_{ij}(u)$, $D_{ij}(u')$, and $\tilde{D}_{ij}(u)$ are all affine functions of their arguments. It follows that there must exist four “memory tensors” $M_{ij}^{(\dots)}$ such that

$$B_{ij}(u, u') = (u - u')\delta_{ij} + M_{ij}^{v \rightarrow d} + uM_{ij}^{v \rightarrow v} - u'M_{ij}^{d \rightarrow d} - uu'M_{ij}^{d \rightarrow v}. \quad (2.30)$$

These tensors are all *constant*. Applying Eq. (2.22), it also follows that

$$A_{ij}(u, u') = \delta_{ij} + M_{ij}^{d \rightarrow d} + uM_{ij}^{d \rightarrow v}, \quad (2.31)$$

which does not depend on u' . If the roles of u and u' are reversed, so u' lies in \mathcal{I}_+ while u lies in \mathcal{I}_- , Eqs. (2.22) and (2.25a) can be used to show that Eq. (2.30) is replaced by

$$B_{ij}(u, u') = (u - u')\delta_{ij} - M_{ji}^{v \rightarrow d} + uM_{ji}^{d \rightarrow d} - u'M_{ji}^{v \rightarrow v} + uu'M_{ji}^{d \rightarrow v}, \quad (2.32)$$

while Eq. (2.31) is replaced by

$$A_{ij}(u, u') = \delta_{ij} + M_{ji}^{v \rightarrow v} - uM_{ji}^{d \rightarrow v}. \quad (2.33)$$

Regardless, although there is an infinite-dimensional space of possible waveforms, it follows from these results that the effects of those waveforms on the Jacobi propagators are encoded in the finite-dimensional space of possible memory tensors—at least outside \mathcal{I}_C . Comparison with Eq. (2.27) shows that all memory tensors vanish when the spacetime is globally flat. More generally, the memory tensors can be computed by integrating the matrix Jacobi equation (2.15) through the curved region \mathcal{I}_C . Even when exact analytic solutions are not available, numerical computations are straightforward. Some examples are discussed in Appendix B.

While results equivalent to Eqs. (2.30) and (2.31) have been derived before [26], describing the various terms in the Jacobi propagators as “memory tensors” is new. We shall see in Section III B below—in particular in Eqs. (3.9) and (3.10)—that the superscripts on the memory tensors roughly explain how they affect pairs of geodesics: The “displacement-displacement memory” $M_{ij}^{d \rightarrow d}$ determines how initial relative displacements affect final relative displacements, the “velocity-displacement memory” $M_{ij}^{v \rightarrow d}$ determines how initial relative velocities affect final relative displacements, the “displacement-velocity memory” $M_{ij}^{d \rightarrow v}$ determines how initial relative displacements affect final relative velocities, and the “velocity-velocity memory”

$M_{ij}^{v \rightarrow v}$ determines how initial relative velocities affect final relative velocities. $M_{ij}^{d \rightarrow v}$ has dimension $(\text{length})^{-1}$, $M_{ij}^{d \rightarrow d}$ and $M_{ij}^{v \rightarrow v}$ are dimensionless, and $M_{ij}^{v \rightarrow d}$ has dimension $(\text{length})^1$.

Our displacement-velocity memory $M_{ij}^{d \rightarrow v}$ is closely related to what has been referred to elsewhere as the “velocity memory” [27, 28, 31, 40, 41, 95]. However, the final relative velocities of two geodesics depend not only on their initial displacements, but also on their initial velocities. This motivates us to adopt a more precise terminology that distinguishes between contributions associated with initial displacements and contributions associated with initial velocities. What we call velocity-velocity memory $M_{ij}^{v \rightarrow v}$ is closely related to what has been referred to before as the “kick memory” [31, 96]. Our displacement-displacement memory is instead related to what has previously been referred to as “the” memory tensor [12, 25, 97], or sometimes (at least part of) the “displacement memory” [28]. Lastly, our $M_{ij}^{v \rightarrow d}$ is related to what has previously been referred to as the “subleading displacement memory” [28] or the “drift memory” [31], which is in turn connected to the “spin” [18] and the “center-of-mass” [21] memories.

Regardless of terminology, the goal in much of this paper is to determine how various observables depend on the four memory tensors. From this perspective, it is important to know which memory tensors are “possible” (for some waveform) and which are not: The space of possible memory tensors is not equivalent to the space of four 2×2 matrices. Instead, the memory tensors are, for example, constrained by the conserved Wronskian (2.20). In combination with Eqs. (2.30) and (2.31), this implies that

$$M_{ij}^{v \rightarrow v} + M_{ji}^{d \rightarrow d} = M_{ki}^{d \rightarrow v} M_{kj}^{v \rightarrow d} - M_{ki}^{d \rightarrow d} M_{kj}^{v \rightarrow v}, \quad (2.34a)$$

$$M_{ij}^{d \rightarrow v} - M_{ji}^{v \rightarrow d} = M_{ki}^{d \rightarrow v} M_{kj}^{d \rightarrow d} - M_{kj}^{d \rightarrow v} M_{ki}^{d \rightarrow d}. \quad (2.34b)$$

Additional constraints would result from instead combining the conserved Wronskian with the time-reversed Jacobi propagators given by Eqs. (2.32) and (2.33). Additional constraints can also be generated by antisymmetrizing the symmetric tensors in Eq. (2.24). For example, Eq. (2.30) and the symmetry of $B_{ki} \partial_u B^k_j$ implies that

$$M_{ij}^{v \rightarrow d} - M_{ji}^{d \rightarrow v} = M_{ki}^{v \rightarrow d} M_{kj}^{v \rightarrow v} - M_{kj}^{v \rightarrow d} M_{ki}^{v \rightarrow v}. \quad (2.35)$$

Regardless, Eq. (2.34a) allows the velocity-velocity memory $M_{ij}^{v \rightarrow v}$ to be computed from the other three memory tensors. In a weak-field limit where terms quadratic in the curvature are ignored, it implies that

$$M_{ij}^{v \rightarrow v} = -M_{ji}^{d \rightarrow d} + \mathcal{O}(H^2). \quad (2.36)$$

Equations (2.34b) and (2.35) instead constrain the anti-symmetric components of $M_{ij}^{d \rightarrow v}$ and $M_{ij}^{v \rightarrow d}$, implying that those components vanish in a weak-field limit. In fact,

we shall see in Section IID below that all four memory tensors are symmetric (and also trace-free) in such a limit.

It may be noted that our definition for the memory tensors in terms of B_{ij} effectively singles out the $u = 0$ hyperplane as a “reference” hypersurface. However, there is nothing intrinsically special about this choice, and others can be used instead. Referencing a different $u = \text{constant}$ hypersurface is very similar to performing a constant translation of the u coordinate, which transforms one Brinkmann coordinate system into another. It is therefore interesting to understand how the memory tensors are related to each other in different Brinkmann coordinate systems. Using the *general* Brinkmann-to-Brinkmann coordinate transformation (2.3), comparison of Eqs. (2.18) and (2.30) shows that the memory tensors transform via

$$\hat{M}_{ij}^{d \rightarrow v} = \gamma r^k_i r^l_j M_{kl}^{d \rightarrow v}, \quad (2.37a)$$

$$\hat{M}_{ij}^{v \rightarrow v} = r^k_i r^l_j (M_{kl}^{v \rightarrow v} - u_0 M_{kl}^{d \rightarrow v}), \quad (2.37b)$$

$$\hat{M}_{ij}^{d \rightarrow d} = r^k_i r^l_j (M_{kl}^{d \rightarrow d} + u_0 M_{kl}^{d \rightarrow v}), \quad (2.37c)$$

$$\hat{M}_{ij}^{v \rightarrow d} = \gamma^{-1} r^k_i r^l_j [M_{kl}^{v \rightarrow d} - u_0^2 M_{kl}^{d \rightarrow v} + u_0 (M_{kl}^{v \rightarrow v} - M_{kl}^{d \rightarrow d})]. \quad (2.37d)$$

Varying the origin of the u coordinate by varying u_0 thus mixes the various memory tensors. In some cases, this freedom can be used to eliminate certain memory tensors. However, varying u_0 can never affect $M_{ij}^{d \rightarrow v}$ or $M_{ij}^{d \rightarrow d} + M_{ij}^{v \rightarrow v}$, both of which are invariant up to overall scalings and orthogonal transformations. As noted above, $M_{ij}^{d \rightarrow d} + M_{ij}^{v \rightarrow v}$ always vanishes at least through first order in the curvature. We shall see in Section IID below that in many (though not all) cases, $M_{ij}^{d \rightarrow v}$ also vanishes at first order.

Although our primary concern in this paper is with gravitational waves, it can be instructive to compare with the electromagnetic case. Appendix D considers charged-particle scattering in an electromagnetic sandwich wave in flat spacetime, and shows that instead of obtaining four rank-2 memory tensors, there are two memory *vectors* in that context. These are essentially the zeroth and the first moments of the electromagnetic waveform \mathcal{A}_i . We now show that at leading order, the gravitational memory tensors are instead given by the zeroth, the first, and the second moments of the gravitational waveform H_{ij} .

D. Approximate memory tensors

If a gravitational wave is weak, which means that the memory tensors are all “small,” they can be related to the waveform by perturbatively solving Eqs. (2.15) and (2.16). Through second order in the curvature H_{ij} , a straightforward calculation shows that

$$B_{ij}(u, u') = (u - u')\delta_{ij} + \int_{u'}^u dw (u - w) \left[(w - u')H_{ij}(w) + \int_{u'}^w dw' (w - w')(w' - u')H_{ik}(w)H_{kj}(w') \right] + \mathcal{O}(H^3). \quad (2.38)$$

Applying Eq. (2.22) then results in

$$A_{ij}(u, u') = \delta_{ij} + \int_{u'}^u dw (u - w) \left[H_{ij}(w) + \int_{u'}^w dw' (w - w')H_{ik}(w)H_{kj}(w') \right] + \mathcal{O}(H^3). \quad (2.39)$$

Both of these expressions are valid for all u , for all u' , and for all plane waves in which the relevant integrals exist; they are not restricted only to sandwich waves. One implication is that the first-order contributions to the Jacobi propagators are always symmetric and trace-free in vacuum. However, antisymmetric components and nonzero traces can arise at second order [27, 29].

If we restrict ourselves to sandwich wave spacetimes, the leading-order memory tensors can be extracted by comparing Eq. (2.38) with Eq. (2.30). Through first order in the curvature, this results in

$$M_{ij}^{\text{d}\rightarrow\text{v}} = \int_{-\infty}^{\infty} dw H_{ij}(w) + \mathcal{O}(H^2), \quad (2.40a)$$

$$\begin{aligned} M_{ij}^{\text{v}\rightarrow\text{v}} &= -M_{ij}^{\text{d}\rightarrow\text{d}} + \mathcal{O}(H^2) \\ &= \int_{-\infty}^{\infty} dw w H_{ij}(w) + \mathcal{O}(H^2), \end{aligned} \quad (2.40b)$$

$$M_{ij}^{\text{v}\rightarrow\text{d}} = -\int_{-\infty}^{\infty} dw w^2 H_{ij}(w) + \mathcal{O}(H^2). \quad (2.40c)$$

In vacuum, all four memory tensors are therefore symmetric and trace-free at leading order. They encode the zeroth, the first, and the second moments of H_{ij} . These are all that are needed (at leading order) for the observables considered in this paper. However, higher moments of the waveform can be relevant for certain other “persistent observables” [28, 31].

If a plane wave spacetime is viewed as a “local” idealization of the far-field geometry around a radiating compact system in an asymptotically flat spacetime, the quadrupole approximation [98] suggests that the waveform—which is a curvature, not a transverse-traceless metric perturbation—must be proportional to the fourth derivative of the system’s quadrupole moment. If all gravitational waves are sourced, for example, by a violent collision or by an explosion involving multiple masses, then the third derivatives of the quadrupole moment would be expected to vanish at both early and late times [27, 46, 99]. The waveform would thus be given by

$$H_{ij}(u) = \partial_u \mathfrak{H}_{ij}(u), \quad (2.41)$$

where $\mathfrak{H}_{ij}(u)$ vanishes for all $u \in \mathcal{I}_{\pm}$. Substitution into Eq. (2.40a) shows that in this case, the displacement-velocity memory vanishes through first order in the curvature. Although Einstein’s equations do not constrain

$M_{ij}^{\text{d}\rightarrow\text{v}}$ purely in a plane wave context, they are likely to do so for the plane waves which are local approximations of astrophysically relevant gravitational waves.

Nevertheless, vanishing displacement-velocity memory is not typically a feature of the plane waves that arise from Penrose limits. For example, the Penrose limit of a null geodesic with angular momentum L in a Schwarzschild spacetime with mass M is [39]

$$H_{ij}(u) = \frac{3ML^2}{[r(u)]^5} \text{diag}[1, -1]_{ij}, \quad (2.42)$$

where $r(u)$ denotes the areal radius of the given geodesic³. Since $3ML^2/[r(u)]^5 \geq 0$, substitution into Eq. (2.40a) shows that, except in the radial case where $L = 0$, the displacement-velocity memory cannot vanish at first order in H_{ij} .

It may also be noted that if we again assume a waveform given by Eq. (2.41), use of Eq. (2.39) shows that although $M_{ij}^{\text{d}\rightarrow\text{v}}$ vanishes at first order in the curvature, it *cannot* vanish at second order:

$$M_{ij}^{\text{d}\rightarrow\text{v}} = -\frac{1}{2} \left[\int_{-\infty}^{\infty} du \mathfrak{H}^{kl}(u) \mathfrak{H}_{kl}(u) \right] \delta_{ij} + \mathcal{O}(H^3). \quad (2.43)$$

Initially comoving geodesics are therefore focused isotropically in the two transverse directions. That $M_{ij}^{\text{d}\rightarrow\text{v}}$ must be nonzero at second order is closely related to statements in, e.g., Refs. [40, 41] that it is impossible for the velocity memory to vanish.

Unless otherwise noted, we place no constraints below on the leading-order behavior of $M_{ij}^{\text{d}\rightarrow\text{v}}$. We also do not assume that H_{ij} necessarily has the form (2.41).

III. GEODESIC MOTION AND MEMORY EFFECTS

The Jacobi propagators discussed in the previous section govern all properties of geodesics in plane wave space-

³ This is technically not a sandwich wave. However, if the null geodesic is only scattered—and not captured or bound—its radius grows rapidly as $u \rightarrow \pm\infty$. Memory tensors then remain a useful concept. The same could not be said for, e.g., the Penrose limit which is associated with a circular null geodesic in which $r(u) = 3M$.

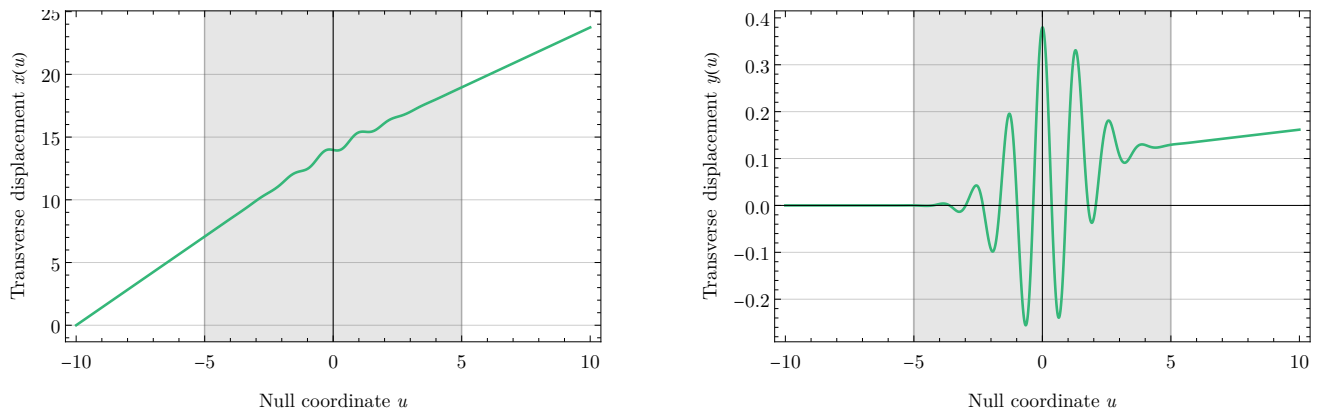


FIG. 2. Example transverse coordinates of a geodesic in a sandwich wave spacetime. The geodesic has a vanishing initial velocity in the y direction but not in the x direction, and there is a clear (non-diagonal) velocity-velocity memory. However, note the different vertical scales in these plots. The gravitational wave profile used here is given by Eq. (B.10) in Appendix B, with center point $U_0 = 0$, frequency $\nu = 5/U$, curvature lengthscales $l_+ = l_- = U/\sqrt{2}$, and phases $\phi_- = 0$ and $\phi_+ = -\pi/2$. This wave might be interpreted as circularly polarized with a Gaussian profile. These plots also employ units in which the characteristic burst width U is equal to unity. The shaded region roughly corresponds to the curved region \mathcal{I}_C ; at the edge of the shading, the exponential in the waveform is 0.002 times its maximum value.

times⁴. We now make this explicit by describing how geodesics are scattered in sandwich wave spacetimes. Section III A begins by reviewing known results on geodesics in plane wave spacetimes. Those results are then specialized to sandwich waves in Section III B, where the memory tensors introduced above are used to describe the transverse properties of scattered geodesics. “Time-reversed” memory tensors, which describe initial states in terms of final states, are also derived there. Section III C completes the treatment of geodesic motion by describing both transverse and longitudinal memory effects. We focus in particular on how null geodesics are affected by gravitational wave memory, which differs considerably from the more typical cases involving slowly moving time-like geodesics. Lastly, Section III D explains how memory tensors affect Synge’s world function, which provides an alternative way to encode the geodesics of sandwich wave spacetimes. As an application, we describe how memory effects deform light cones.

A. Geodesics in plane wave spacetimes

The geodesic structure of plane wave spacetimes has been extensively described in, e.g., Refs. [39, 74]. To briefly review the results needed here, suppose that $x^\alpha(\tau)$ describes an affinely parametrized geodesic. Then, since ℓ^α is Killing, $\ell_\alpha dx^\alpha/d\tau = -du/d\tau$ must be constant. If that constant vanishes, the geodesic lies on a $u = \text{constant}$ hypersurface, and is either spacelike or null. However, the vast majority of geodesics are not of that type, and in all

such cases, we are free to identify the affine parameter τ with u . Doing so,

$$\ell_\alpha \frac{dx^\alpha}{du} = -1. \quad (3.1)$$

The two transverse coordinates of a geodesic are then given by

$$x^i(u) = A^i_j(u, u')x^j(u') + B^i_j(u, u')\dot{x}^j(u'), \quad (3.2)$$

where A_{ij} and B_{ij} are the Jacobi propagators introduced in Section II B. In terms of this transverse motion, the v coordinate of a geodesic may be shown to be

$$v(u) = v(u') + \kappa(u - u') + \frac{1}{2}[x^i(u)\dot{x}_i(u) - x^i(u')\dot{x}_i(u')], \quad (3.3)$$

where

$$\kappa \equiv -\frac{1}{2}g_{\alpha\beta} \frac{dx^\alpha}{du} \frac{dx^\beta}{du} \quad (3.4)$$

is a constant. If a geodesic is timelike, $\kappa > 0$; if it is null, $\kappa = 0$. Nevertheless, there exist families of timelike geodesics in which the limits $\kappa \rightarrow 0$ and $\kappa \rightarrow \infty$ both approach null geodesics. This is described in more detail below Eq. (3.18).

Regardless, it follows from Eqs. (3.2) and (3.3) that all interesting properties of geodesics in plane wave spacetimes are determined by their two transverse coordinates x^i , which are in turn determined by the two Jacobi propagators A_{ij} and B_{ij} . Moreover, whether a geodesic is timelike, null, or spacelike affects only its v coordinate. Some examples of geodesics in specific plane wave spacetimes are plotted in Figs. 2 and 3. Additional examples may be found in, e.g., Refs. [40, 41, 46, 100].

⁴ In more general spacetimes, Jacobi propagators only encode the behavior of *nearby* geodesics.

As noted above, the Brinkmann coordinates used in this paper are essentially Fermi normal coordinates constructed around the null geodesic $x^i(u) = v(u) = 0$. However, there is nothing physically distinct about this origin. If we choose any other null geodesic, appropriate choices for $x_0^i(u)$ and for v_0 in the coordinate transformation (2.3) may be used to construct Brinkmann coordinates $(\hat{u}, \hat{v}, \hat{x}^i)$ in which that geodesic is given by $\hat{x}^i(\hat{u}) = \hat{v}(\hat{u}) = 0$. Moreover, doing so does not change the waveform. Similar recenterings may also be performed for non-null geodesics, which can always be mapped to $\hat{x}^i(\hat{u}) = 0$ and $\hat{v}(\hat{u}) = \kappa\hat{u} + \text{constant}$. These results provide a sense in which the plane wave spacetimes are indeed planar; the origin is of no intrinsic geometrical significance. The freedom to recenter is also useful below, where it allows us, without loss of generality, to place a geodesic observer at the origin.

One last point to note is that plane wave spacetimes generically admit caustics, or more precisely conjugate points. Given a pair of points in a plane wave spacetime, there typically exists exactly one geodesic that passes between them. However, if two points have phase coordinates u and u' in which

$$\det B_{ij}(u, u') = 0, \quad (3.5)$$

there are either an infinite number of connecting geodesics or there are none [74]. The pairs of hypersurfaces $u' = \text{constant}$ and $u = \text{constant}$ are then referred to as “conjugate hyperplanes.” All null geodesics emanating from a point on the $u' = \text{constant}$ hypersurface are focused into either a line or (in exceptional cases) a point on the $u = \text{constant}$ hypersurface. Timelike geodesics are instead focused into either two- or one-dimensional subsets of that three-dimensional hypersurface. In the case of a sandwich wave, fixing some $u' \in \mathcal{I}_-$ results in at most two solutions to Eq. (3.5) in which $u \in \mathcal{I}_+$ [26]. An example with one solution is described in Appendix B 1 below.

B. Transverse memory effects in sandwich wave spacetimes

Before a gravitational wave arrives and after it has left, all geodesics in a sandwich wave spacetime are straight lines in Brinkmann coordinates. However, these lines are not necessarily trivial continuations of one other; geodesics are scattered by the gravitational wave in the curved region \mathcal{I}_C . We now show that all possible scatterings are determined by the memory tensors introduced in Section II C above.

If initial data $x^i = x^i(u')$ and $\dot{x}^i = \dot{x}^i(u')$ for a particular geodesic is specified at the phase coordinate $u' \in \mathcal{I}_-$, and if $u \in \mathcal{I}_+$, it follows from Eqs. (2.30), (2.31) and (3.2) that the transverse displacement at late times is

$$x_i(u) = (\delta_{ij} + M_{ij}^{\text{d}\rightarrow\text{d}} + uM_{ij}^{\text{d}\rightarrow\text{v}})(x'^j - u'\dot{x}'^j) + [M_{ij}^{\text{v}\rightarrow\text{d}} + u(\delta_{ij} + M_{ij}^{\text{v}\rightarrow\text{v}})]\dot{x}'^j. \quad (3.6)$$

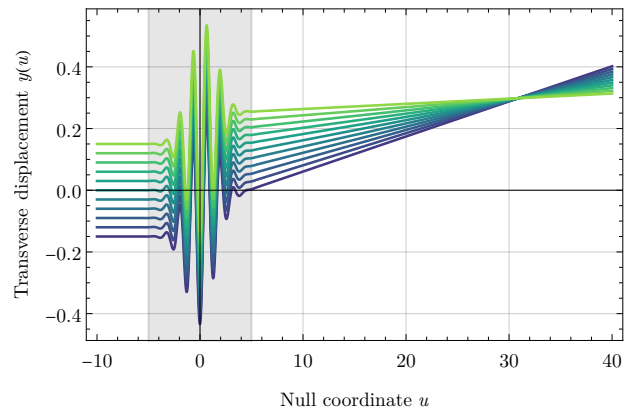


FIG. 3. Scattering of a bundle of initially parallel geodesics traveling in the x -direction, illustrating a nontrivial displacement-velocity effect. The sandwich gravitational wave (shaded region) is seen to act as a lens for these geodesics. The waveform and other conventions here are the same as in Fig. 2.

Differentiation with respect to u gives the final transverse velocity

$$\dot{x}_i(u) = (\delta_{ij} + M_{ij}^{\text{v}\rightarrow\text{v}})\dot{x}'^j + M_{ij}^{\text{d}\rightarrow\text{v}}(x'^j - u'\dot{x}'^j). \quad (3.7)$$

These equations are exact, and can be used to predict the results of various memory experiments that compare the initial and the final states of freely falling objects.

One consequence is that the memory tensors can be viewed as the components of a linear map which relates the initial and the final transverse states of all geodesics in a sandwich wave spacetime. In particular, the memory tensors determine a “scattering matrix” \mathcal{S} that relates the initial transverse displacements and the initial transverse velocities to the final transverse displacements and the final transverse velocities. In order to construct this matrix, it is first convenient to introduce the initial and the final “projected displacements”

$$x_+^i \equiv x^i(u) - u\dot{x}^i(u), \quad x_-^i \equiv x^i(u') - u'\dot{x}^i(u'), \quad (3.8)$$

which do not depend on precisely how we choose u or u' . Physically, these are the transverse coordinates which the initial and the final geodesics would have if they were extrapolated onto the $u = 0$ hypersurface while ignoring any intervening curvature; see Fig. 4. Regardless, if we additionally define⁵ $\dot{x}_+^i \equiv \dot{x}^i(u)$ and $\dot{x}_-^i \equiv \dot{x}^i(u')$, Eqs. (3.6) and (3.7) imply that

$$\begin{pmatrix} x_+^i \\ \dot{x}_+^i \end{pmatrix} = \mathcal{S} \begin{pmatrix} x_-^j \\ \dot{x}_-^j \end{pmatrix}, \quad (3.9)$$

where the scattering matrix is

$$\mathcal{S} = \begin{pmatrix} \delta_{ij} + M_{ij}^{\text{d}\rightarrow\text{d}} & M_{ij}^{\text{v}\rightarrow\text{d}} \\ M_{ij}^{\text{d}\rightarrow\text{v}} & \delta_{ij} + M_{ij}^{\text{v}\rightarrow\text{v}} \end{pmatrix}. \quad (3.10)$$

⁵ Despite the notation, the \dot{x}_\pm^i are not derivatives of x_\pm^i .

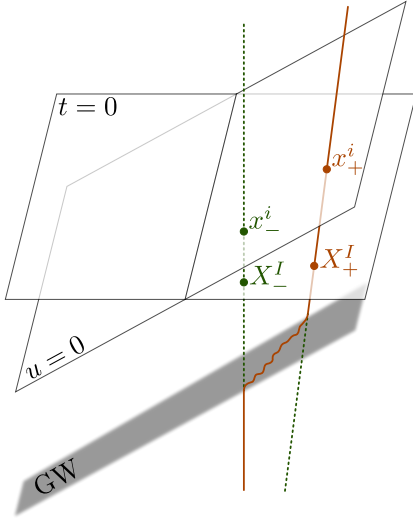


FIG. 4. The projected displacements x_{\pm}^i and X_{\pm}^I . Following Eq. (3.8), the constants x_{\pm}^i denote the flat projections of the two transverse coordinates of the initial and the final geodesics onto the hypersurface $u = 0$. Following Eq. (3.17), the constants X_{\pm}^I denote the flat projections of the three Cartesian coordinates of the initial and the final geodesics onto the hypersurface $t = 0$. Dashed lines denote extrapolations of the worldlines which ignore the spacetime curvature.

This justifies the names for the memory tensors that were introduced in Section II C above: $M_{ij}^{d \rightarrow d}$ is the displacement-displacement memory, $M_{ij}^{d \rightarrow v}$ is the displacement-velocity memory, and so on.

The scattering matrix \mathcal{S} determines the final state of a system in terms of its initial state. However, the initial state can instead be determined from the final state by using Eqs. (2.32) and (2.33) to show that

$$\begin{pmatrix} x_{-}^i \\ \dot{x}_{-}^i \end{pmatrix} = \mathcal{S}^{-1} \begin{pmatrix} x_{+}^j \\ \dot{x}_{+}^j \end{pmatrix}, \quad (3.11)$$

where

$$\mathcal{S}^{-1} = \begin{pmatrix} \delta_{ij} + M_{ji}^{v \rightarrow v} & -M_{ji}^{v \rightarrow d} \\ -M_{ji}^{d \rightarrow v} & \delta_{ij} + M_{ji}^{d \rightarrow d} \end{pmatrix}. \quad (3.12)$$

This inverse can also be derived from Eq. (3.10) using the memory tensor identities in Eqs. (2.34) and (2.35). Regardless, it follows that all information contained in the “future-directed” memory tensors ($M_{ij}^{d \rightarrow d}$, $M_{ij}^{v \rightarrow v}$, $M_{ij}^{v \rightarrow d}$, $M_{ij}^{d \rightarrow v}$) can be equivalently encoded in their “past-directed” counterparts ($M_{ij}^{d \leftarrow d}$, $M_{ij}^{v \leftarrow v}$, $M_{ij}^{v \leftarrow d}$, $M_{ij}^{d \leftarrow v}$), which are related via

$$\begin{aligned} M_{ij}^{d \leftarrow d} &= +M_{ji}^{v \rightarrow v}, & M_{ij}^{v \leftarrow v} &= +M_{ji}^{d \rightarrow d}, \\ M_{ij}^{d \leftarrow v} &= -M_{ji}^{v \rightarrow d}, & M_{ij}^{v \leftarrow d} &= -M_{ji}^{d \rightarrow v}. \end{aligned} \quad (3.13)$$

The memory tensor $M_{ij}^{d \leftarrow v}$, for example, describes how final transverse velocities affect initial transverse displacements.

No matter which memory tensors are employed, the scattering matrix \mathcal{S} plays a similar role to the ABCD ray transfer matrix, which is used in optics to describe the propagation of light rays through optical elements in the paraxial approximation [101, 102] (see also Ref. [90] for an implementation of the ABCD ray transfer matrix for light propagation in general relativity). Thus, the transverse action of plane gravitational waves on test particles can be compared to that of lenses and other optical elements on light rays. The focusing mentioned above in connection with conjugate hyperplanes is, e.g., reminiscent of the focusing of a nearby point source by a lens. Focusing of initially parallel rays instead occurs when $\det A_{ij}(u, u') = 0$ [rather than $\det B_{ij}(u, u') = 0$], and an example of this is presented in Fig. 3. In both cases, however, focusing by vacuum gravitational waves is typically astigmatic.

It may also be noted that the transverse scattering of a geodesic by a gravitational plane wave may be compared with the transverse scattering of a charged particle by an electromagnetic plane wave. It is shown in Appendix D that, unlike their gravitational counterparts, electromagnetic memory effects do not depend on a particle’s initial state; they are “inhomogeneous.”

C. Transverse and longitudinal memory effects in three-dimensional space

The scattering matrix \mathcal{S} provides a simple relation between the gravitational memory tensors and the two transverse coordinates of a scattered geodesic. However, this simplicity can be misleading. The longitudinal dynamics can be considerably more complicated, particularly in the inertial coordinates which are most natural in the flat regions to the past and to the future of the gravitational wave. We now provide a full three-dimensional picture of geodesic scattering in sandwich wave spacetimes, including both longitudinal and transverse effects. Unlike in the purely transverse discussion above, there are significant differences between the behaviors of slowly and rapidly moving geodesics (including null geodesics).

Before a gravitational wave arrives, it follows from Eqs. (3.3) and (3.8) that any geodesic which is not confined to a $u = \text{constant}$ hypersurface may be parameterized by

$$v(u) = v_{-} + u(\kappa + \frac{1}{2}\delta_{ij}\dot{x}_{-}^i\dot{x}_{-}^j), \quad (3.14a)$$

$$x^i(u) = x_{-}^i + u\dot{x}_{-}^i, \quad (3.14b)$$

where κ , v_{-} , x_{-}^i , and \dot{x}_{-}^i are all constant. After the wave has left,

$$v(u) = v_{+} + u(\kappa + \frac{1}{2}\delta_{ij}\dot{x}_{+}^i\dot{x}_{+}^j), \quad (3.15a)$$

$$x^i(u) = x_{+}^i + u\dot{x}_{+}^i, \quad (3.15b)$$

where v_{+} , x_{+}^i , and \dot{x}_{+}^i are also constant. The final transverse state (x_{+}^i, \dot{x}_{+}^i) is related to the initial transverse

state (x_-^i, \dot{x}_-^i) via Eq. (3.9), while v_+ and v_- are related via

$$v_+ = v_- + \frac{1}{2}\delta_{ij}(x_+^i \dot{x}_+^j - x_-^i \dot{x}_-^j). \quad (3.16)$$

Although these expressions encode all transverse and longitudinal aspects of geodesic scattering in sandwich wave spacetimes, the parameters used here are not particularly intuitive. Real observers would not naturally be inclined to project onto $u = \text{constant}$ hypersurfaces, nor would they be inclined to measure velocities with respect to u .

Interpretations can be simplified by adopting the inertial coordinates t and z that are related to u and v through Eq. (2.11). The timelike worldline $x = y = z = 0$ is then a geodesic, even inside the gravitational wave. *We take this worldline to be the trajectory of a canonical observer, and measure everything with respect to it.* Doing so does not entail any loss of generality, since the argument at the end of Section III A implies that given any timelike geodesic, there will exist a Brinkmann coordinate system in which that geodesic lies at the origin. In that context, the coordinates (t, x, y, z) form a local Lorentz frame for the given observer. They are ordinary inertial coordinates both before the gravitational wave arrives and after it has left.

Employing capitalized indices I, J, \dots to refer to the three spatial coordinates (x, y, z) , it is convenient to parameterize the initial and the final geodesics by

$$x^I(t) = X_{\pm}^I + V_{\pm}^I t, \quad (3.17)$$

where the constants V_{\pm}^I denote the initial and the final 3-velocities dx^I/dt . The constant displacements X_{\pm}^I represent 3-dimensional projections of the initial and final geodesics onto the $t = 0$ hypersurface. This contrasts with the x_{\pm}^i defined above, which are i) purely transverse and ii) projected onto the $u = 0$ hypersurface rather than the $t = 0$ one; see Fig. 4.

It is now possible to translate between the ‘‘Brinkmann parameters’’ $(\kappa, v_{\pm}, x_{\pm}^i, \dot{x}_{\pm}^i)$ appearing in Eqs. (3.14) and (3.15), and the ‘‘inertial parameters’’ (X_{\pm}^I, V_{\pm}^I) appearing in Eq. (3.17). Defining $V_{\pm} \in [0, 1)$ to be the three-dimensional Euclidean norm of V_{\pm}^I , and θ_{\pm} as the angle between the velocity vector and the direction of propagation of the gravitational wave, comparing expressions first shows that

$$\kappa = \frac{1 - V_{\pm}^2}{(1 - V_{\pm} \cos \theta_{\pm})^2}. \quad (3.18)$$

The fact that κ is not affected by the gravitational wave constrains the relation between possible pairs (V_-, θ_-) and (V_+, θ_+) . Regardless, $\kappa = 1$ for an object that is at rest with respect to the canonical observer, and also in some cases where $V_{\pm} \neq 0$. In an ultra-relativistic limit where $V_{\pm} \rightarrow 1$ at fixed $\theta_{\pm} \neq 0$, $\kappa \rightarrow 0$. However, if $\theta_{\pm} = 0$, the limit $V_{\pm} \rightarrow 1$ instead results in $\kappa \rightarrow \infty$. Both $\kappa \rightarrow 0$ and $\kappa \rightarrow \infty$ are therefore ultra-relativistic limits, although it is only the former case that is generic. The

divergent latter case arises due to the breakdown of the parameterization (3.1) for null geodesics that propagate in the same direction as the gravitational wave.

For an arbitrary timelike or null geodesic, further calculations show that the remaining Brinkmann parameters are related to the inertial parameters via

$$v_{\pm} = \frac{\sqrt{2}Z_{\pm}}{1 - V_{\pm} \cos \theta_{\pm}}, \quad (3.19a)$$

$$x_{\pm}^i = X_{\pm}^i + \frac{Z_{\pm}V_{\pm}^i}{1 - V_{\pm} \cos \theta_{\pm}}, \quad (3.19b)$$

$$\dot{x}_{\pm}^i = \frac{\sqrt{2}V_{\pm}^i}{1 - V_{\pm} \cos \theta_{\pm}}, \quad (3.19c)$$

where $(X^I) = (X_{\pm}^1, X_{\pm}^2, Z_{\pm})$. The nontrivial nature of these expressions implies that the apparent simplicity of (at least transverse) scattering in terms of the Brinkmann parameters is lost when using inertial parameters. Nevertheless, these latter parameters remain useful due to their familiar interpretations.

1. Low-speed memory effects

The conversions between Brinkmann and inertial parameters simplify considerably at slow speeds relative to the canonical observer. Applying Eq. (3.19) for a timelike geodesic in which, say, $V_- = 0$,

$$x_-^i = x_-^i, \quad Z_- = \frac{1}{\sqrt{2}}v_- . \quad (3.20)$$

The projected v coordinate thus serves as a proxy for the longitudinal Cartesian coordinate z . Allowing for nonzero speeds which are nevertheless small, Eq. (3.18) reduces to

$$\kappa = 1 + 2V_{\pm} \cos \theta_{\pm} + \mathcal{O}(V_{\pm}^2). \quad (3.21)$$

This is conserved for every scattering process, so gravitational waves cannot affect the longitudinal speeds $V_{\pm} \cos \theta_{\pm}$ of slowly moving geodesics. Any effects on their velocities must be transverse to the gravitational wave.

However, it is not necessarily true that there are no longitudinal effects at all. Again setting $V_- = 0$ for simplicity, an expansion through first order in the curvature H_{ij} yields

$$\Delta Z = \frac{1}{2\sqrt{2}}M_{ij}^{\text{d}\rightarrow\text{v}}X_-^iX_-^j + \mathcal{O}(H^2), \quad (3.22)$$

where $\Delta Z \equiv Z_+ - Z_-$. Longitudinal displacements can therefore arise when $M_{ij}^{\text{d}\rightarrow\text{v}} \neq 0$. However, this effect is quadratic in the initial displacement, and is therefore negligible for sufficiently nearby geodesics. The transverse displacement

$$\Delta X_i = \left(M_{ij}^{\text{d}\rightarrow\text{d}} - \frac{1}{\sqrt{2}}Z_-M_{ij}^{\text{d}\rightarrow\text{v}} \right) X_-^j + \mathcal{O}(H^2), \quad (3.23)$$

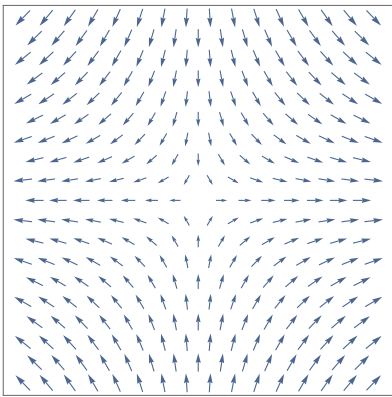


FIG. 5. Contribution to the displacement vector field ΔX^i from $M_{ij}^{d \rightarrow d}$ for initially stationary timelike geodesics, through first order in H_{ij} . Different points here correspond to different points in the plane which is transverse to the gravitational wave. The vertical and the horizontal axes here are aligned with the eigenvectors of $M_{ij}^{d \rightarrow d}$.

dominates for slowly moving geodesics that are sufficiently close to the canonical observer. It may also be shown that when the initial velocity vanishes, the transverse components of the final 3-velocity are

$$\Delta V_i = \frac{1}{\sqrt{2}} M_{ij}^{d \rightarrow v} X_-^j + \mathcal{O}(H^2). \quad (3.24)$$

These expressions are mostly complicated by the displacement-velocity memory $M_{ij}^{d \rightarrow v}$. If that memory vanishes through first order in the curvature, as it usually does when a gravitational wave is generated by a compact source, the only nontrivial effect which remains is the standard displacement memory

$$\Delta X_i = M_{ij}^{d \rightarrow d} X_-^j + \mathcal{O}(H^2). \quad (3.25)$$

This is plotted in Fig. 5.

2. Memory effects and null geodesics

Memory effects are considerably more complicated at high speeds. There is, e.g., no longer any sense in which longitudinal effects can be ignored. Nevertheless, there is relatively little discussion in the literature on gravitational-wave memory in this regime. What has been discussed—with varying degrees of generality—is the effect of memory on optical observables, including frequency shifts, astrometric deflections, changes in luminosity and angular-diameter distances, and multiple imaging [26, 27, 103, 104]. These observables, of course, involve the effects of a gravitational wave on an observer, a source(s), and the light which passes between them. What does not appear to be available is a direct description of what happens to individual null geodesics as seen by a single canonical observer. We now provide such a description.

First note that if a null geodesic is initially comoving with the gravitational wave, the wave does not affect it. For all other null geodesics, $\kappa = 0$, $V_\pm = 1$, and Eq. (3.19) implies that

$$\delta_{ij} \dot{x}_\pm^i \dot{x}_\pm^j = 2 \cot^2(\frac{1}{2}\theta_\pm). \quad (3.26)$$

The magnitudes of the \dot{x}_\pm^i therefore encode the longitudinal angles θ_\pm . This is also true for the magnitudes $\delta_{ij} V_\pm^i V_\pm^j = \sin^2 \theta_\pm$ of the transverse components of the 3-velocities V_\pm^I . From this perspective, it is useful to introduce the unit 2-vectors

$$n_\pm^i \equiv V_\pm^i \csc \theta_\pm, \quad (3.27)$$

which describe only the transverse direction of motion. Equations (2.40), (3.9), (3.10), (3.19) and (3.26) then imply that through first order in the curvature, the perturbation to the propagation direction of a null geodesic is described by

$$\Delta\theta = \left\{ M_{ij}^{d \rightarrow d} n_-^i n_-^j - \frac{1}{\sqrt{2}} M_{ij}^{d \rightarrow v} n_-^i [Z_- n_-^j + X_-^j \tan(\frac{1}{2}\theta_-)] \right\} \sin \theta_- + \mathcal{O}(H^2), \quad (3.28)$$

and

$$\Delta n^i = (n_-^i n_-^j - \delta^{ij}) \left\{ M_{jk}^{d \rightarrow d} n_-^k - \frac{1}{\sqrt{2}} M_{jk}^{d \rightarrow v} \times [Z_- n_-^k + X_-^k \tan(\frac{1}{2}\theta_-)] \right\} + \mathcal{O}(H^2). \quad (3.29)$$

Note that there is no sense in which $\Delta\theta$ is generically small compared to Δn^i . Therefore, gravitational wave memory affects both the longitudinal and the transverse properties of null geodesics. It is also apparent that null geodesics can exhibit memory effects which are independent of their initial projected displacements X_-^I .

If those displacements are small, or if $M_{ij}^{d \rightarrow v}$ is negligible at $\mathcal{O}(H)$, only $M_{ij}^{d \rightarrow d}$ can significantly affect the propagation directions. The longitudinal deflection $\Delta\theta$ is then maximized when n_-^i is an eigenvector of $M_{ij}^{d \rightarrow d}$. In that case, the transverse deflection Δn^i vanishes. If n_-^i instead lies midway between the two eigenvectors of $M_{ij}^{d \rightarrow d}$, it is the transverse deflection that is maximized and the longitudinal deflection which vanishes. More generally, $\Delta\theta$ and Δn^i can both be nonzero. The transverse velocity changes here are illustrated in Fig. 6. A full three-dimensional picture is provided in Fig. 7, where it is seen that an initially planar collection of null geodesic rays does not remain planar after it passes through a gravitational wave (even when displacements are ignored).

Although 3-velocities of null geodesics are easier to measure than displacements, the latter may be important as well. Similar calculations to the ones which led to Eqs. (3.28) and (3.29) [but which also use Eq. (3.16)] can be used to show that the projected longitudinal displacements of null geodesics are given by

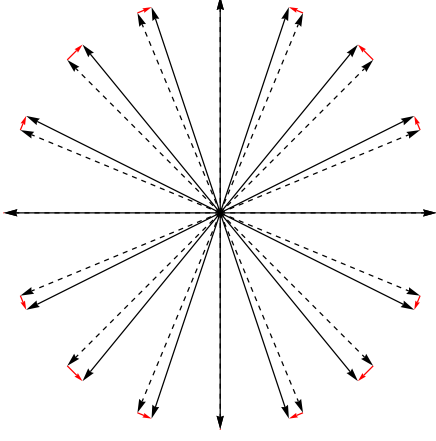


FIG. 6. Effect of the displacement-displacement memory on the transverse propagation of null geodesics. Arrows represent propagation directions in the 2-plane which appears, at fixed t , to be orthogonal to the propagation of the gravitational wave (according to the canonical observer). The horizontal and the vertical axes are aligned with the eigenvectors of $M_{ij}^{d \to d}$. Dashed arrows denote propagation directions before the gravitational wave arrives. Solid black arrows denote propagation directions after the wave has left. Red arrows denote shifts in the transverse velocities. Displacements of the null geodesics are not shown.

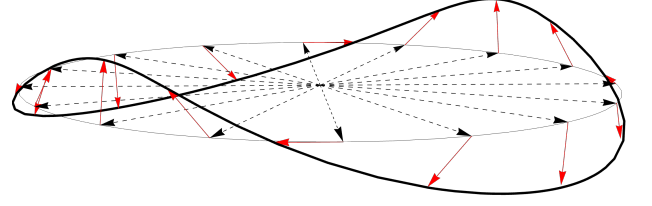


FIG. 7. Effect of the displacement-displacement memory on the propagation of null geodesics in three dimensions. The dashed arrows represent initial propagation directions for the null geodesics, all of which are assumed here to lie in the $\theta_- = \pi/2$ plane which is orthogonal to the gravitational wave. The thick black line is formed from the tips of all velocity vectors after the gravitational wave has passed. The red arrows show some particular shifts in the 3-velocities of various geodesics. Displacements are not shown. A top-down projection of this diagram is given in Fig. 6.

$$\Delta Z = \frac{1 + \cos \theta_-}{\sqrt{2}} \left\{ \left(M_{ij}^{v \to d} + \sqrt{2} Z_- M_{ij}^{d \to d} \right) n_-^i n_-^j + \frac{1}{2} M_{ij}^{d \to v} \left[X_-^i X_-^j \tan^2(\frac{1}{2} \theta_-) - Z_-^2 n_-^i n_-^j \right] \right\} + \mathcal{O}(H^2), \quad (3.30)$$

while their transverse counterparts are

$$\begin{aligned} \Delta X^i = & M_{ij}^{d \to d} X^j + \frac{1}{\sqrt{2}} \cot(\frac{1}{2} \theta_-) [2\delta^{ij} - (1 + \cos \theta_-) n_-^i n_-^j] \left(M_{jk}^{v \to d} + \sqrt{2} Z_- M_{jk}^{d \to d} - \frac{1}{2} Z_-^2 M_{jk}^{d \to v} \right) n_-^k \\ & - \frac{1}{2\sqrt{2}} [2Z_- \delta^{ij} + n_-^i X_-^j \sin \theta_-] M_{jk}^{d \to v} X_-^k + \mathcal{O}(H^2). \end{aligned} \quad (3.31)$$

The first term in ΔX^i clearly matches the displacement memory (3.25) that is associated with slowly moving time-like geodesics. However, there is much more in this null setting. The displacement-displacement memory not only maps initial transverse displacements to final transverse displacements; it also maps initial *longitudinal* displacements to final transverse *and* longitudinal displacements. Moreover, these latter effects depend on the direction in which the null geodesic is propagating. The effect of $M_{ij}^{d \to d}$ on the three-dimensional displacement field of a collection of initially comoving null geodesics is shown in Fig. 8.

Perhaps more interestingly, our results show that null geodesics can be used to measure the velocity-displacement memory $M_{ij}^{v \to d}$. That affects both ΔZ and ΔX^i , but not $\Delta \theta$ or Δn^i , nor any memory effects that are associated with slowly moving geodesics. Unlike the

effects due to $M_{ij}^{d \to d}$ or $M_{ij}^{d \to v}$, those of $M_{ij}^{v \to d}$ are independent of the initial displacement. If we consider a collection of initially parallel null geodesics, their final displacements will be shifted by a constant that depends on $M_{ij}^{v \to d}$, a linear transformation which depends on $M_{ij}^{d \to d}$, and a quadratic displacement which depends on $M_{ij}^{d \to v}$.

D. Memory effects and the world function

A somewhat different perspective on geodesic memory is provided by Synge's world function $\sigma(x, x')$, which returns one-half of the squared geodesic distance between

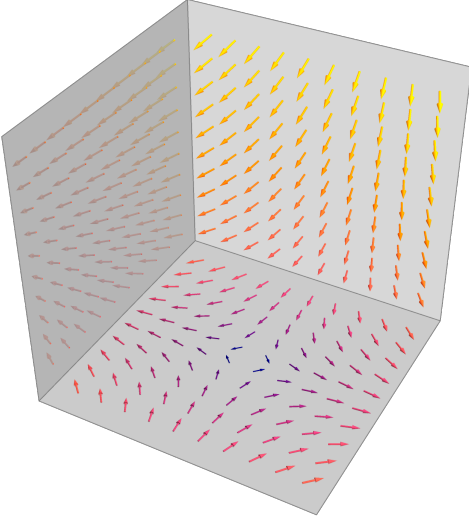


FIG. 8. Effect of the displacement-displacement memory on the displacements of initially comoving null geodesics. Each point here corresponds to a different initial projected position X_-^I for a null geodesic. The vectors at each point represent the displacements $\Delta X^I = X_+^I - X_-^I$. The bottom plane here is $Z_- = 0$, where a standard quadrupolar displacement can be observed; cf. Fig. 5. Projections of displacement vectors onto different $Z_- = \text{constant}$ planes result in similar quadrupolar patterns, but with different singular points. However, displacements are not purely transverse when $Z_- \neq 0$. Also note that this figure describes only the effects of $M_{ij}^{\text{d}\rightarrow\text{d}}$. The effect of $M_{ij}^{\text{v}\rightarrow\text{d}}$ would be to add a constant displacement at every point, while that of $M_{ij}^{\text{d}\rightarrow\text{v}}$ would be more complicated. Also note that we have chosen a particular θ_- and n_-^i for all displacements here; somewhat different patterns result for geodesics which propagate in different directions.

the spacetime points⁶ x and x' . From this biscalar, all properties of (timelike, null, and spacelike) geodesics can be extracted simply by differentiation [105]. The world function also plays a central role in the discussion of wave propagation in curved spacetimes [106], and we use it for this purpose in Section V below.

In terms of the Jacobi propagators A_{ij} and B_{ij} , the world function in any plane wave spacetime is known to be given by [74, 81]

$$\sigma = \frac{1}{2}(u - u') \left[-2(v - v') + \partial_u B_{ik} (B^{-1})^k{}_j x^i x^j + (B^{-1})_{ik} A^k{}_j x'^i x'^j - 2(B^{-1})_{ij} x'^i x^j \right], \quad (3.32)$$

where $(B^{-1})_{ij}$ denotes the matrix inverse of B_{ij} . This is exact and holds for all pairs of points that do not lie on conjugate hyperplanes (where B_{ij} is not invertible). If we

now assume that the gravitational wave is weakly curved, Eqs. (2.38) and (2.39) imply that

$$\sigma = \bar{\sigma} + \frac{1}{2(u - u')} \int_{u'}^u dw H_{ij}(w) \left[(w - u') x^i + (u - w) x'^i \right] \left[(w - u') x^j + (u - w) x'^j \right] + \mathcal{O}(H^2), \quad (3.33)$$

where

$$\bar{\sigma} \equiv -(u - u')(v - v') + \frac{1}{2} \delta_{ij} (x^i - x'^i)(x^j - x'^j) \quad (3.34)$$

is the world function in flat spacetime. In a weakly curved sandwich wave where u' lies in \mathcal{I}_- while u lies in \mathcal{I}_+ , Eq. (2.40) can now be used to write the perturbed world function in terms of the memory tensors:

$$\sigma = \bar{\sigma} + \frac{1}{2(u - u')} \left[M_{ij}^{\text{d}\rightarrow\text{v}} (u' x^i - u x'^i)(u' x^j - u x'^j) + 2M_{ij}^{\text{d}\rightarrow\text{d}} (x^i - x'^i)(u' x^j - u x'^j) - M_{ij}^{\text{v}\rightarrow\text{d}} (x^i - x'^i) \times (x^j - x'^j) \right] + \mathcal{O}(H^2). \quad (3.35)$$

One application of this expression is that it can be used to immediately see how proper times are affected by gravitational-wave memory: If two timelike-separated events are considered, the proper time along the geodesic that connects them is simply $\sqrt{-2\sigma}$. In general, all memory tensors can contribute to that time.

The perturbed world function can also be used to easily see how light-cones are deformed by gravitational wave memory. A future-pointing light-cone whose vertex lies at (u', v', x'^i) , before the gravitational wave has arrived, is given by the surface $\sigma = 0$, or equivalently by

$$v = v' + \frac{1}{2(u - u')^2} \left\{ [(u - u') \delta_{ij} - M_{ij}^{\text{v}\rightarrow\text{d}}] (x^i - x'^i) \times (x^j - x'^j) + M_{ij}^{\text{d}\rightarrow\text{v}} (u' x^i - u x'^i)(u' x^j - u x'^j) + 2M_{ij}^{\text{d}\rightarrow\text{d}} (x^i - x'^i)(u' x^j - u x'^j) \right\} + \mathcal{O}(H^2) \quad (3.36)$$

after the wave has left. To better interpret this, use the inertial coordinates in Eq. (2.11) and suppose that the light cones emanate from the canonical observer at $x'^i = z' = 0$. Then,

$$(t - t')^2 = \left[\delta_{ij} + \frac{\sqrt{2}}{t - t' - z} \left(2t'^2 M_{ij}^{\text{d}\rightarrow\text{v}} + \sqrt{2} t' M_{ij}^{\text{d}\rightarrow\text{d}} - M_{ij}^{\text{v}\rightarrow\text{d}} \right) \right] x^i x^j + z^2 + \mathcal{O}(H^2). \quad (3.37)$$

For light emitted long ago, the effect of $M_{ij}^{\text{d}\rightarrow\text{v}}$ dominates over that of $M_{ij}^{\text{d}\rightarrow\text{d}}$ (when the former tensor is nonzero), and the effect of $M_{ij}^{\text{d}\rightarrow\text{d}}$ dominates over that of $M_{ij}^{\text{v}\rightarrow\text{d}}$.

⁶ Here, we use x and x' to denote events in spacetime rather than individual coordinates. When doing so below, the distinction should be clear from context.

It also follows that light cones projected onto a transverse plane with constant t and z are necessarily elliptical. More precisely, the eccentricity of each ellipse is $2\sqrt{\Lambda}$, where Λ denotes the positive eigenvalue of

$$\frac{1}{t - t' - z} (2t'^2 M_{ij}^{d \rightarrow v} + \sqrt{2} t' M_{ij}^{d \rightarrow d} - M_{ij}^{v \rightarrow d}). \quad (3.38)$$

At fixed t and z , this eigenvalue generically depends on t' , meaning that the cross-sections of the observer's forward light-cones can have varying eccentricities. These cross-sections can also be rotated with respect to one another, as the (generically t' -dependent) eigenvector which is associated with Λ provides the minor axis of the ellipse. These nontrivial eccentricities and the orientations of the associated cross-sections are consequences of gravitational wave memory. Eq. (3.37) can also be used to determine how light cones are projected into, e.g., planes with constant t and y . However, the shapes of those projections are more complicated.

IV. NON-GEODESIC MOTION, SPIN, AND MEMORY

The geodesic scattering described in the previous section can, in general, only approximate the scattering of an actual extended object. Trajectories can accelerate due to an object's angular momentum, as well as from the quadrupole and higher-order multipole moments of its stress-energy tensor [83]. We now discuss how angular momentum interacts with gravitational wave memory, focusing on the scattering of massless objects. Physically, this corresponds to considering the trajectories of, e.g., electromagnetic wave packets one order beyond geometric optics.

We begin in Section IV A by reviewing the spin Hall equations, which describe the linear-in-spin corrections to the trajectories of massless particles. Next, Section IV B discusses conservation laws for the spin Hall equations, showing that every conformal Killing vector is associated with a conserved quantity. This result is true not only in plane wave spacetimes, but in any spacetime which admits a conformal Killing vector field. Finally, Section IV C applies these results in sandwich wave spacetimes to describe how gravitational wave memory scatters massless wave packets with angular momentum.

A. Review of the spin Hall equations

If angular momentum and other extended-body characteristics are ignored, there are various senses in which the “center” of a high-frequency electromagnetic wave packet moves along a null geodesic. However, wave packets can exhibit significant angular momentum one order beyond geometric optics. To understand the effect of an angular momentum $S^{\alpha\beta} = S^{[\alpha\beta]}(\tau)$, we first define the centroid $x^\alpha(\tau)$ of an extended wave packet by

choosing a timelike vector field t^α and then imposing the Corinaldesi–Papapetrou spin supplementary condition [53, 107, 108]

$$S_{\alpha\beta} t^\beta = 0. \quad (4.1)$$

If $S^{\alpha\beta}$ is purely longitudinal⁷, its first nontrivial contribution to the motion of such a centroid may then be shown to be described by the spin Hall equations [52, 53, 55]

$$\frac{dx^\mu}{d\tau} \nabla_\mu p_\alpha = -\frac{1}{2} R_{\alpha\beta\gamma\delta} \frac{dx^\beta}{d\tau} S^{\gamma\delta}, \quad (4.2a)$$

$$\frac{dx^\alpha}{d\tau} = p^\alpha + \frac{1}{p \cdot t} S^{\alpha\beta} p^\gamma \nabla_\gamma t_\beta, \quad (4.2b)$$

$$S^{\alpha\beta} = \left(\frac{\epsilon s}{p \cdot t} \right) \varepsilon^{\alpha\beta\gamma\delta} p_\gamma t_\delta, \quad (4.2c)$$

where p_α denotes the wave packet's linear momentum, which is null⁸, τ is a dimensionless parameter along the worldline, ϵ and s are constant parameters, and $\varepsilon^{\alpha\beta\gamma\delta}$ denotes the Levi-Civita tensor. The spin Hall equations are intended to hold up to terms of order ϵ^2 , where the small parameter ϵ relates the (large) dominant frequency of a wave packet to its momentum: If U^α denotes the 4-velocity of an observer, the angular frequency seen by that observer is $\omega = (-p \cdot U)/\epsilon$. The parameter s instead provides a dimensionless magnitude for the angular momentum, in the sense that

$$S^{\alpha\beta} S_{\alpha\beta} = 2(\epsilon s)^2. \quad (4.3)$$

For some electromagnetic wave packets, circular polarization results in $s = \pm 1$, depending on the handedness of the polarization state. However, there are other electromagnetic wave packets for which $|s|$ can be much larger than 1. In optics, these are termed wave packets or beams that carry intrinsic orbital angular momentum [112, 113].

The spin Hall equations can be used to describe wave packets composed not only of electromagnetic fields [53, 55–59], but also of linearized gravitational fields [60–64], massless Dirac fields [65], or even scalar fields (which can

⁷ Here, $S^{\alpha\beta}$ is said to be “longitudinal” if it is orthogonal to the linear momentum p_β . The angular momentum tensor is then dual to a vector which is proportional to p^α . In other contexts, $S^{\alpha\beta} p_\beta = 0$ would typically be interpreted as an implicit definition for the centroid of an object, and would then be referred to as the Tulczyjew–Dixon spin supplementary condition [108]. However, this spin supplementary condition does not define a unique worldline when the momentum is null; cf. [53] and [109, p. 70]. The vanishing of $S^{\alpha\beta} p_\beta$ here is instead interpreted as a physical restriction on the nature of the angular momentum. Wave packets with non-longitudinal angular momentum are possible [53], with examples sometimes described as spatiotemporal vortex beams [110, 111]. Regardless, we focus only on the longitudinal case.

⁸ More precisely, $p_\alpha p^\alpha = \mathcal{O}(\epsilon^2)$. It is not possible for any wave packet with a nonzero angular momentum to have an *exactly* null linear momentum [53].

carry orbital angular momentum). For these different cases, the spin Hall equations might differ only in the parameter s that determines the magnitude of the angular momentum tensor.

It may also be noted that the spin Hall equations are a special case of the Mathisson–Papapetrou equations [together with the Corinaldesi–Papapetrou spin supplementary condition (4.1)], which have long been known to describe the motion of spinning objects in curved spacetimes [53]. However, specializing to the case of a nearly massless wave packet with longitudinal angular momentum allows the usual evolution equation for the angular momentum to be solved explicitly, yielding Eq. (4.2c). Therefore, all that remains is an evolution equation (4.2a) for the linear momentum and a momentum-velocity relation (4.2b) which relates p^α to $dx^\alpha/d\tau$.

To offer some intuition for these frequency- and angular momentum-dependent effects, some examples of spin Hall rays propagating through a sandwich wave spacetime are presented in Figs. 9 and 10. These are obtained by numerically integrating Eq. (4.2), although the same trajectories can also be obtained using the analytical results derived below in Eqs. (4.16) and (4.17). Regardless, it is clear that memory effects depend, in general, on an object’s angular momentum.

B. Conservation laws and the spin Hall equations

It is well known in the context of the Mathisson–Papapetrou equations that if ξ^α is a Killing vector field, the generalized momentum [54, 85]

$$\mathcal{P}_\xi \equiv p_\alpha \xi^\alpha + \frac{1}{2} S^{\alpha\beta} \nabla_\alpha \xi_\beta \quad (4.4)$$

must be conserved. It was already noted in Ref. [53] that since the spin Hall equations are a special case of the Mathisson–Papapetrou equations, these conservation laws continue to hold. However, we now establish a more general result for the spin Hall equations: Eq. (4.4) is conserved not only for ordinary Killing vectors, but for all *conformal* Killing vectors. We require only that

$$\mathcal{L}_\xi g_{\alpha\beta} = 2\Upsilon g_{\alpha\beta} \quad (4.5)$$

for some scalar field Υ . The ordinary Killing case is recovered if $\Upsilon = 0$.

To motivate why this might be so, note that the generalized momentum is given by

$$\mathcal{P}_\xi(\tau) = \int_{\Sigma_\tau} dS_\alpha T^\alpha{}_\beta \xi^\beta, \quad (4.6)$$

where ξ^α is now a *generalized* Killing field [85] and $T^{\alpha\beta}$ is the stress-energy tensor of the object—here an electromagnetic wave packet. The hypersurfaces Σ_τ are assumed to foliate the worldtube of the object. Using the stress-energy conservation, it follows that

$$\frac{d}{d\tau} \mathcal{P}_\xi(\tau) = \frac{1}{2} \int_{\Sigma_\tau} dS_\gamma \tau^\gamma T^{\alpha\beta} \mathcal{L}_\xi g_{\alpha\beta}, \quad (4.7)$$

where τ^γ is a time evolution vector field for the foliation. This clearly vanishes in the Killing case. However, $T^\alpha{}_\alpha = 0$ for any electromagnetic field, and in that case, \mathcal{P}_ξ is constant whenever ξ^α is conformally Killing.

This motivates our result, but does not prove it. First, the spin Hall equations can be applied to, e.g., scalar wave packets, which are not necessarily trace-free. Second, although ordinary Killing fields are also generalized Killing fields, the same cannot be said of proper conformal Killing fields. Third, there are a number of approximations inherent in the spin Hall equations, and we have not made any of these precise. Instead of doing so, we shall establish by direct calculation that given any conformal Killing field, the spin Hall equations imply that \mathcal{P}_ξ is indeed conserved, at least through first order in ϵ .

From Eq. (4.2a) and from $DS^{\alpha\beta}/d\tau = 2p^{[\alpha} dx^{\beta]}/d\tau$, which is one of the Mathisson–Papapetrou equations, direct differentiation of Eq. (4.4) results in

$$\frac{d\mathcal{P}_\xi}{d\tau} = \frac{1}{2} \frac{dx^\beta}{d\tau} [p^\alpha \mathcal{L}_\xi g_{\alpha\beta} + S^{\alpha\gamma} (\nabla_\beta \nabla_\alpha \xi_\gamma + R_{\alpha\gamma\beta\delta} \xi^\delta)]. \quad (4.8)$$

This holds for any vector field ξ^α . However, if that vector field is conformally Killing [33, Eq. (11.4b)],

$$\nabla_\gamma \nabla_\alpha \xi_\beta = R_{\beta\alpha\gamma\delta} \xi^\delta + g_{\alpha\beta} \nabla_\gamma \Upsilon - 2g_{\gamma[\alpha} \nabla_{\beta]} \Upsilon. \quad (4.9)$$

Using this results in

$$\frac{d\mathcal{P}_\xi}{d\tau} = (\Upsilon p_\alpha - S_\alpha{}^\beta \nabla_\beta \Upsilon) \frac{dx^\alpha}{d\tau}. \quad (4.10)$$

The null character of p_α , together with Eqs. (4.2b) and (4.2c), show that both terms on the right-hand side of this equation are individually $\mathcal{O}(\epsilon^2)$. It follows that for each conformal Killing field ξ^α ,

$$\mathcal{P}_\xi = p_\alpha \left[\xi^\alpha + \left(\frac{\epsilon s}{2p \cdot t} \right) \epsilon^{\alpha\beta\gamma\delta} t_\beta \nabla_\gamma \xi_\delta \right] \quad (4.11)$$

is conserved through first order in ϵ . This is true not only in plane wave spacetimes, but in any spacetime which admits a conformal Killing vector.

However, in the plane wave spacetimes of interest here, there are at least five Killing vector fields. There is also the homothety (2.14), which is a special type of conformal Killing vector in which $\Upsilon = 1$. The spin Hall equations therefore admit at least six conservation laws in plane wave spacetimes.

C. Massless spinning particles in plane wave spacetimes

We may now apply the aforementioned conservation laws to solve the spin Hall equations in plane wave spacetimes. Before doing so, it is first necessary to choose a timelike vector field t^α with which to define the centroid. One simple possibility is to set

$$t_\alpha = -\nabla_\alpha t = -\frac{1}{\sqrt{2}} \nabla_\alpha (u + v) \quad (4.12)$$

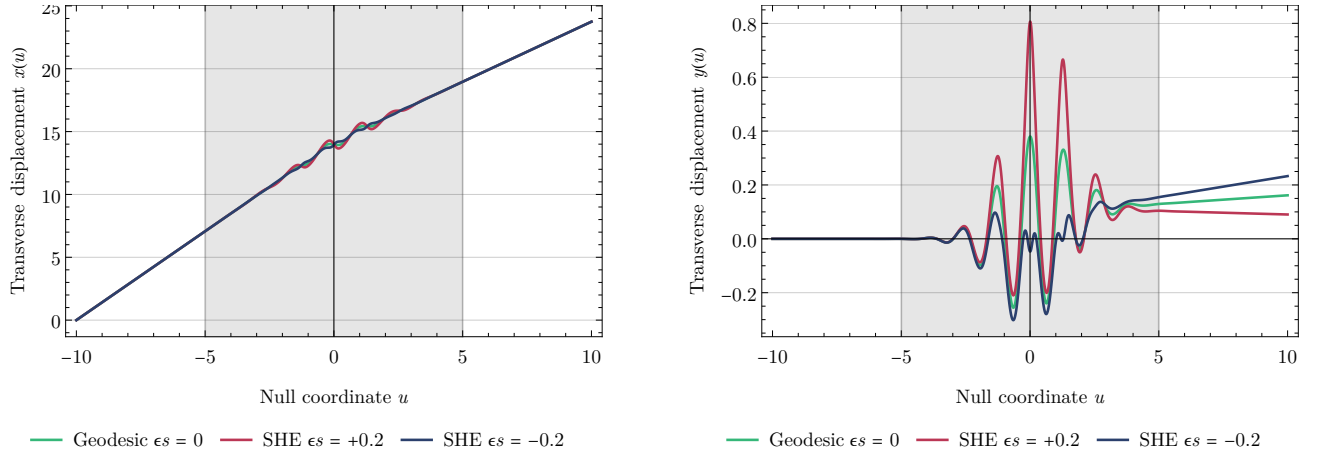


FIG. 9. Transverse motion of massless spinning particles in a gravitational sandwich wave. Three particles are considered with the same initial conditions, one with vanishing angular momentum (which is a geodesic), and two with opposite and nonzero angular momenta. The trajectories of these particles coincide on \mathcal{I}_- , but not in \mathcal{I}_C or \mathcal{I}_+ . More specifically, the final velocities of these particles are seen to depend on ϵ_s , illustrating that memory effects can depend on angular momentum. The gravitational waveform and other conventions here are the same as in Fig. 2; indeed, the $\epsilon_s = 0$ curves here are identical to the curves in that figure. Centroids of the underlying wave packets are defined here by assuming that the t^α in Eq. (4.1) is given by $-\nabla_\alpha t$.

at least in the flat regions \mathcal{I}_\pm , where it reduces to the 4-velocity of the canonical observer at $x = y = z = 0$.

The simplest Killing vector in a plane wave spacetime is $\ell_\alpha = -\nabla_\alpha u$, and since this is covariantly constant,

$$E \equiv -\mathcal{P}_\ell = -p_v = \text{constant}. \quad (4.13)$$

In exceptional cases where $E = 0$, both the momentum and the velocity of the wave packet remain parallel to ℓ^α . Wave packets that are traveling in the same direction as the background gravitational wave are therefore unaffected either by that wave or by their own angular momentum. The cases in which $E \neq 0$ are more interesting, and we focus on them in the following.

If ξ^α is used to denote one of the Killing fields with the form given in Eq. (2.8), a calculation shows that

$$\nabla_\alpha \xi_\beta = 2\dot{\Xi}_i \ell_{[\beta} \nabla_{\alpha]} x^i. \quad (4.14)$$

Substituting this and Eq. (4.12) into Eq. (4.11), we obtain

$$p_i \left[\Xi^i - \left(\frac{\epsilon_s \epsilon^{ij}}{\sqrt{2} p \cdot t} \right) \dot{\Xi}_j \right] - E \dot{\Xi}_i x^i = \text{constant}, \quad (4.15)$$

where $\epsilon^{ij} = \epsilon^{uvij}$ is a two-dimensional permutation symbol. Varying over all possible Ξ^i , this encodes four conservation laws. Using Eqs. (2.17), (2.22) and (2.25) to evaluate these laws at u and at u' shows that

$$p_i = p'^j \partial_u B_{ij} + E \left[x'^j + \frac{\epsilon_s}{\sqrt{2} E} \left(\frac{p'_k \epsilon^{kj}}{p' \cdot t'} \right) \right] \partial_u A_{ij}, \quad (4.16)$$

and

$$x_i = A_{ij} x'^j + \frac{B_{ij} p'^j}{E} + \frac{\epsilon_s \epsilon^{jk}}{\sqrt{2} E} \left(\frac{\delta_{ij} p_k}{p \cdot t} - \frac{A_{ij} p'_k}{p' \cdot t'} \right), \quad (4.17)$$

where all instances of the Jacobi propagators are evaluated at (u, u') . As in the geodesic case, the final position and the final momentum therefore depend on the initial position and the initial momentum only via the Jacobi propagators A_{ij} and B_{ij} .

In the trivial case where u and u' both lie in one of the flat regions \mathcal{I}_- or \mathcal{I}_+ , so there is no curvature between the initial and the final states, it follows from Eqs. (4.16) and (4.17) that

$$x^i = x'^i + \frac{1}{E} (u - u') p'^i, \quad p_i = p'_i. \quad (4.18)$$

The transverse velocity

$$\dot{x}^i = dx^i/du = p^i/E \quad (4.19)$$

is therefore constant and the spin is irrelevant; wave packets follow null geodesics in flat regions. However, the initial and the final geodesics may appear to be “different” due to the presence of the intervening gravitational wave.

This can be understood by assuming that u lies in \mathcal{I}_+ while u' lies in \mathcal{I}_- . Doing so, we can effectively correct the scattering matrix (3.10) which was derived above for geodesic motion. Using the projected spatial positions x_\pm^i which were defined by Eq. (3.8), it follows from Eqs. (2.30), (2.31) and (4.16) that the momentum after the wave has left is

$$p_i^+ = \left[\delta_{ij} + M_{ij}^{v \rightarrow v} + \frac{\epsilon_s}{E} \sin^2(\frac{1}{2}\theta_-) M_{ik}^{d \rightarrow v} \epsilon^k{}_j \right] p_-^j + E M_{ij}^{d \rightarrow v} x_-^j \quad (4.20)$$

where $\theta_- = 2 \arctan([2E^2/\delta_{ij} p_-^i p_-^j]^{1/2})$ again denotes the initial angle between the wave packet and the gravitational wave, as seen by the canonical observer at the origin [cf.

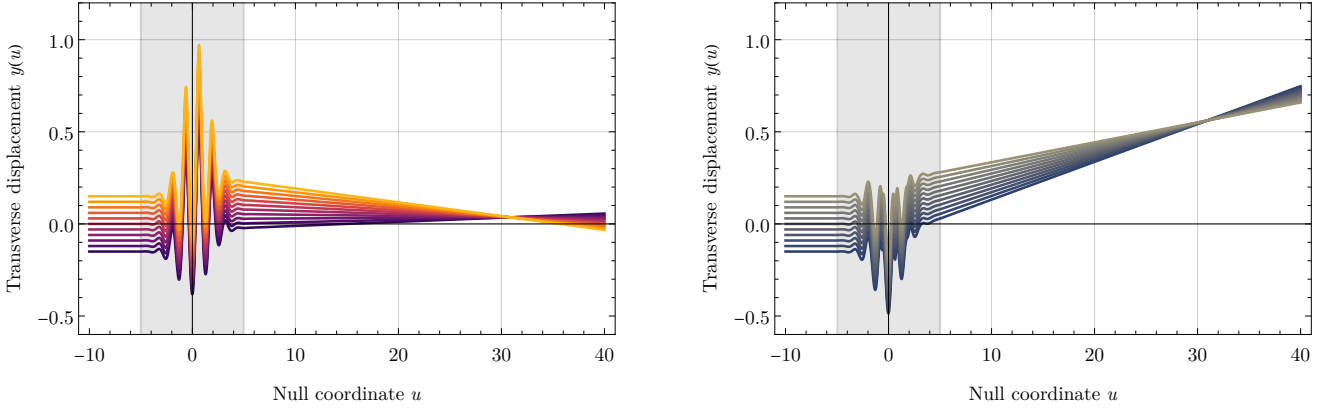


FIG. 10. Bundles of initially parallel massless spinning particles in a gravitational sandwich wave. The left and the right panels here illustrate cases in which $\epsilon_s = +0.2$ and $\epsilon_s = -0.2$, respectively. Angular momentum is thus seen to affect where a bundle is focused. This figure is analogous to Fig. 3 in the geodesic case. The gravitational waveform and other conventions here are the same as in Fig. 2.

Eq. (3.26)]. It follows that $M_{ij}^{d \rightarrow v}$ is the only memory tensor that can produce spin-dependent corrections to the transverse momentum. It may also be noted that since θ_- depends on p_i^- , nonzero spin results in a nonlinear mapping from the initial state (x_-^i, p_-^i) to the final state (x_+^i, p_+^i) .

Applying a similar calculation to Eq. (4.17), the projected transverse position of a potentially spinning wave packet is given by

$$x_+^i = (\delta_{ij} + M_{ij}^{d \rightarrow d})x_-^j + \frac{1}{E}M_{ij}^{v \rightarrow d}p_-^j + \frac{\epsilon_s \epsilon^{jk}}{E^2} \times \{(\delta_{ij} + M_{ij}^{d \rightarrow d})p_k^- \sin^2(\frac{1}{2}\theta_-) - \delta_{ij}[(\delta_{kl} + M_{kl}^{v \rightarrow v})p_-^l + EM_{kl}^{d \rightarrow v}x_-^l] \sin^2(\frac{1}{2}\theta_+)\}. \quad (4.21)$$

Angular momentum therefore affects x_+^i via all memory tensors except $M_{ij}^{v \rightarrow d}$ (although $M_{ij}^{v \rightarrow d}$ does affect the spin-independent contribution to the projected position). Finally, we can write

$$\begin{pmatrix} x_+^i \\ \dot{x}_+^i \end{pmatrix} = \left(\mathcal{S} + \frac{\epsilon_s}{E} \mathcal{S}_1 \right) \begin{pmatrix} x_-^j \\ \dot{x}_-^j \end{pmatrix}, \quad (4.22)$$

where \mathcal{S} is given by Eq. (3.10) and the spin-dependent corrections to the scattering matrix can be written as

$$\mathcal{S}_1 = \begin{pmatrix} \sin^2(\frac{1}{2}\theta_+) \epsilon^{ik} M_{kj}^{d \rightarrow v} & \sin^2(\frac{1}{2}\theta_-) \epsilon^{kj} (\delta_{ik} + M_{ik}^{d \rightarrow d}) - \sin^2(\frac{1}{2}\theta_+) \epsilon^{ik} (\delta_{kj} + M_{kj}^{v \rightarrow v}) \\ 0 & \sin^2(\frac{1}{2}\theta_-) \epsilon_{kj} M_{ik}^{d \rightarrow v} \end{pmatrix}. \quad (4.23)$$

Note, however, that despite the matrix form of Eq. (4.22), the map from initial states to final states is not linear when $\epsilon \neq 0$; the corrected scattering matrix \mathcal{S}_1 depends not only on the geometry, but also on the particle's state.

Regardless, Eqs. (4.20) and (4.21) fully determine the transverse scattering of a spinning wave packet through first order in ϵ . Furthermore, the full 4-momentum p_α^\pm can be determined from its transverse components p_α^i and from the null constraint $p_\alpha^\pm p_\pm^\alpha = 0$. This is not, however, sufficient to determine what happens to the v component of a wave packet's projected position. That follows from the conservation law associated with the homothety λ^α . Using Eqs. (2.14) and (4.11), as well as $S^{\alpha\beta} \nabla_\alpha \lambda_\beta = 0$, its associated conservation law is

$$\mathcal{P}_\lambda = x^i p_i - 2vE = \text{constant}. \quad (4.24)$$

It follows that the projected coordinates v_\pm are still related by the geodesic expression (3.16). *Full* solutions to the spin Hall equations can thus be determined entirely in terms of their transverse components. Moreover, the memory tensors involved in the solution of the spin Hall equations are exactly the same as the ones that are relevant already for geodesics. In this sense, experiments involving the effects of a gravitational wave on light with angular momentum cannot provide more information about the gravitational wave than experiments without angular momentum.

V. MEMORY EFFECTS AND WAVE PROPAGATION IN PLANE WAVE SPACETIMES

So far, we have discussed the scattering of geodesics, and of massless spinning particles as approximate models for wave packets with angular momentum. Now we remove the “particle” idealization and consider the scattering of test fields by gravitational sandwich waves. For simplicity, we focus on massless scalar fields and compare, where appropriate, with results in the previous sections. Although we shall not do so here, various spin-raising procedures can be applied to our scalar results to understand the behaviors of electromagnetic and other higher-spin fields [51, 68–71].

Our first result, in Section V A, is a general Kirchhoff-type integral formula for scalar fields on plane wave backgrounds. This describes a field in terms of initial data on a given null hypersurface. It is exact and is nontrivially related to a certain representation formula originally due to Ward [72]. We use our integral formula in Section V B to show that in a weak field approximation, any solution to the wave equation in flat spacetime can be used to find a solution in a plane wave spacetime. More precisely, scattered fields can be found simply by differentiating “unscattered” fields in flat spacetime.

Sections V C and V D both investigate the scattering of particular types of scalar waves on plane wave backgrounds. We first consider scalar waves which are initially planar, both exactly and in a weak field approximation. In the latter context, scattered plane waves remain planar whenever $M_{ij}^{d \rightarrow v} = \mathcal{O}(H^2)$, and in those cases, most interesting features can be understood from the scattering of null geodesics. We also consider the weak-field scattering of certain localized solutions which are constructed from counter-propagating Hermite–Gauss and Laguerre–Gauss beams. In these cases, we find that gravitational waves excite a finite number of scalar side modes.

Lastly, Section V E compares the exact dynamics of high frequency scalar wave packets which carry angular momentum with the dynamics predicted by the spin Hall equations. This is done by numerically evaluating an appropriate Kirchhoff integral.

A. A Kirchhoff-like integral for massless scalar fields

In the absence of sources, it can be convenient to propagate fields forward in time using a Kirchhoff-like integral. For a massless scalar field ψ that satisfies $\nabla^\alpha \nabla_\alpha \psi = 0$, as well as a Green function $G(x, x')$ that satisfies

$$\nabla^\alpha \nabla_\alpha G(x, x') = -4\pi \delta(x, x'), \quad (5.1)$$

first define the current

$$J^{\alpha'}(x', x) \equiv \psi(x') \nabla^{\alpha'} G(x', x) - G(x', x) \nabla^{\alpha'} \psi(x'). \quad (5.2)$$

Integrating $\nabla_{\alpha'} J^{\alpha'} = -4\pi \psi(x) \delta(x, x')$ throughout a 4-volume that includes the point x and that has the bound-

ary Σ ,

$$\psi(x) = -\frac{1}{4\pi} \oint_{\Sigma} J^{\alpha'}(x', x) dS_{\alpha'}. \quad (5.3)$$

This expresses ψ in terms of its boundary values on Σ . By appropriately choosing Σ and G , the integral here can sometimes be reduced to one which involves only a single spacelike hypersurface in the past of the point x [106]. Physically, such a result expresses a field in terms of initial data on a spacelike hypersurface, and is referred to as a Kirchhoff integral.

Unfortunately, such a representation is not globally possible in plane wave spacetimes. This is because the focusing associated with the conjugate hyperplanes mentioned in Section III A implies that plane wave spacetimes do not admit Cauchy surfaces; they are not globally hyperbolic [36, 74]. Separately, it can also be inconvenient to use large spacelike initial-data surfaces, as these cannot be placed entirely before a gravitational wave arrives.

We can work around these problems by i) restricting to regions with no conjugate hyperplanes, and ii) allowing for “incomplete” initial data which is compatible with more than one field. In particular, we now identify Σ with the null hypersurface⁹ $u' = \text{constant}$, and specify initial data only on that hypersurface. Then, if $G(x', x)$ denotes an advanced Green function which vanishes whenever x' is in the future of x , one solution to the massless scalar wave equation may be written as

$$\psi(x) = \frac{1}{4\pi} \int_{\Sigma} J^{\alpha'}(x', x) dS_{\alpha'}. \quad (5.4)$$

This expresses the field in terms of initial data on the null hypersurface Σ . Unlike with an ordinary Kirchhoff integral, this does not produce the only field which is compatible with the given initial data: One may add to ψ , e.g., any function which depends only on u and which vanishes in a neighborhood of Σ . Physically, these extra solutions correspond to scalar waves which are co-propagating with the background gravitational wave. Regardless, *one* solution to the scalar wave equation is given by Eq. (5.4), and we can examine its properties.

Assuming that x is sufficiently close to the $u' = \text{constant}$ hypersurface that there are no intervening conjugate hyperplanes¹⁰, the advanced Green function may be shown to have the form [74, 114]

$$G(x', x) = \sqrt{\Delta(x, x')} \delta(\sigma(x, x')) \Theta(x' < x), \quad (5.5)$$

⁹ Unlike in Eq. (5.3), this Σ is not the boundary of a 4-volume. Eq. (5.4) nevertheless follows by assuming that a sufficiently large portion of the $u' = \text{constant}$ hypersurface is part of such a boundary, and also that $\psi(x') = \nabla_{\alpha'} \psi(x') = 0$ on remaining parts of that boundary which lie in the support of $G(\cdot, x)$.

¹⁰ This means that if u denotes the phase coordinate of the event x , $\det B_{ij}(u'', u') \neq 0$ for all $u'' \in (u', u]$. Although they are not needed here, Green functions in the presence of intervening conjugate hyperplanes may be found in [74].

where $\sigma(x, x')$ is the world function described in Section III D,

$$\Delta(u, u') = \frac{(u - u')^2}{\det B_{ij}(u, u')} \quad (5.6)$$

denotes the van Vleck determinant [106], and $\Theta(x' < x)$ is a Heaviside-type distribution which is equal to one if x' is in the past of x and which vanishes otherwise. The van Vleck determinant reduces to unity in the coincidence limit $u' \rightarrow u$. It would instead diverge if u and u' are conjugate in the sense of Eq. (3.5), although such cases are not relevant here. In a weak-field vacuum limit, $\Delta = 1 + \mathcal{O}(H^2)$.

Now consider a sandwich wave and suppose that u' lies in \mathcal{I}_- so all initial data is specified in the flat region before the gravitational wave arrives. Then, since Δ depends only on u and u' , Eqs. (3.32), (5.4), and (5.5) imply that when $u > u'$,

$$\psi(u, v, x^i) = \frac{\Delta^{1/2}(u, u')}{2\pi(u - u')} \int d^2x' \partial_{v'} \psi(u', v_{\text{ret}}, x'^j), \quad (5.7)$$

where $v_{\text{ret}} = v_{\text{ret}}(v, u, u', x^i, x'^j)$ denotes the value of v' which corresponds to the retarded event on Σ with given x'^j . It is found by solving

$$\sigma(u, v, x^i; u', v_{\text{ret}}, x'^j) = 0, \quad (5.8)$$

which results in

$$v_{\text{ret}} = v - \frac{1}{2} [(\partial_u B B^{-1})_{ij} x^i x^j + (B^{-1} A)_{ij} x'^i x'^j - 2(B^{-1})_{ij} x'^i x^j]. \quad (5.9)$$

Substituting this into Eq. (5.7) gives an exact expression for a scalar field in terms of initial data on Σ . A direct calculation can be used to verify that Eq. (5.7) is indeed a solution. We show in Appendix C that although it is not obvious, this integral representation is related to one which was previously obtained by Ward [72]. However, it differs from other specializations of Ward's result which have been used in, e.g., [51, 115, 116].

One physical consequence of Eq. (5.7) is that scalar waves which are scattered in plane wave spacetimes depend on the spacetime geometry only via the Jacobi propagators $A_{ij}(u, u')$ and $B_{ij}(u, u')$. In a sandwich wave context where $u' \in \mathcal{I}_-$ and $u \in \mathcal{I}_+$, all nontrivial effects can thus be described in terms of the same memory tensors which arose in our study of scattered geodesics. No new information about a gravitational wave can be learned by measuring memory effects in wave optics rather than geometric optics.

B. Fields in plane wave spacetimes from fields in flat spacetime

Assuming that a gravitational wave is weak, we may now apply the integral representation Eq. (5.7) perturbatively in the gravitational waveform H_{ij} . Doing so

allows us to generate (scattered) scalar fields in plane wave spacetimes simply by applying an appropriate differential operator to (unscattered) scalar fields in flat spacetime. The form of this operator will illustrate how each memory tensor contributes to scattering.

When the spacetime curvature is weak, its only non-trivial effect on the ψ in Eq. (5.7) is via the v_{ret} given by Eq. (5.9). Furthermore, use of Eq. (3.33) shows that if $v_{\text{ret}} = \bar{v}_{\text{ret}} + v_{\text{ret}}^{(1)} + \mathcal{O}(H^2)$, the flat-spacetime limit of v_{ret} is

$$\bar{v}_{\text{ret}} = v - \frac{\delta_{ij}(x^i - x'^i)(x^j - x'^j)}{2(u - u')}, \quad (5.10)$$

while its first-order correction is

$$v_{\text{ret}}^{(1)} = -\frac{1}{2(u - u')^2} \int_{u'}^u dw H_{ij}(w) [(w - u')x^i + (u - w)x'^i] [(w - u')x^j + (u - w)x'^j]. \quad (5.11)$$

Assuming that $v_{\text{ret}}^{(1)}$ remains sufficiently small, it follows from Eq. (5.7) that

$$\psi = \bar{\psi} + \frac{1}{2\pi(u - u')} \int d^2x' v_{\text{ret}}^{(1)} \partial_{v'}^2 \psi(u', \bar{v}_{\text{ret}}, x'^j) + \mathcal{O}(H^2), \quad (5.12)$$

where

$$\bar{\psi} \equiv \frac{1}{2\pi(u - u')} \int d^2x' \partial_{v'} \psi(u', \bar{v}_{\text{ret}}, x'^j) \quad (5.13)$$

denotes a flat-spacetime field which agrees with ψ on the $u' = \text{constant}$ hypersurface Σ . The perturbation to the field due to a gravitational wave can therefore be written as an integral involving $v_{\text{ret}}^{(1)}$. However, since Eq. (5.11) shows that $v_{\text{ret}}^{(1)}$ is quadratic in x'^i , the perturbed field is really a linear combination of the zeroth, the first, and the second ‘‘transverse moments’’ of $\partial_{v'}^2 \psi$ on Σ .

Interestingly, these moments can largely be computed simply by differentiating (rather than integrating) the background field $\bar{\psi}$. Using Eqs. (5.10) and (5.13), the zeroth and the first transverse moments of $\partial_{v'}^2 \psi$ are

$$\int d^2x' \partial_{v'}^2 \psi = 2\pi(u - u') \partial_v \bar{\psi}, \quad (5.14)$$

$$\int d^2x' x'_i \partial_{v'}^2 \psi = 2\pi(u - u') [x_i \partial_v \bar{\psi} + (u - u') \partial_i \bar{\psi}]. \quad (5.15)$$

Although the second moment of the second derivative $\partial_{v'}^2 \psi$ cannot be written quite so simply, the second moment of the *third* derivative $\partial_{v'}^3 \psi$ can be shown to be given by

$$\begin{aligned} \int d^2x' x'_i x'_j \partial_{v'}^3 \psi &= 2\pi(u - u') [x_i x_j \partial_v^2 \bar{\psi} + (u - u') \\ &\times (\delta_{ij} \partial_v \bar{\psi} + 2x_{(i} \partial_{j)} \partial_v \bar{\psi}) + (u - u')^2 \partial_i \partial_j \bar{\psi}]. \end{aligned} \quad (5.16)$$

Now, since $\ell^\alpha \partial_\alpha = \partial_v$ is Killing and ψ is a solution to the scalar wave equation in a plane wave spacetime, $\Psi \equiv \mathcal{L}_\ell \psi = \partial_v \psi$ is also a solution in that spacetime. Similarly, $\bar{\Psi} \equiv \partial_v \bar{\psi}$ is a solution to the scalar wave equation in flat spacetime whenever $\bar{\psi}$ is a solution in flat spacetime. It then follows from Eq. (5.12) that

$$\Psi = \bar{\Psi} + \frac{1}{2\pi(u-u')} \int d^2x' v_{\text{ret}}^{(1)} \partial_v^3 \psi(u', \bar{v}_{\text{ret}}, x'^j) \quad (5.17)$$

is an approximate solution on a plane wave background. The integral here involves the zeroth, the first, and the second moments of $\partial_v^3 \psi$ on Σ , all of which can be extracted from Eqs. (5.14) to (5.16). If $\bar{\psi}$ is any solution to the flat-spacetime wave equation, these results show that

$$\Psi = \partial_v \bar{\psi} - \frac{1}{2} \left(\int_{u'}^u dw H^{ij}(w) [x_i \partial_v + (u-w) \partial_i] \right. \\ \left. \times [x_j \partial_v + (u-w) \partial_j] \right) \bar{\psi} \quad (5.18)$$

is an approximate solution to the wave equation on a plane wave background. *Scattered solutions can thus be generated simply by differentiating unscattered solutions.* However, we emphasize that the above equation describes a process in which the field before the arrival of the gravitational wave is $\partial_v \bar{\psi}$, not $\bar{\psi}$. Despite the roundabout nature in which we have obtained this result, it may be applied to any $\bar{\psi}$ that satisfies the massless scalar wave equation in flat spacetime. If desired, spin-raising operations [51, 68–71] could be used to obtain similar results for the scattering of electromagnetic fields or of metric perturbations on plane wave backgrounds.

Regardless, our result can be simplified by evaluating Ψ in the flat region \mathcal{I}_+ after the gravitational wave has left, in which case all integrals in Eq. (5.18) reduce to memory tensors. Applying Eq. (2.40),

$$\Psi = \partial_v \bar{\psi} + \frac{1}{2} [M_{ij}^{v \rightarrow d} \partial^i \partial^j - 2M_{ij}^{d \rightarrow d} (x^i \partial_v + u \partial^i) \partial^j \\ - M_{ij}^{d \rightarrow v} (x^i \partial_v + u \partial^i) (x^j \partial_v + u \partial^j)] \bar{\psi}. \quad (5.19)$$

All derivatives which appear here may be seen to be Lie derivatives with respect to flat-spacetime Killing fields. The velocity-displacement memory thus contributes pairs of translations, the displacement-displacement memory contributes a combination of translations mixed with null rotations, and the displacement-velocity memory contributes pairs of null rotations. Regardless, the bracketed differential operator in Eq. (5.19) may be viewed as a kind of “continuum” memory effect. Various “before and after” comparisons could be performed with scattered fields, and these would be determined by that operator and by the initial field configuration.

C. Scattering of plane waves

Sections III and IV above both consider the effects of a gravitational plane wave on highly localized objects:

geodesics and massless spinning particles. However, we may also consider the effects of a gravitational sandwich wave on scalar plane waves, which are completely *delocalized*. Suppose that for $u \in \mathcal{I}_-$, we have the “incoming” flat spacetime plane wave

$$\psi_- = \exp \left\{ i\omega_- (t - z \cos \theta_- - n_i^- x^i \sin \theta_-) \right\} \\ = \exp \left\{ \frac{i\omega_-}{\sqrt{2}} \left[(1 - \cos \theta_-)v + (1 + \cos \theta_-)u \right. \right. \\ \left. \left. - \sqrt{2} n_i^- x^i \sin \theta_- \right] \right\}, \quad (5.20)$$

where ω_- denotes the initial frequency (as seen by the canonical observer at the origin), θ_- the initial angle of propagation relative to the gravitational wave, and n_i^- a unit 2-vector which describes the initial direction of propagation in the transverse plane. At least in a weak field limit, we could apply Eq. (5.19) in order to determine how such a scalar wave is scattered by a gravitational wave. However, we instead solve this problem *exactly*¹¹ by employing Ward’s progressing-wave solutions [72]. This expands upon results which initially appeared in, e.g., Ref. [51].

As described Appendix C, Ward found that the wave equation in an arbitrary plane wave spacetime can be solved by

$$\psi = (\det h_{ij})^{-1/4} f(S_P), \quad (5.21)$$

where f is an arbitrary function, the eikonal $S_P(\mathcal{U}, \mathcal{V}, \mathcal{X}^i)$ is given by Eq. (C.2) in terms of the Rosen coordinates $(\mathcal{U}, \mathcal{V}, \mathcal{X}^i)$, and $h_{ij}(\mathcal{U})$ denotes the 2-metric in the Rosen line element (C.1). We would like to identify a solution in this class which is equal to ψ_- before the gravitational wave arrives. However, ψ is written in terms of Rosen coordinates while ψ_- is written in terms of Brinkmann coordinates.

In order to compare, first recall that h_{ij} is given, via Eq. (C.8), by the square of some E_{ij} which satisfies the differential equation (2.15) and the constraint (C.7). It is always possible to choose $E_{ij} = A_{ij}(u, u')$ for some fixed $u' \in \mathcal{I}_-$, which guarantees that the Rosen metric is trivial before the gravitational wave arrives: $h_{ij} = \delta_{ij}$ in \mathcal{I}_- . Using that same E_{ij} to transform from Rosen to Brinkmann coordinates using Eq. (C.6), both coordinate systems can be seen to coincide before the gravitational wave arrives. The progressing wave ψ therefore matches the incoming plane wave ψ_- in \mathcal{I}_- when the f in Eq. (5.21) is chosen to be

$$f(S_P) = \exp \left[\frac{i\omega_-}{\sqrt{2}} (1 - \cos \theta_-) S_P \right], \quad (5.22)$$

¹¹ If Eq. (5.19) is used to find a scattered scalar field Ψ , it is natural to employ the seed field $\bar{\psi} = -i\sqrt{2}\psi_- / [\omega_-(1 - \cos \theta_-)]$ so $\partial_v \bar{\psi} = \psi_-$. The result matches Eq. (5.26) through first order in the memory tensors.

while the constants \mathcal{U}_0 , h_0^{ij} , and P_i which appear in $S_{\mathcal{P}}$ are given by

$$\mathcal{U}_0 = u', \quad h_0^{ij} = u' \delta^{ij}, \quad (5.23a)$$

$$P_i = -\sqrt{2} \cot(\frac{1}{2}\theta_-) n_i^-. \quad (5.23b)$$

Although the resulting ψ coincides with ψ_- before the gravitational wave arrives, it can differ at later times. In order to evaluate the scattered field more generally,

note that it follows from Eq. (C.2) that ψ depends on an integral of $(h^{-1})^{ij} = (A^{-1})^{ik}(A^{-1})^j{}_k$. However, this integral can be evaluated by using Eqs. (2.20) and (2.24) to see that

$$\partial_u[(A^{-1})^{ik} B_k^j] = (A^{-1})^i{}_k (A^{-1})^{jk}. \quad (5.24)$$

The Brinkmann-to-Rosen coordinate transformation (C.6) then implies that as long as $\det A_{ij}(u'', u') \neq 0$ for all $u'' \in [u', u]$, which avoids so-called focal points [89], the scalar field (5.21) reduces to

$$\psi = \frac{1}{(\det A_{kl})^{1/2}} \exp \left\{ \frac{i\omega_-}{\sqrt{2}} \left[(1 - \cos \theta_-) \left(v - \frac{1}{2} (\partial_u A A^{-1})_{ij} x^i x^j \right) - \sqrt{2} (A^{-1})_{ij} n_-^i x^j \sin \theta_- \right. \right. \\ \left. \left. + (1 + \cos \theta_-) \left((A^{-1} B)_{ij} n_-^i n_-^j + u' \right) \right] \right\} \quad (5.25)$$

in Brinkmann coordinates. This is an exact solution to the massless wave equation which agrees with the incoming plane wave ψ_- when $u \in \mathcal{I}_-$.

In a scattering context where u lies in \mathcal{I}_+ while u' lies in \mathcal{I}_- , the Jacobi propagators which appear here can be written in terms of the memory tensors using Eqs. (2.30) and (2.31). It follows from those expressions that the outgoing wave does not depend on the precise value of u' . Regardless, working only to first order in the curvature for simplicity, we find that the outgoing wave $\psi_+ \equiv \psi|_{u \in \mathcal{I}_+}$ is given by

$$\psi_+ = \exp \left\{ \frac{i\omega_-}{\sqrt{2}} \left[(1 - \cos \theta_-) v + (1 + \cos \theta_-) \left(M_{ij}^{v \rightarrow d} + (\delta_{ij} - 2M_{ij}^{d \rightarrow d}) u \right) n_-^i n_-^j - \sqrt{2} (\delta_{ij} - M_{ij}^{d \rightarrow d}) n_-^i x^j \sin \theta_- \right. \right. \\ \left. \left. - \frac{1}{2} M_{ij}^{d \rightarrow v} \left((1 - \cos \theta_-) x^i x^j - 2\sqrt{2} u n_-^i x^j \sin \theta_- + 2u^2 (1 + \cos \theta_-) n_-^i n_-^j \right) \right] \right\} + \mathcal{O}(H^2). \quad (5.26)$$

In general, the phase of this exponential depends quadratically on both u and x^i , implying that the outgoing wave is not necessarily a plane wave. However, quadratic terms arise only when $M_{ij}^{d \rightarrow v} \neq 0$. At first order in H_{ij} , plane waves are therefore scattered into plane waves only when the displacement-velocity memory vanishes. This can be understood heuristically by noting that initially parallel null geodesics remain parallel only when $M_{ij}^{d \rightarrow v}$ vanishes.

When the displacement-velocity memory *does* vanish at leading order, which is the what typically occurs in astrophysical applications, the outgoing wave (5.26) can be written as

$$\psi_+ = \exp \left\{ \frac{i\omega_+}{\sqrt{2}} \left[(1 - \cos \theta_+) v + (1 + \cos \theta_+) u \right. \right. \\ \left. \left. - \sqrt{2} n_+^i x^i \sin \theta_+ + \phi_+ \right] \right\} + \mathcal{O}(H^2). \quad (5.27)$$

Comparing with the ingoing wave (5.20), this may be interpreted as a plane wave with the outgoing frequency

$$\omega_+ = \left[1 - (1 + \cos \theta_-) M_{ij}^{d \rightarrow d} n_-^i n_-^j \right] \omega_-, \quad (5.28)$$

and an outgoing propagation direction which is deter-

mined by the angles

$$\theta_+ = \theta_- + M_{ij}^{d \rightarrow d} n_-^i n_-^j \sin \theta_-, \quad (5.29a)$$

$$n_+^i = n_-^i + (n_-^i n_-^j - \delta^{ij}) M_{jk}^{d \rightarrow d} n_-^k. \quad (5.29b)$$

There is also the phase shift

$$\phi_+ = (1 + \cos \theta_-) M_{ij}^{v \rightarrow d} n_-^i n_-^j. \quad (5.30)$$

While the displacement-displacement memory perturbs both the frequency and the propagation direction of a scattered plane wave, the velocity-displacement memory imparts only a phase shift. More specifically, the plane wave deflections given by Eq. (5.29) agree with our results (3.28) and (3.29) for null geodesics. The frequency shift Eq. (5.28) can also be seen to agree with the frequency shifts that have been computed in geometric optics [117–119], often in connection with pulsar timing measurements. In these senses, (delocalized) plane waves behave like (localized) null geodesics, at least when H_{ij} is small and $M_{ij}^{d \rightarrow v}$ can be neglected.

One other point to note is that our expressions are not meaningful when $\theta_- = 0$. Physically, this corresponds to the case in which a scalar wave is co-propagating with a gravitational wave. However, there is no sense in which

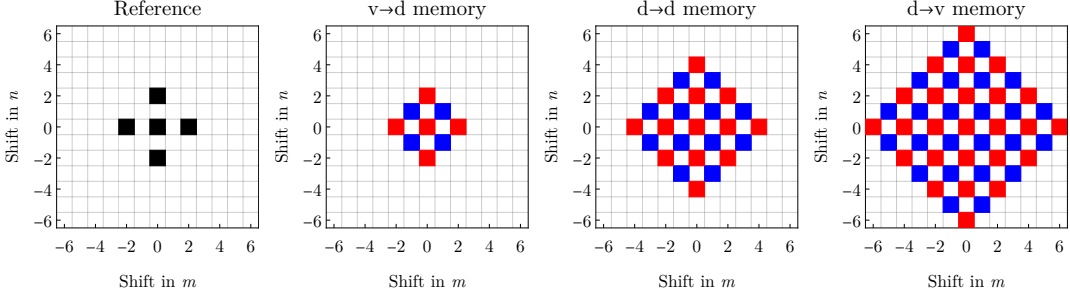


FIG. 11. Graphical representation of Hermite–Gauss modes that are generically excited by gravitational wave memory. The leftmost pane illustrates the HG modes which compose the ingoing field $\partial_v \psi_{m,n}^{\text{HG}}$. The three right panes indicate which modes are affected by different memory tensors in the outgoing field. Red squares are used to indicate that the corresponding mode is excited only by diagonal components of the corresponding memory tensor; blue squares are instead excited by off-diagonal components.

two co-propagating waves can pass through each other; one cannot be scattered by the other. Mathematically, note that both ψ_- and the “outgoing wave” given by Eq. (5.25) depend only on u in this context. However, *any* function of u is a globally valid solution to the scalar wave equation. This ambiguity is related to the aforementioned fact that we are effectively treating the null $u = u'$ hypersurface as if it were a Cauchy surface even though it is not. Solutions are not unique because we have effectively chosen not to control radiation which is co-propagating with the gravitational wave.

D. Scattering of higher-order Gaussian beams

Having now considered the scattering of both null geodesics, which are fully localized, and scalar plane waves, which are completely delocalized, we now discuss an intermediate between these two extremes: scalar beams that are strongly (but not “fully”) localized in two spatial directions while being weakly localized in the third. In order to accommodate this generality without undue complication, we work only to first order in the memory tensors, applying the perturbative scattering formula (5.19). We also assume for simplicity that the scalar beams are initially counter-propagating with respect to the background gravitational wave.

It follows from Eq. (5.26) that, at first order, a counter-propagating scalar wave which is initially planar generically has its wavefronts deformed into hyperbolic paraboloids. However, this effect is purely due to the displacement-velocity memory. When $M_{ij}^{\text{d}\rightarrow\text{v}}$ vanishes at leading order, an incoming plane wave is actually unaffected by a counter-propagating gravitational sandwich wave. This contrasts with what happens for the localized beams we now consider, where nontrivial memory effects arise even in the absence of first order displacement-velocity memory.

These beams are constructed from the Hermite–Gauss (HG) and Laguerre–Gauss (LG) families [120–122], which are exact solutions of the massless scalar wave equation

in Minkowski spacetime. Choosing a direction of propagation opposite to that of the gravitational wave (whose effects are incorporated below), the HG solutions $\psi_{m,n}^{\text{HG}}$ and the LG solutions $\psi_{l,p}^{\text{LG}}$ are explicitly given by

$$\psi_{m,n}^{\text{HG}} \equiv \frac{\mathcal{N}_{m,n}}{w(v)} H_m \left(\frac{\sqrt{2}x}{w(v)} \right) H_n \left(\frac{\sqrt{2}y}{w(v)} \right) e^{\chi(u,v,r)}, \quad (5.31a)$$

$$\psi_{l,p}^{\text{LG}} \equiv \frac{\mathcal{N}_{l,p}}{w(v)} \left(\frac{\sqrt{2}r}{w(v)} \right)^{|l|} L_p^{|l|} \left(\frac{2r^2}{w(v)^2} \right) e^{\chi(u,v,r) - il\phi}, \quad (5.31b)$$

where $r^2 = x^2 + y^2$ is the squared transverse radius, $\phi = \arg(x + iy)$ is a polar coordinate along the beam axis, and

$$\chi(u, v, r) \equiv -\frac{r^2}{[w(v)]^2} + i \left[\sqrt{2}k \left(u - \frac{r^2}{2R(v)} \right) + (m + n + 1) \arctan \left(\frac{\sqrt{2}v}{w_0^2 k} \right) \right]. \quad (5.32)$$

The transverse beam width is characterized by the length-scale

$$w(v) \equiv w_0 \sqrt{1 + \frac{2v^2}{w_0^4 k^2}}, \quad (5.33)$$

while

$$R(v) \equiv v \left(1 + \frac{w_0^4 k^2}{2v^2} \right) \quad (5.34)$$

may be interpreted as the curvature radius of the wave fronts. It is also convenient to introduce the normalization constants

$$\mathcal{N}_{m,n} \equiv \sqrt{\frac{2}{\pi 2^{m+n} m! n!}}, \quad \mathcal{N}_{l,p} \equiv \sqrt{\frac{2p!}{\pi (p + |l|)!}}, \quad (5.35)$$

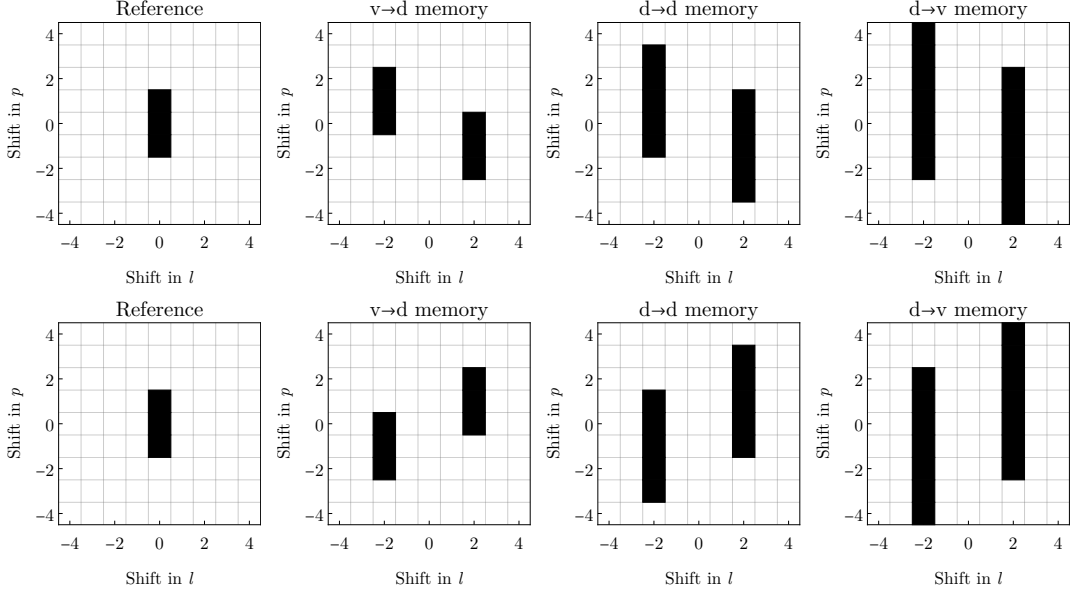


FIG. 12. Graphical representation of Laguerre–Gauss modes that are excited by gravitational wave memory. The leftmost panes illustrate the LG modes which compose the ingoing field $\partial_v \psi_{l,p}^{\text{LG}}$. The figures in the upper row correspond to $l \geq 2$, whereas figures in the lower row describe $l \leq -2$. In contrast to the case of Hermite–Gauss modes (as illustrated in Fig. 11), where different components of the memory tensors excite different modes, all modes marked here are excited by both diagonal and off-diagonal terms of the various memory tensors.

which ensure that if an asterisk is used to denote complex conjugation,

$$\int (\psi_{m,n}^{\text{HG}})^* \psi_{m',n'}^{\text{HG}} dx dy = \delta_{mm'} \delta_{nn'}, \quad (5.36a)$$

$$\int (\psi_{l,p}^{\text{LG}})^* \psi_{l',p'}^{\text{HG}} dx dy = \delta_{ll'} \delta_{pp'}. \quad (5.36b)$$

Both integrals here are to be evaluated on a screen with constant u and v . On such a screen, the HG beams are naturally expressed in Cartesian coordinates (x, y) in terms of Hermite polynomials H_m , whereas the LG beams are written in terms of polar coordinates (r, ϕ) and generalized Laguerre polynomials L_p^l . Each beam is uniquely characterized by its waist radius w_0 , its wave number k , and the mode numbers (m, n) or (l, p) , where $m, n, p \in \mathbb{N}$ and $l \in \mathbb{Z}$. The HG mode numbers m and n describe how many nodes there are in the x and the y directions, respectively. The LG mode number l provides a measure of the orbital angular momentum carried by $\psi_{l,p}^{\text{LG}}$ [112]. The cases $m = n = 0$ and $l = p = 0$ coincide, and are referred to as Gaussian beams. More general cases may be described as “higher order” Gaussian beams.

Both the HG and the LG solutions decay exponentially in the transverse x and y directions. The characteristic lengthscale for this decay is given by $w(v)$, which has a minimum value of w_0 at the $v = 0$ “focus,” but grows linearly with v when $|v| \gg w_0^2 k$. The beam therefore focuses inward at an initial angle and then diverges outward at that same angle. A beam with a smaller $w_0 k$ spreads out more rapidly away from its focus. This transverse spread causes both the HG and the LG beams to decay longitu-

dinally as well as transversely. However, the longitudinal decay is slower, being only polynomial in v .

Regardless, we now consider a gravitational sandwich-wave background and let the seed field $\bar{\psi}$ in the scattering formula (5.19) be equal either to $\psi_{m,n}^{\text{HG}}$ or to $\psi_{l,p}^{\text{LG}}$. Before the gravitational wave arrives, the “incoming” fields here reduce either to $\partial_v \psi_{m,n}^{\text{HG}}$ or to $\partial_v \psi_{l,p}^{\text{LG}}$, which are *not* pure HG or LG modes. Eqs. (E.1a) and (E.3a) in Appendix E nevertheless imply that these derivatives can be written as linear combinations of at most five HG or LG modes. The “outgoing” fields that appear after the gravitational wave has passed are more complicated, with the perturbed field involving both the memory tensors and the second partial derivatives of $\bar{\psi}$. However, it is shown in Appendix E that all such derivatives can be explicitly written in terms of a finite number of undifferentiated HG or LG modes. Although it is possible to write down these combinations explicitly, the resulting expressions are unwieldy and we omit them.

It is nevertheless straightforward to explain at least which side modes are excited by different types of gravitational wave memory. In the HG case, the complete list is illustrated in Fig. 11. The incoming beam $\partial_v \psi_{m,n}^{\text{HG}}$ is, generically, a linear combination of HG fields with the five modes (m, n) , $(m \pm 2, n)$, and $(m, n \pm 2)$. If the velocity-displacement memory $M_{ij}^{v \rightarrow d}$ is purely diagonal, it affects only these five modes. However, an off-diagonal component of $M_{ij}^{v \rightarrow d}$ can instead excite only the four new modes $(m \pm 1, n \pm 1)$. The effect of the displacement-displacement memory is more complicated, generally coupling to modes up to $(m \pm 4, n)$ and $(m, n \pm 4)$. The

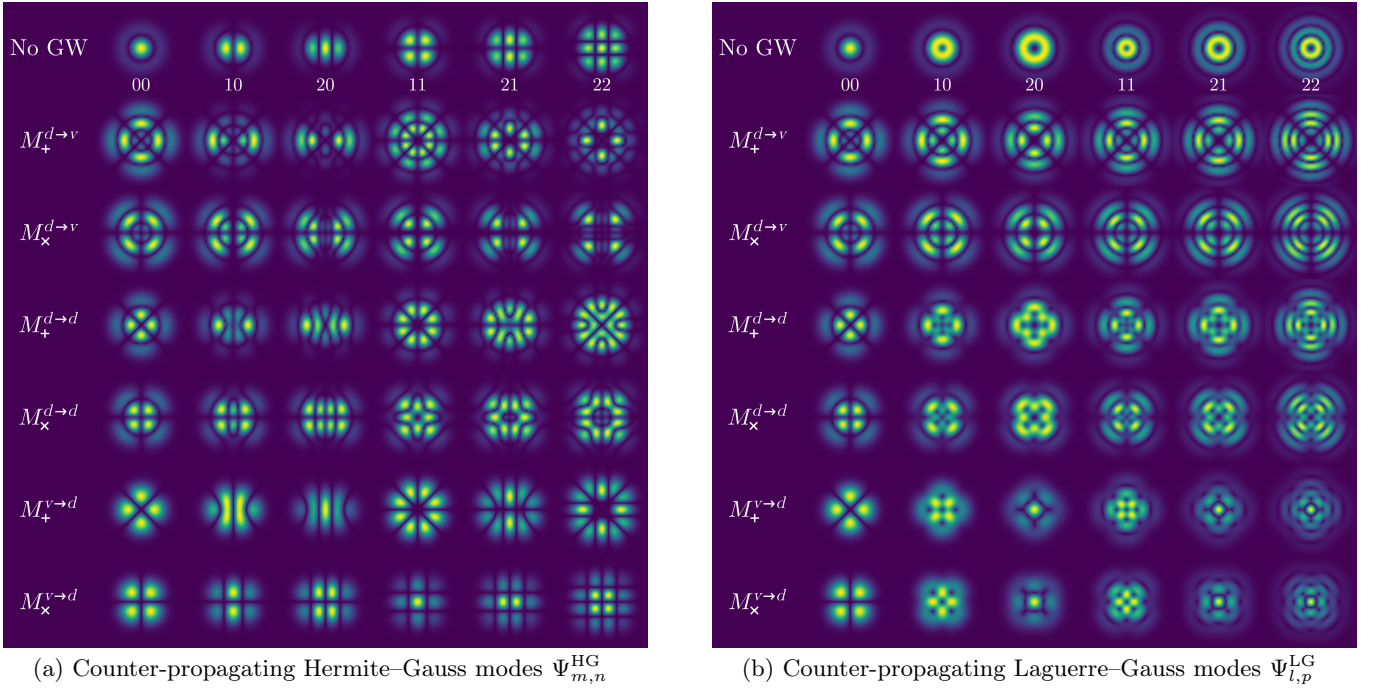


FIG. 13. Slices of fields seeded by HG modes (a) and LG modes (b) which are counter-propagating with the gravitational wave, all evaluated $t = z = 0$. It is assumed that $w_0 k = 100$. The first row corresponds to the magnitude of the unperturbed reference field $\partial_v \bar{\psi}$, while the numbers refer to the HG or LG mode used for the seed field $\bar{\psi}$. Subsequent rows correspond to the magnitudes of the first-order field perturbations associated with different memory tensors. For example, the row labelled by $M_+^{d \rightarrow v}$ plots the difference fields associated with a purely diagonal displacement-velocity memory. The row labelled by $M_x^{d \rightarrow v}$ instead plots the results of a purely off-diagonal displacement-velocity memory. In the LG (but not the HG) cases, magnitudes of perturbations due to the diagonal and the off-diagonal components of a given memory tensor differ only by a 45° rotation.

effect of the displacement-velocity memory is more complicated still, exciting side modes as high as $(m \pm 6, n)$ and $(m, n \pm 6)$. In all cases here, the diagonal and the off-diagonal components of each memory tensor affect disjoint sets of modes. However, this separation would not occur if the HG modes that we employed were not aligned with the x and y axes.

A similar analysis can also be performed for LG beams, where the side modes excited by the various memory tensors are illustrated in Fig. 12. An incoming beam $\partial_v \psi_{l,p}^{\text{LG}}$ is generally made up of a linear combination of the three modes (l, p) and $(l, p \pm 1)$. Unlike in the HG case, the diagonal and the off-diagonal components of the memory tensors affect such beams similarly, essentially because $\psi_{l,p}^{\text{LG}}$ is rotationally symmetric except for the phase $l\phi$. In any case, the excitations generated by the different memory tensors have the form $(l \pm 2, p \pm \Delta p)$. For the velocity-displacement memory, $-2 \leq \Delta p \leq 2$, for the displacement-displacement memory, $-3 \leq \Delta p \leq 3$, and for the displacement-velocity memory, $-4 \leq \Delta p \leq 4$.

Another way to illustrate memory effects in this context is to plot example cross-sections of different scattered beams. This is done in Fig. 13, which plots the magnitudes of the difference fields which are associated with the various memory tensors on a screen at $t = z = 0$ (or equivalently, at $u = v = 0$). This corresponds to the focus of the unperturbed beam at $t = 0$. If one were to

instead evaluate on a screen in which $|u|$ is sufficiently large, the u -dependent factors on the right-hand side of Eq. (5.19) would cause the effects of $M_{ij}^{d \rightarrow v}$ to dominate over those of $M_{ij}^{d \rightarrow d}$, and the effects of $M_{ij}^{d \rightarrow d}$ to dominate over those of $M_{ij}^{v \rightarrow d}$. Plots analogous to Fig. 13 would then show no significant differences between the effects of the different memory tensors (at least when comparing only diagonal memory tensors or only off-diagonal ones). Regardless, the strong difference between the effects of diagonal and off-diagonal terms in the various memory tensors suggests that the induced transverse deformations of the beams are highly dependent on the polarization of an intervening gravitational wave. It may also be noted that similar deformations of HG beams propagating in curved spacetimes have been reported in Ref. [123].

E. Scattering of wave packets and comparison with the spin Hall equations

The analysis of scalar wave scattering in Sections VB and VD is restricted to weak gravitational waves and perturbative methods. In the non-perturbative regime, wave propagation can be described by the Kirchhoff-like integral (5.7). However, that integral cannot generally be evaluated in closed form. Non-perturbative scattering for

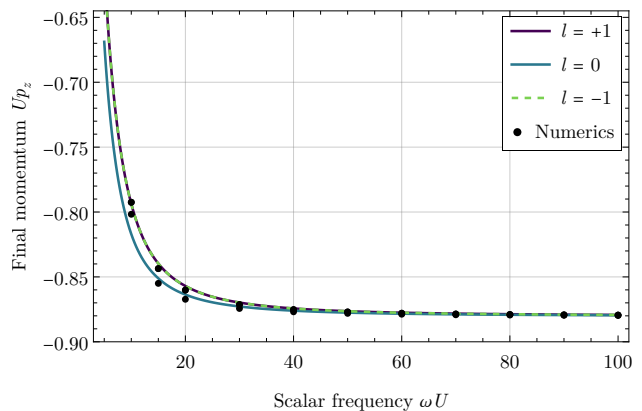
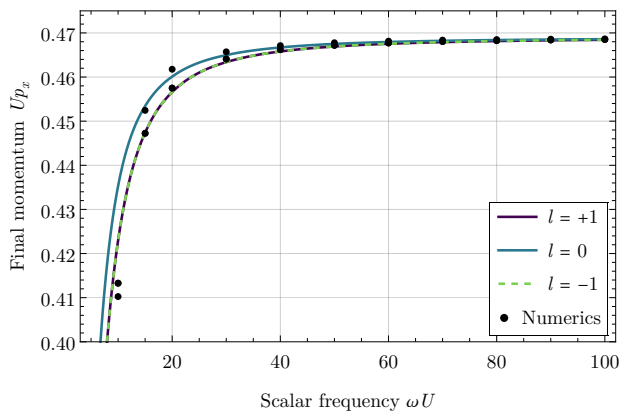


FIG. 14. Final momentum components p_x and p_z (both initially nonzero) due to scattering off a circularly polarized gravitational sandwich wave, as a function of the initial scalar wave frequency ω . The dots indicate data obtained by numerical quadrature of Eq. (5.37), while the solid curves were obtained by solving the spin Hall equations (4.2) using initial data derived from the initial scalar wave packet. The spin Hall equations are seen to agree with the full numerical evolution, especially when ω is large. It can also be seen that there is little dependence on l at high frequencies. The gravitational wave here has amplitude $A = 1/2U^2$ and frequency $\nu = 5/U$. The scales in these plots use units in which $U = 1$. The remaining momentum component p_y is plotted in Fig. 15.

generic scalar fields could instead be understood by summing the initially planar waves described in Section V C. However, using analytic methods to extract interesting features from such sums is again nontrivial. As a consequence, we now turn to a numerical analysis of scalar waves scattered by non-perturbative gravitational sandwich waves. This section presents results obtained from the numerical evaluation of a Kirchhoff integral which yields exact solutions to the complex scalar wave equation in specific plane wave spacetimes (up to numerical error). We consider the scattering of small, high-frequency wave packets and show that their dynamics are in good agreement with the ray description provided by the spin Hall equations (4.2). This provides evidence that the spin Hall effect of wave packets carrying angular momentum is indeed described by those equations.

We choose here to use a “standard” Kirchhoff integral where the initial hypersurface Σ that appears in Eq. (5.4) is spacelike rather than null. This is possible because (i) we work in a sufficiently small region that conjugate hyperplanes are not encountered, and (ii) the initial data considered here (very nearly) vanish outside of a sufficiently compact region that all relevant portions of Σ can be placed in \mathcal{I}_- , before any significant portion of the gravitational wave arrives. In particular, we identify Σ with the hypersurface $t' = \text{constant}$, where the time coordinate is again defined by Eq. (2.11). Then it is convenient to introduce spherical coordinates r', θ', φ' for the source point x' which are centered around the three spatial coordinates x^I of the field point x . Combining Eqs. (5.2), (5.4) and (5.5) then yields the Kirchhoff integral

$$\psi(x) = \frac{1}{4\pi} \int_{S_2} \frac{d\Omega'}{|\partial_{r'}\sigma|} \left[r'^2 (\sqrt{\Delta} \partial_{t'} \psi' - \psi' \partial_{t'} \sqrt{\Delta}) + \partial_{r'} (r'^2 \sqrt{\Delta} \psi' \partial_{t'} \sigma / \partial_{r'} \sigma) \right]_{r'=r_{\text{ret.}}}, \quad (5.37)$$

when $t > t'$, where $d\Omega = \sin\theta' d\theta' d\varphi'$ is the standard measure on the round unit two-sphere S_2 and $r_{\text{ret.}} = r_{\text{ret.}}(x; t', \theta', \varphi')$ describes the radius of the past light cone with vertex x on the initial $t' = \text{constant}$ hypersurface and in the direction determined by the angles (θ', φ') . This last function can be obtained by transforming Eq. (3.32) into the given coordinates and then solving $\sigma = 0$. Regardless, the Jacobi propagators A_{ij} and B_{ij} are computed numerically, and then σ follows from Eq. (3.32) and Δ from Eq. (5.6).

Scalar wave propagation can be related to the predictions of the gravitational spin Hall equations by (i) prescribing initial data for a scalar field at $t' = \text{constant}$, before the gravitational wave arrives, (ii) computing the 4-momentum, the energy centroid, and the angular momentum of this data, (iii) evolving the spin Hall equations with these parameters as initial data, (iv) numerically evaluating the Kirchhoff integral Eq. (5.37) to find the field after the gravitational wave has left, and (v) computing the 4-momentum and the centroid of scattered field. Finally, the 4-momenta and the centroids of steps (iii) and (v) can be directly compared.

In order to describe this in more detail, we first explain how to compute 4-momenta and centroids. These are derived from the generalized momentum given by Eqs. (4.4) and (4.6). Integrating over a constant- t hypersurface while assuming that the stress-energy tensor of the scalar field $T^{\alpha\beta}$ is nonzero only where the spacetime is (very nearly) flat, the 4-momentum in \mathcal{I}_- and in \mathcal{I}_+ can be computed using

$$p^\alpha = \int T^{\alpha t} d^3x. \quad (5.38)$$

We take ψ to be a genuinely complex field, as opposed to a complex field interpreted so that only its real component

is physical. Denoting by ψ^* its complex conjugate, the stress-energy tensor is

$$T_{\alpha\beta} = (\delta_{(\alpha}^{\gamma} \delta_{\beta)}^{\lambda} - \frac{1}{2}g_{\alpha\beta}g^{\gamma\lambda})\nabla_{\gamma}\psi^*\nabla_{\lambda}\psi. \quad (5.39)$$

Stress-energy conservation implies that although the 4-momentum can be changed by a passing gravitational wave, it is conserved within each of the two flat regions. Its components are the generalized momentum \mathcal{P}_{ξ} evaluated for vector fields ξ^{α} which locally generate translations.

The centroid of a scalar field can be extracted by first noting from Eqs. (4.4) and (4.6) that the angular momentum with respect to an origin with coordinates \bar{x}^{α} is given by

$$S^{\alpha\beta} = 2 \int (x - \bar{x})^{[\alpha} T^{\beta]t} d^3x \quad (5.40)$$

in any flat region. Applying the spin supplementary condition (4.1) with the frame vector given by Eq. (4.12), the spatial coordinates of the centroid in any flat region are therefore

$$\bar{x}^I = \frac{1}{p^t} \int T^{tt} x^I d^3x. \quad (5.41)$$

Unlike in Section IV, we now use \bar{x}^I to denote the centroid position instead of x^I , reserving the latter for the spatial coordinates of a general field point. Regardless, comparison with the spin Hall equations requires that we also evaluate ϵ_s . This is done by computing $S^{\alpha\beta}$ and then applying Eq. (4.3), which determines the absolute value of ϵ_s . Its sign is chosen to coincide with the sign of the angular momentum parameter l introduced in Eq. (5.44) below. The u -derivatives needed to compute the stress-energy tensor were obtained using finite differences. All other derivatives were determined using the fact that derivatives along the four Killing vector fields described by Eq. (2.8) also satisfy the scalar wave equation and can thus also be propagated forward in time using the Kirchoff integral (5.37).

We work with gravitational waves that can be interpreted as circularly polarized with Gaussian profiles. More precisely, we consider the waveforms given by Eq. (B.10), with center point $U_0 = 10U$, phase offsets $\phi_+ = \pi/2$ and $\phi_{\times} = 0$, and equal curvature length scales $l_+ = l_{\times}$. We also define the curvature amplitude

$$A \equiv \frac{2}{\sqrt{\pi}l_+^2}, \quad (5.42)$$

where this and the gravitational wave frequency ν are both kept as adjustable parameters. The given waveform never decays entirely to zero, so these are not technically sandwich waves. However, the ‘‘flat regions’’ \mathcal{I}_{\pm} can be roughly identified as those in which $|u - U_0| \gg U$.

Next, we impose initial data for $\psi(x')$ on the $t' = 0$ hypersurface, which amounts to specifying the field and its first time derivative there. Introducing an initial scalar amplitude profile $a(x^J)$, a scalar frequency ω , and a unit

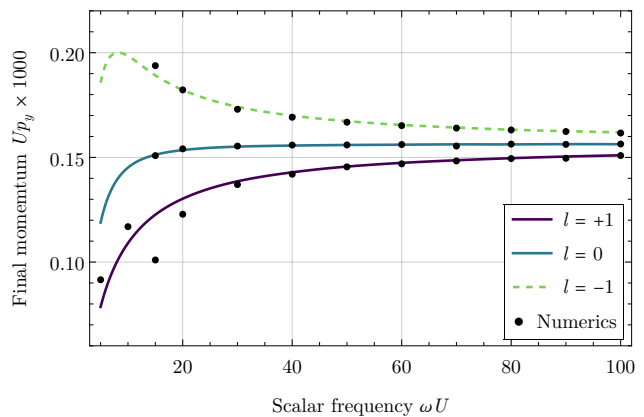


FIG. 15. Final momentum component p_y (which initially vanishes) due to scattering off a circularly polarized gravitational sandwich wave, as a function of the initial scalar wave frequency ω . All conventions here are the same as in Fig. 14, which plots p_x and p_z . Here, p_y is seen to converge to the $l = 0$ case of a null geodesic at large ω , and the first corrections are well described by the spin Hall equations. Unlike for the p_x and p_z components, those corrections are nontrivial: There is a clear dependence on the angular momentum of the wave packet.

3-vector n^I (unlike the unit 2-vector n^i used above) which describes the initial direction of propagation, we let

$$\psi|_{t=0} = a(x^J) e^{i\omega n_I x^I}, \quad (5.43a)$$

$$\partial_t \psi|_{t=0} = -[i\omega a(x^J) + n^K \nabla_K a(x^J)] e^{i\omega n_I x^I}. \quad (5.43b)$$

This choice is motivated by the high-frequency (or WKB) approximation, in which a family of fields on spacetime has the form $[a(x) + \mathcal{O}(\omega^{-1})] e^{i\omega u(x)}$ as $\omega \rightarrow \infty$. Working in flat spacetime, planar wavefronts result from $\mathbf{u} = n_I x^I - t$, and the scalar wave equation implies that $\partial_{\alpha} u \partial^{\alpha} a = 0$. Evaluating these results on the initial hypersurface while dropping the $\mathcal{O}(\omega^{-1})$ correction recovers the initial data above. Despite the approximation used to produce these data, their evolution into the future takes into account all finite-frequency effects. Up to numerical error, its use in the Kirchoff integral (5.37) produces an exact solution to the scalar wave equation in a sandwich wave background.

Comparison with the spin Hall equations requires a small wave packet, so we choose the initial amplitude profile of the scalar field to decay exponentially—though anisotropically—in all spatial directions. Introducing a constant, positive-definite matrix W_{IJ} that controls this decay,

$$a(x^I) = \mathcal{N} |x|_{\perp}^2 \exp(-W_{JK} x^J x^K + i l \phi), \quad (5.44)$$

where \mathcal{N} is a normalization constant, $|x|_{\perp}^2 \equiv (\delta_{IJ} - n_I n_J) x^I x^J$ is the squared distance away from the propagation axis, l is an integer controlling the orbital angular momentum (OAM) of the field¹², and ϕ is an angle

¹² Using the given initial data to compute the angular momentum,

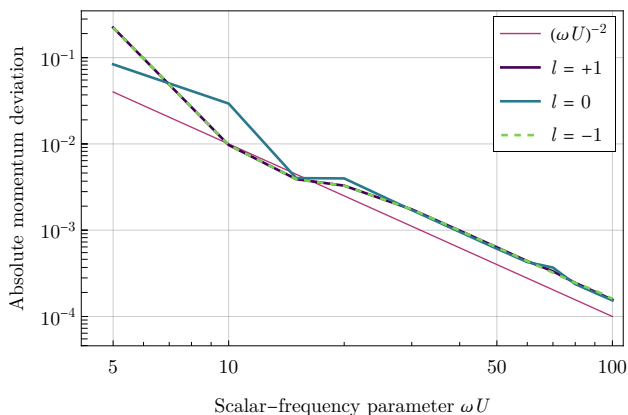


FIG. 16. Frequency dependence of the differences between the final 3-momenta obtained using the Kirchhoff integral and the spin Hall equations. The vertical scale plots the norm of the difference between these two momenta. As the scalar frequency ω increases, this difference scales like $1/\omega^2$, which is plotted in red. All conventions here are the same as in Fig. 14.

around the propagation direction. Using rotated coordinates \hat{x}^I which are aligned with the propagation direction, so $\hat{n}^3 = 1$, this last angle is more precisely defined to be $\arg(\hat{x}^1 + i\hat{x}^2)$. Although ϕ is uniquely defined only up to an overall additive constant, that constant is irrelevant to our discussion. In our implementation, we choose $\hat{W}_{IJ} = (2\pi/U^2) \text{diag}[1, 1, 1/9]_{IJ}$ in these same rotated coordinates, so that the wave packet decays more rapidly away from its propagation direction rather than along it. All calculations are carried out with the propagation direction $(n_I) = (\sin \beta, 0, -\cos \beta)$, where $\beta = 1/2$, and, for convenience, \mathcal{N} is chosen such that the initial energy $p^t|_{t=0}$ is equal to the gravitational wave width U .

We implemented the above scheme using **Wolfram Mathematica** [124]. As a first test, the scattering of scalar wave packets in a fixed gravitational wave background was considered for various values of the initial scalar wave frequency ω . Since wave packets with different values of l did not acquire significant spatial separation during the integration time $\Delta t = 20U$, after which they had propagated to the region \mathcal{I}_+ , our analysis focuses mainly on the final 3-momentum p_I . Figures 14 and 15 show the final momentum of the wave packet as a function of its initial angular frequency ω . In these plots, the dots represent the numerical results obtained from the Kirchhoff formula (5.4), applied to the initial data mentioned above, while the solid lines represent the numerical results obtained from numerical solutions to the spin Hall equations (4.2). As demonstrated in Fig. 14, the momentum components that are initially nonzero show only little dependence on

it can be shown that $\epsilon s = (p^t/\omega)l + \mathcal{O}(\omega^{-3})$. That the leading term here is of order $1/\omega$ implies that the angular momentum of the wave packet first appears at one order beyond geometric optics.

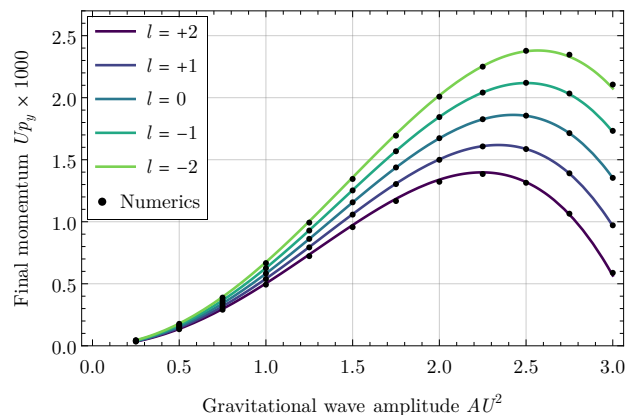


FIG. 17. Variation of the final momentum p_y (which initially vanishes) as a function of the gravitational wave amplitude A . Conventions are the same as in Fig. 14, except that A is free in this plot. The initial frequency of the scalar wave is also fixed at $\omega = 50/U$. The spin Hall predictions are seen to remain valid even for very large gravitational wave amplitudes.

the OAM parameter l : Defining the relative momentum splitting as

$$\delta p_I = \frac{p_I(l=+1) - p_I(l=-1)}{\max\{|p_I(l=+1)|, |p_I(l=-1)|\}}, \quad (5.45)$$

we find that δp_x and δp_y do not exceed 1.6×10^{-5} in the considered parameter regime. However, Fig. 15 shows a clear l -dependence of the final value of p_y (which is initially zero): The relative splitting ranges from $\delta p_y \approx -2$ at $\omega = 5/U$ to $\delta p_y \approx -0.06$ at $\omega = 100/U$.

Figure 16 shows that the final momenta of the considered scalar wave packets converge to the spin Hall predictions at a rate that is proportional to ω^{-2} . This result is to be expected from the construction of the spin Hall equations using high-frequency asymptotics, though the present comparison provides the first quantitative measures of the quality of the gravitational spin Hall model. To further analyze this quality in the present setup, the dependence of p_y on the gravitational wave amplitude A was investigated for a fixed value of the scalar wave frequency, $\omega = 50/U$, but different values of the OAM parameter l , namely 0, ± 1 , and ± 2 . Figure 17 shows a clear l -dependent change in p_y for gravitational wave amplitudes up to $A = 3/U^2$ that is consistent with the spin Hall predictions. All of these results were obtained without weak-field approximations.

VI. CONCLUSIONS

This paper discusses a wide range of memory effects in gravitational plane wave spacetimes. All memory effects involving geodesics, spinning massless particles, and even full test fields were found to depend only on solutions to the geodesic deviation equation. In particular, they can be written in terms of the Jacobi propagators

$A_{ij}(u, u')$ and $B_{ij}(u, u')$. Although there is an infinite-dimensional space of possible waveforms, and there are different Jacobi propagators for each waveform, there is only a finite-dimensional space of possibilities for the “initial” and “final” Jacobi propagators in sandwich-wave contexts where the waveform is nontrivial only for a finite time. All memory effects we consider can then be encoded in the four memory tensors introduced in Section II; cf. Eqs. (2.30) and (2.31). Since the memory tensors encode only a relatively small amount of information about the gravitational waveform, memory effects of the types considered here can probe only certain characteristics of a gravitational wave. In a weak-field limit, the memory tensors encode only the zeroth, the first, and the second moments of the curvature.

Applied to geodesics, our memory tensors $M_{ij}^{d \rightarrow d}$, $M_{ij}^{d \rightarrow v}$, $M_{ij}^{v \rightarrow d}$, and $M_{ij}^{v \rightarrow v}$ determine the transverse displacement-displacement, displacement-velocity, velocity-displacement, and velocity-velocity memory effects, respectively; cf. Eqs. (3.9) and (3.10). Although longitudinal memory effects occur as well—as discussed in Section III C particularly for null geodesics—these effects are determined by the same four memory tensors.

The memory tensors also determine a number of memory effects which are not necessarily associated with geodesics. For example, we find in Section IV that they completely characterize the scattering of massless particles (or compact wave packets) with longitudinal angular momentum, a process which is described by the spin Hall equations. Although spinning wave packets are scattered differently than null geodesics, nothing more can be learned about a gravitational wave by using them to perform memory experiments.

This is also true when considering the scattering of arbitrary test fields: The memory tensors determine Synge’s world function σ , as well as the van Vleck determinant Δ , and these are all that enter the relevant Green functions for (massless or massive [82]) scalar fields in plane wave spacetimes. Memory effects in the propagation of massless scalar fields are discussed from several perspectives in Section V. One result is that we use the aforementioned Green function to derive a Kirchhoff-like integral formula for the final field in terms of an initial one. We also compute the exact scattering of an initially planar scalar wave by a gravitational wave. If the outgoing wave is also planar (which is not necessarily the case), the initial and the final waves are shown to be scattered similarly to a null geodesic.

We also show that when a gravitational wave is weak, its effect on an arbitrary scalar field can be obtained simply by applying a differential operator to an appropriate “seed” solution which satisfies the wave equation in flat spacetime. The perturbative portion of this operator involves pairs of Lie derivatives with respect to four of the relevant Killing fields, where these derivatives are weighted by the various memory tensors; cf. Eq. (5.19). We apply this result for seed solutions involving counter-propagating Hermite–Gauss and Laguerre–Gauss beams in flat space-

time, where different memory tensors are found to excite different side modes. The number of excited modes is found to be finite.

Lastly, we numerically analyze the behavior of massless scalar wave packets in fully nonlinear gravitational waves. Our main result is that the momenta of these wave packets are well approximated by the spin Hall equations, which are described and solved in Section IV. This provides the first numerical evidence for the convergence of scalar-wave-packet dynamics to the behavior predicted by the spin Hall equations.

This paper has focused on memory effects in plane wave spacetimes. Physically, plane wave geometries might be expected to approximate the geometry in a spatially small region far from a gravitating source. Given the Penrose limit, plane waves might also be expected to be relevant for memory effects which involve systems confined to remain near a null geodesic in an arbitrary spacetime. However, precise translations to these contexts are left for later work.

ACKNOWLEDGMENTS

We are grateful to Tim Adamo, Andrea Cristofoli, Peter Horvathy, Anton Ilderton, and Sonja Klisch for helpful discussions. FS was supported in part by the Austrian Science Fund (FWF), Project P34274. Research by T.B.M. is supported by the European Union (ERC, GRAVITES, project no 101071779). Views and opinions expressed are however those of the authors only and do not necessarily reflect those of the European Union or the European Research Council Executive Agency. Neither the European Union nor the granting authority can be held responsible for them.

Appendix A: Notation

We work on smooth Lorentzian spacetimes $(M, g_{\alpha\beta})$, where the metric tensor $g_{\alpha\beta}$ has signature $(-+++)$. Greek letters are used for spacetime indices and range from 0 to 3. We mostly describe plane wave spacetimes in Brinkmann coordinates (u, v, x^i) , although Rosen coordinates $(\mathcal{U}, \mathcal{V}, \mathcal{X}^i)$ are also used. In this context, overset dots are used to denote derivatives with respect to u or \mathcal{U} . Also, Latin letters from the middle of the alphabet, (i, j, k, \dots) , which run from 1 to 2, are used to label the transverse and spacelike coordinates in these spacetimes. The components of 3-vectors are labeled with capitalized Latin letters from the middle of the alphabet, (I, J, K, \dots) , and range from 1 to 3. We work in geometrized units in which $G = c = 1$, the Einstein summation convention is assumed, and we use the notation $a_\alpha b^\alpha = a \cdot b$. The Riemann tensor is defined so that $2\nabla_{[\alpha}\nabla_{\beta]}\omega_\gamma = R_{\alpha\beta\gamma}{}^\lambda\omega_\lambda$ for any smooth ω_γ . A summary of the important symbols used throughout the paper is given in Table I.

Symbol	Description	Reference
$u, v, x^1 = x, x^2 = y$	Brinkmann coordinates	Eq. (2.1)
t, z	Time and longitudinal coordinates	Eq. (2.11)
$\mathcal{U}, \mathcal{V}, \mathcal{X}^i$	Rosen coordinates	Eq. (C.1)
H_{ij}	Plane wave waveform (Brinkmann)	Eqs. (2.1), (2.2)
h_{ij}	Plane wave waveform (Rosen)	Eqs. (C.1), (C.8)
ℓ^α	Plane wave propagation direction	Eq. (2.6)
λ^α	Homothety	Eq. (2.14)
Ξ^i	Solution to transverse vector Jacobi equation	Eqs. (2.8), (2.9)
E_{ij}	Solution to transverse matrix Jacobi equation	Eqs. (2.15), (C.8)
A_{ij}, B_{ij}	Transverse Jacobi propagators	Eq. (2.16)
$M_{ij}^{d \rightarrow v}, M_{ij}^{d \rightarrow d}, M_{ij}^{v \rightarrow v}, M_{ij}^{v \rightarrow d}$	Memory tensors	Eqs. (2.30), (2.40), (3.10)
$\mathcal{I}_\pm, \mathcal{I}_C$	Flat and curved regions of a sandwich wave	Fig. 1
γ, u_0, v_0, r^i_j	Transformations between Brinkmann coordinates	Eq. (2.3)
κ	Geodesic constant	Eqs. (3.4), (3.18)
x_\pm^i	Positions projected on $u = 0$ hyperplane	Eqs. (3.8), (3.9), Fig. 4
X_\pm^I	Positions projected on $t = 0$ hyperplane	Eq. (3.17), Fig. 4
\dot{x}_\pm^i	Initial and final transverse velocities	Eq. (3.9)
V_\pm^I	Initial and final 3-velocities	Eq. (3.17)
n_\pm^i	Initial and final unit propagation directions	Eqs. (3.27), (5.20), (5.26)
p_α	Linear momentum	Eqs. (4.2), (4.4)
$S^{\alpha\beta}$	Angular momentum	Eqs. (4.1), (4.2), (4.4)
$\epsilon s, l$	Angular momentum parameters	Eqs. (4.3), (5.31b), (5.43)
\mathcal{P}_ξ	ξ^α component of generalized momentum	Eqs. (4.4), (4.6)
$\mathcal{S}, \mathcal{S}_1$	Scattering matrices	Eqs. (3.9), (3.10), (4.22)
σ	Synge's world function	Eq. (3.32)
Δ	van Vleck determinant	Eq. (5.6)
G	Scalar Green function	Eq. (5.5)
Σ, Σ_τ	Hypersurfaces	Eqs. (4.6), (5.4)
$\psi_{m,n}^{\text{HG}}$	Hermite–Gauss modes	Eq. (5.31a)
$\psi_{l,p}^{\text{LG}}$	Laguerre–Gauss modes	Eq. (5.31b)
$T^{\alpha\beta}$	Stress-energy tensor	Eqs. (4.6), (5.39)
a, ω	Initial scalar wave packet amplitude and frequency	Eqs. (5.43), (5.44)
U, U_0	Gravitational wave width and center	Eq. (B.10)
ν, ϕ_+, ϕ_\times	Gravitational wave frequency and phase offsets	Eq. (B.10)
l_+, l_\times	Curvature lengthscales	Eqs. (B.1), (B.10)
$A \equiv 2/\sqrt{\pi}l_+^2$	Curvature amplitude	Eqs. (5.42), Fig. 18

TABLE I. Table of symbols.

Appendix B: Example plane waves and their memory tensors

This paper mostly takes the perspective that the precise waveform of a gravitational plane wave is less relevant than its associated memory tensors. However, it is always possible to compute the latter from the former, at least numerically. This appendix provides three examples of specific plane wave spacetimes in which the memory tensors can be computed analytically: one exactly and two approximately. Our first example is a constant, finite-width pulse. Although this does not model any astrophysically relevant radiation, all memory tensors can easily be computed in the fully nonlinear regime. Our latter two examples are treated only in the linear approximation. One of these describes an oscillating burst while the other models the radiation which is emitted by the head-on

collision of two masses.

1. Exact constant pulse

Perhaps the simplest nontrivial examples of vacuum sandwich waves are constant pulses with duration $U > 0$ and curvature lengthscale $l > 0$ (which is not to be confused with the angular momentum parameters l employed in Sections VD and VE). Any such pulse must be linearly polarized, so coordinates can be chosen in which its waveform is diagonal: Letting Θ denote the Heaviside step function,

$$H_{ij}(u) = l^{-2}\Theta(u)\Theta(U-u)\text{diag}[1, -1]_{ij}. \quad (\text{B.1})$$

Gravitational waves of this kind are not reasonable models for the far-field radiation emitted by any compact

system in an asymptotically flat context. However, if the Heaviside functions in Eq. (B.1) were omitted, the resulting constant-curvature wave could be obtained by applying a Penrose limit to the Schwarzschild light ring; cf. Ref. [39] and also Eq. (2.42). Our waveform might, therefore, be viewed as a crude model for the Penrose limit of a null geodesic in the Schwarzschild spacetime which comes in from infinity, circles multiple times near the light ring, and then leaves. Regardless of interpretation, the

waveform (B.1) provides a simple example in which all memory tensors can be computed exactly. Square pulses of this kind have also been considered, from a different perspective, in Ref. [125].

In order to compute the memory tensors here, it is sufficient to obtain the Jacobi propagator $B_{ij}(u, u')$ as described in Section II B. Supposing that u and u' both lie in $\mathcal{I}_- = (-\infty, 0)$, this is simply $(u - u')\delta_{ij}$. However, if $u' \in \mathcal{I}_-$ while $u \in \mathcal{I}_C = (0, U)$, solving Eq. (2.15) with $E_{ij} = B_{ij}$ results in

$$B_{ij}(u, u') = l \operatorname{diag}[\sinh(u/l) - (u'/l) \cosh(u/l), \sin(u/l) - (u'/l) \cos(u/l)]_{ij}. \quad (\text{B.2})$$

Finally, if $u' \in \mathcal{I}_-$ while $u \in \mathcal{I}_+ = (U, \infty)$,

$$B_{ij}(u, u') = l \operatorname{diag}[\sinh(U/l) - (u'/l) \cosh(U/l) + (\cosh(U/l) - (u'/l) \sinh(U/l))(u - U)/l, \sin(U/l) - (u'/l) \cos(U/l) + (\cos(U/l) + (u'/l) \sin(U/l))(u - U)/l]_{ij}. \quad (\text{B.3})$$

Applying Eq. (2.22) allows us to use this to obtain the other Jacobi propagator,

$$A_{ij}(u, u') = \operatorname{diag}[\cosh(U/l) + l^{-1}(u - U) \sinh(U/l), \cos(U/l) - l^{-1}(u - U) \sin(U/l)]_{ij}. \quad (\text{B.4})$$

Comparison with Eq. (2.30) then shows that the memory tensors are given by

$$M_{ij}^{y \rightarrow v} = \operatorname{diag}[\cosh(U/l) - 1, \cos(U/l) - 1]_{ij}, \quad M_{ij}^{d \rightarrow v} = l^{-1} \operatorname{diag}[\sinh(U/l), -\sin(U/l)]_{ij}, \quad (\text{B.5a})$$

$$M_{ij}^{d \rightarrow d} = \operatorname{diag}[\cosh(U/l) - (U/l) \sinh(U/l) - 1, \cos(U/l) + (U/l) \sin(U/l) - 1]_{ij}, \quad (\text{B.5b})$$

$$M_{ij}^{y \rightarrow d} = l \operatorname{diag}[\sinh(U/l) - (U/l) \cosh(U/l), \sin(U/l) - (U/l) \cos(U/l)]_{ij}. \quad (\text{B.5c})$$

These expressions are exact. Unlike in the linear context, it is clear that none of these tensors are trace-free and also that $M_{ij}^{d \rightarrow d} \neq -M_{ij}^{y \rightarrow v}$.

If we linearize in H_{ij} , which is equivalent to expanding through quadratic order in $1/l$, the memory tensors here reduce to

$$M_{ij}^{d \rightarrow v} = U^{-1}(U/l)^2 \operatorname{diag}[1, -1]_{ij} + \mathcal{O}(l^{-4}), \quad (\text{B.6a})$$

$$\begin{aligned} M_{ij}^{y \rightarrow v} &= -M_{ij}^{d \rightarrow d} + \mathcal{O}(l^{-4}) \\ &= \frac{1}{2}(U/l)^2 \operatorname{diag}[1, -1]_{ij} + \mathcal{O}(l^{-4}), \end{aligned} \quad (\text{B.6b})$$

$$M_{ij}^{y \rightarrow d} = -\frac{1}{3}U(U/l)^2 \operatorname{diag}[1, -1]_{ij} + \mathcal{O}(l^{-4}). \quad (\text{B.6c})$$

These expressions *are* trace-free, as expected. They can also be interpreted as the leading-order expansions in U . Of course, these tensors (and their non-perturbative counterparts) depend on a choice of origin for the u coordinate. It follows from Eq. (2.37) that although no shift in the u coordinate can be used to eliminate $M_{ij}^{y \rightarrow d}$ or $M_{ij}^{d \rightarrow v}$, both $M_{ij}^{d \rightarrow d}$ and $M_{ij}^{y \rightarrow v}$ can be simultaneously eliminated in the weak-field limit. Doing so has the consequence of leaving $M_{ij}^{d \rightarrow v}$ unchanged while dividing $M_{ij}^{y \rightarrow d}$ by 4.

Regardless, if the origin of the u coordinate is left as-is, the first nonlinearities here result in, e.g.,

$$M_{ij}^{d \rightarrow d} + M_{ij}^{y \rightarrow v} = -\frac{1}{12}(U/l)^4 \delta_{ij} + \mathcal{O}(l^{-6}). \quad (\text{B.7})$$

More general results on how perturbative and non-perturbative nonlinearities affect the Jacobi propagators may be found in Ref. [27].

Another point which can be noted here is that there may be cases in which $B_{ij}(u, u')$ fails to be invertible. Recalling the discussion surrounding Eq. (3.5), the corresponding values of u and u' fix the conjugate hyperplanes [74]. These are associated with geodesic focusing, as well as, e.g., the breakdown of both the Green function (5.5) and of the Kirchhoff-like formula (5.7). For the constant pulse considered here, it follows from Eq. (B.3) that if $u' \in \mathcal{I}_-$ is fixed, there exists some $u \in \mathcal{I}_+$ which is conjugate to u' whenever

$$\frac{l \tan(U/l) - u'}{1 + (u'/l) \tan(U/l)} < 0. \quad (\text{B.8})$$

There are two possibilities here, depending on the sign of $\tan(U/l)$. If $\tan(U/l) > 0$, which occurs, e.g., for short

or weak pulses, the relevant criterion reduces to $u'/l < -\cot(U/l)$. All geodesics which begin somewhere in the sufficiently distant past are thus focused in the future of the gravitational wave pulse. For pulses where $\tan(U/l)$ is instead negative, focusing from \mathcal{I}_- to \mathcal{I}_+ occurs only from the finite interval in which $\tan(U/l) < u'/l < 0$.

A similar analysis may be used to find when $A_{ij}(u, u')$ fails to be invertible, which signals the divergence of the initially planar scalar wave given by Eq. (5.25). Using Eq. (B.4), such waves diverge for some $u \in \mathcal{I}_+$ only when

$$\tan(U/l) > 0. \quad (\text{B.9})$$

This criterion also describes the existence of a focal point [89], a location where an initially comoving collection of geodesics would be focused after passing through the given gravitational wave (as in, e.g., Fig. 3).

2. Oscillating waves

The list of waveforms whose effects can be understood non-perturbatively (and non-numerically) is rather short. However, it is straightforward to perturbatively compute memory tensors in a wide range of scenarios. One class of possibilities are the waveforms

$$H_{ij}(u) = \frac{e^{-[(u-U_0)/2U]^2}}{2\sqrt{\pi}} \begin{pmatrix} l_+^{-2} \sin(\nu u + \phi_+) & l_\times^{-2} \sin(\nu u + \phi_\times) \\ l_\times^{-2} \sin(\nu u + \phi_\times) & -l_+^{-2} \sin(\nu u + \phi_+) \end{pmatrix}_{ij}. \quad (\text{B.10})$$

A wave in this class oscillates with angular frequency ν , and those oscillations are modulated by a Gaussian centered at $u = U_0$ and with width U . The curvature lengths of the $+$ and the \times polarized components of the wave are parameterized by l_+ and l_\times , and these components can also have the constant phase offsets ϕ_+ and ϕ_\times [where the ϕ_+ here should not be confused with the phase in Eq. (5.30)]. Such a wave is $+$ polarized when $l_\times \rightarrow \infty$ and \times polarized when $l_+ \rightarrow \infty$. More generally, it is linearly polarized in both of these cases, but also whenever $\phi_+ = \phi_\times$. The wave may be described as circularly polarized whenever $l_\times = l_+$ and $\phi_\times = \phi_+ \pm \pi/2$.

Although these are technically not sandwich waves, they decay sufficiently fast that memory tensors remain a useful concept. If we assume that the amplitudes here are sufficiently small, Eq. (2.40) can be used to show that

$$M_{ij}^{\text{d}\rightarrow\text{v}} = U e^{-\nu^2 U^2} \begin{pmatrix} l_+^{-2} \sin(\nu U_0 + \phi_+) & l_\times^{-2} \sin(\nu U_0 + \phi_\times) \\ l_\times^{-2} \sin(\nu U_0 + \phi_\times) & -l_+^{-2} \sin(\nu U_0 + \phi_+) \end{pmatrix}_{ij} + \mathcal{O}(H^2), \quad (\text{B.11a})$$

$$M_{ij}^{\text{d}\rightarrow\text{d}} = -2\nu U^3 e^{-\nu^2 U^2} \begin{pmatrix} l_+^{-2} \cos(\nu U_0 + \phi_+) & l_\times^{-2} \cos(\nu U_0 + \phi_\times) \\ l_\times^{-2} \cos(\nu U_0 + \phi_\times) & -l_+^{-2} \cos(\nu U_0 + \phi_+) \end{pmatrix}_{ij} - U_0 M_{ij}^{\text{d}\rightarrow\text{v}} + \mathcal{O}(H^2), \quad (\text{B.11b})$$

$$M_{ij}^{\text{v}\rightarrow\text{d}} = [2U^2(2\nu^2 U^2 - 1) + U_0^2] M_{ij}^{\text{d}\rightarrow\text{v}} + 2U_0 M_{ij}^{\text{d}\rightarrow\text{d}} + \mathcal{O}(H^2), \quad (\text{B.11c})$$

and $M_{ij}^{\text{v}\rightarrow\text{v}} = -M_{ij}^{\text{d}\rightarrow\text{d}} + \mathcal{O}(H^2)$. All memory tensors are generically nonzero at this order. However, some of these tensors can be made to vanish in special cases. For example, $M_{ij}^{\text{d}\rightarrow\text{v}}$ vanishes at linear order when, e.g., $\phi_+ = \phi_\times = -\nu U_0$, which would correspond to a particular class of linearly polarized waves. If one would like to construct a more general class of oscillating bursts in which $M_{ij}^{\text{d}\rightarrow\text{v}}$ vanishes at linear order, one way to do so would be to let H_{ij} be proportional to a u -derivative of the right-hand side of Eq. (B.10); cf. Eq. (2.41).

Regardless, all of the linearized memory tensors given by Eq. (B.11) are exponentially suppressed when $\nu U \gg 1$. In these cases, the waveform nearly averages to zero over many oscillations. However, a similar suppression does not occur at higher orders, essentially because the squared waveform does not average to zero. This is illustrated in Fig. 18. Nonlinearity might therefore be considerably more important in these cases than simple estimates suggest. See also [27, 29] for other cases in which nonlinear effects can be relatively large.

3. Weak gravitational waves from colliding masses

Our final example concerns the gravitational wave burst that is emitted by two massive objects which collide head-on, leaving a single static remnant. Idealizing such a process, the quadrupole formula suggests that it can be modeled by an impulsive plane wave with the waveform

$$H_{ij}(u) = \alpha \delta'(u) \text{diag}[1, -1]_{ij}, \quad (\text{B.12})$$

where α is a constant which can be related to the initial energies of the two objects and their final distance from the observer. A similar waveform arises if, instead, one mass splits into two. Regardless, applying Eq. (2.40) to Eq. (B.12), one finds that $M_{ij}^{\text{d}\rightarrow\text{v}}$ vanishes at linear order, as expected for an ‘‘astrophysically reasonable’’ gravitational wave. In fact, $M_{ij}^{\text{v}\rightarrow\text{d}}$ vanishes as well. The only nontrivial memory tensors here are

$$M_{ij}^{\text{d}\rightarrow\text{d}} = \alpha \text{diag}[1, -1]_{ij} + \mathcal{O}(\alpha^2) \quad (\text{B.13})$$

and $M_{ij}^{\text{v}\rightarrow\text{v}} = -M_{ij}^{\text{d}\rightarrow\text{d}} + \mathcal{O}(\alpha^2)$. In this weak-field approximation, there are no conjugate hyperplanes.

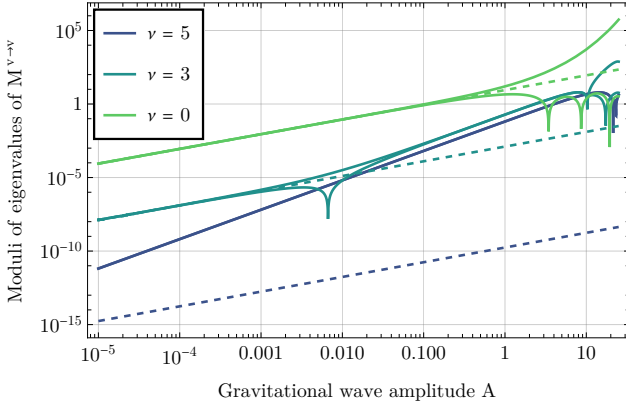


FIG. 18. Absolute values of the eigenvalues of $M_{ij}^{\nu \rightarrow \nu}$, as a function of amplitude, for circularly polarized gravitational plane waves with Gaussian profiles. Solid lines are obtained by numerical integration of the Jacobi equation, while dashed lines are linear approximations obtained from Eq. (B.11b) and $M_{ij}^{\nu \rightarrow \nu} = -M_{ij}^{d \rightarrow d} + \mathcal{O}(H^2)$. In units where $U = 1$, all waveforms here are given by Eq. (B.10) with $U_0 = 10$, $\phi_+ = 0$, $\phi_\times = \pi/2$, and $l_+ = l_\times$, which matches the parameters considered in Section V E. The amplitude plotted here is defined to be $A \equiv 2/\sqrt{\pi}l_+^2$. At larger gravitational wave frequencies ν , the linear approximation is seen to fail even for relatively small amplitudes. It may also be seen that at least in the $\nu = 0$ and $\nu = 3$ cases, the two eigenvalues differ in magnitude at large A , implying that $M_{ij}^{\nu \rightarrow \nu}$ acquires a significant trace.

Appendix C: Ward’s formula for scalar fields on plane wave backgrounds

In Section V A, we have used a Green function for the scalar wave equation in order to derive the Kirchhoff-like scattering formula (5.7) for scalar fields on gravitational plane wave backgrounds. Although the relation is not obvious, this may be shown to be a special case of an integral representation that has been previously derived by Ward [72] using different methods (see also Ref. [68] for an extension to electromagnetic fields). This Appendix explains how the two representations are related and uses that relation to physically interpret the parameters in Ward’s construction.

Ward worked in Rosen coordinates $(\mathcal{U}, \mathcal{V}, \mathcal{X}^i)$, where the line element takes the form

$$ds^2 = -2d\mathcal{U}d\mathcal{V} + h_{ij}(\mathcal{U})d\mathcal{X}^i d\mathcal{X}^j. \quad (\text{C.1})$$

In these coordinates, it is the 2-metric $h_{ij}(\mathcal{U})$ that encodes the waveform of the gravitational wave [rather than the $H_{ij}(u)$ that appears in the Brinkmann line element in Eq. (2.1)]. Ward then introduced the scalar fields

$$S_P(\mathcal{U}, \mathcal{V}, \mathcal{X}^i) \equiv \mathcal{V} + P_i \mathcal{X}^i + \frac{1}{2} P_i P_j \left(h_0^{ij} + \int_{\mathcal{U}_0}^{\mathcal{U}} [h^{-1}(\mathcal{W})]^{ij} d\mathcal{W} \right), \quad (\text{C.2})$$

where \mathcal{U}_0 , h_0^{ij} , and P_i are arbitrary constants. These scalars were shown to satisfy the eikonal equation

$$\nabla^\alpha S_P \nabla_\alpha S_P = 0, \quad (\text{C.3})$$

so constant- S_P hypersurfaces may be viewed as wavefronts in, e.g., geometric optics. However, much more can be said: If f is any scalar function of one variable,

$$(\det h_{ij})^{-1/4} f(S_P) \quad (\text{C.4})$$

is an *exact* solution to the massless scalar wave equation. Since f is arbitrary here, solutions with this form are examples of “progressing waves” [72, 126, 127].

Summing up solutions with different P_i , it follows that given any $F = F(S_P, P_i)$,

$$\psi = \frac{1}{(\det h_{ij})^{1/4}} \int F(S_P, P_k) d^2 P \quad (\text{C.5})$$

is a solution to the massless scalar wave equation. In the flat-spacetime case where coordinates can be chosen such that $h_{ij} = \delta_{ij}$, this reduces to a certain integral formula for solutions to the wave equation which was originally obtained by Whittaker [72, 128].

However, in order to relate Ward’s integral (C.5) to our representation (5.7), we must first translate the former into the Brinkmann coordinates (u, v, x^i) which are used in the latter. Letting $u = \mathcal{U}$, the appropriate transformation is given by [27, 51, 74]

$$x^i = E^i_j(\mathcal{U}) \mathcal{X}^j, \quad v = \mathcal{V} + \frac{1}{2} E^k_i(\mathcal{U}) \dot{E}^k_j(\mathcal{U}) \mathcal{X}^i \mathcal{X}^j, \quad (\text{C.6})$$

where $E_{ij}(\mathcal{U})$ is any solution to the matrix Jacobi equation (2.15) in which

$$E_{k[i} \dot{E}^k_{j]} = 0. \quad (\text{C.7})$$

If this latter constraint is satisfied at any one value of \mathcal{U} , it may be shown to be satisfied for all \mathcal{U} . Regardless, applying this coordinate transformation to the Brinkmann line element (2.1) recovers the Rosen line element (C.1) with the transverse metric

$$h_{ij} = E^k_i E_{kj}. \quad (\text{C.8})$$

Different choices for E_{ij} result in different Rosen coordinate systems, with different (though physically equivalent) transverse metrics. It is clear from the discussion in Section II B that if u' is viewed as a fixed parameter, $E_{ij}(u)$ must be a linear combination of the Jacobi propagators $A_{ij}(u, u')$ and $B_{ij}(u, u')$.

Elsewhere in the literature, it has been common to identify E_{ij} with A_{ij} [51, 72, 115, 116]. We also do so in Section V C above in order to understand how planar test fields are scattered by plane gravitational waves. However, relating Ward’s formula to our Kirchhoff integral (5.7) instead requires the choice

$$E_{ij} = B_{ij}. \quad (\text{C.9})$$

The resulting Rosen coordinate system is then singular at least at $u = u'$, but this is not problematic in Brinkmann coordinates (which are valid everywhere). We also note that from Eqs. (2.20) and (C.8), as well as from the symmetry of $\partial_u B_i^k (B^{-1})_{kj}$ which follows from Eq. (2.24),

$$\partial_u [(B^{-1}A)^{ij}] = -(B^{-1})^{ik} (B^{-1})_{kj} = -(h^{-1})^{ij}. \quad (\text{C.10})$$

Choosing $h_0^{ij} = -(B^{-1})^{ik} A_k^j|_{(\mathcal{U}_0, u')}$ in Eq. (C.2), use of Eq. (C.6) with $P_i = x'_i$ then shows that

$$S_{x'} = v_{\text{ret}}, \quad (\text{C.11})$$

where v_{ret} is given by Eq. (5.9). This provides a clear physical interpretation for the eikonal here: Given an event with Brinkmann coordinates (u, v, x^i) , the event $(u', S_{x'}, x'^i)$ is null-separated from it. Furthermore, it follows from Eq. (5.6) that

$$(\det h_{ij})^{-1/4} = (\det B_{ij})^{-1/2} = \frac{\Delta^{1/2}(u, u')}{u - u'} \quad (\text{C.12})$$

in this case. Our integral (5.7) is therefore equivalent to Ward's (C.5) when $E_{ij} = B_{ij}$, when the constants h_0^{ij} and \mathcal{U}_0 are chosen appropriately, and when $2\pi F(S_{x'}, x') = \partial_{v'} \psi(u', v', x'^i)|_{v'=S_{x'}}$. The parameters P_i which appear in Ward's original result are thus seen to be interpreted as transverse Brinkmann coordinates x'^i on an "initial" null hypersurface. Furthermore, the function F is seen to be a first derivative of the field on that hypersurface. Note however that these simple interpretations arise only when the Rosen coordinate system which is used in the original construction breaks down on the initial hypersurface. Interpretations differ when, e.g., $E_{ij} = A_{ij}$.

Appendix D: Charged particles in an electromagnetic sandwich wave

The majority of this paper is concerned with gravitational wave memory. However, there are also electromagnetic memory effects, and it is instructive to compare them. As in the gravitational context, electromagnetic memory can be considered either as an effect which arises far away from a compact source, or as an effect which is associated with a local plane wave (without reference to any particular source). In the former case, charged particles have been claimed to generically experience a change in velocity due to the passage of electromagnetic radiation [129]. However, this has recently been challenged [130] with the statement that there can be a displacement memory but no velocity memory. Following the gravitational discussion in this paper, which focuses on arbitrary plane waves without reference to their sources, we do not enter here into this disagreement, which depends on the asymptotic properties of electromagnetic fields.

Instead, we consider the motion of a charged particle in flat spacetime which is accelerated by an arbitrary electromagnetic "sandwich wave." The position $x^\alpha(\tau)$ of a particle with charge q and mass m obeys the Lorentz force equation

$$\frac{D}{d\tau} \frac{dx^\alpha}{d\tau} = \frac{q}{m} F^\alpha{}_\beta \frac{dx^\beta}{d\tau}, \quad (\text{D.1})$$

where τ denotes a proper time along the particle's worldline. Furthermore, the electromagnetic field of an arbitrary plane wave can be described by Eq. (2.13). Combining these two expressions shows that

$$\ell_\alpha \frac{dx^\alpha}{d\tau} = -\frac{du}{d\tau} = \text{constant}. \quad (\text{D.2})$$

If Brinkmann coordinates are adopted so $ds^2 = -2dudv + dx^2 + dy^2$, the two transverse components of the Lorentz force equation reduce to

$$\frac{d^2 x^i}{du^2} = \frac{q}{2m} \frac{d\tau}{du} \mathcal{A}^i(u), \quad (\text{D.3})$$

where $\mathcal{A}^i(u)/2\sqrt{2}$ is the electric field which would be seen by an observer at constant x, y, z . Regardless, the Lorentz force equation can be solved to yield

$$x^i(u) = x^i(u') + (u - u') \dot{x}^i(u') + \frac{q}{2m} \frac{d\tau}{du} \int_{u'}^u dw (u - w) \mathcal{A}^i(w). \quad (\text{D.4})$$

This is exact and is valid for arbitrary electromagnetic waveforms.

If we consider a sandwich wave, so $F_{\alpha\beta}$ vanishes for all u outside some finite interval, we can now ask how charged particles are scattered. It follows from Eq. (D.4) that all relevant information is captured by the memory vectors

$$M_v^i \equiv \int_{-\infty}^{\infty} du \mathcal{A}^i(u), \quad M_d^i \equiv - \int_{-\infty}^{\infty} du u \mathcal{A}^i(u), \quad (\text{D.5})$$

which are essentially the zeroth and the first moments of the electric field. If u' lies before the wave has arrived and u after it has left, the transverse scattering variables x_\pm^i and \dot{x}_\pm^i which are defined by Eq. (3.8) are related via

$$\begin{pmatrix} x_+^i \\ \dot{x}_+^i \end{pmatrix} = \begin{pmatrix} x_-^i \\ \dot{x}_-^i \end{pmatrix} + \frac{q}{2m} \frac{d\tau}{du} \begin{pmatrix} M_d^i \\ M_v^i \end{pmatrix}. \quad (\text{D.6})$$

This may be compared with Eqs. (3.9) and (3.10), which describe the transverse scattering of geodesics by a gravitational plane wave. One similarity is that the memory effects in both cases depend on the lowest moments of the relevant waveform (at least when linearizing in the gravitational case). However, this similarity also leads to a difference: Electromagnetic memory is parametrized by memory *vectors* rather than second-rank memory *tensors*. This is essentially because the electromagnetic waveform is a vector while the gravitational waveform is a second-rank symmetric tensor. An even more striking difference is that although the gravitational memory is linear in the initial transverse state, the electromagnetic memory is independent of it. All charged particles with the same $(q/m)d\tau/du$ experience the same transverse kicks and the same transverse displacements.

Appendix E: Derivatives of HG and LG beams

In principle, it is possible to use Eq. (5.19) to understand the scattering of the Hermite–Gauss and Laguerre–Gauss beams analytically, at least in the linear approximation. We now give analytical expressions for the various derivatives that appear in Eq. (5.19) when HG or LG solutions are used as seed fields. These results follow easily by applying the standard properties of Hermite and Laguerre polynomials [131]. They are used in Section VD to understand how gravitational wave memory affects localized scalar beams.

1. Counter-propagating HG beams

For counter-propagating HG beams $\psi_{m,n}^{\text{HG}}$ defined in Eq. (5.31a), the relevant partial derivatives for calculating the scattered beam are

$$\partial_v \psi_{m,n}^{\text{HG}} = \frac{i}{2\sqrt{2}kw_0^2} \left[2(m+n+1)\psi_{m,n}^{\text{HG}} - \sqrt{m(m-1)}\psi_{m-2,n}^{\text{HG}} - \sqrt{n(n-1)}\psi_{m,n-2}^{\text{HG}} - \sqrt{(m+1)(m+2)}\psi_{m+2,n}^{\text{HG}} - \sqrt{(n+1)(n+2)}\psi_{m,n+2}^{\text{HG}} \right], \quad (\text{E.1a})$$

$$\partial_x \psi_{m,n}^{\text{HG}} = \frac{1}{w_0} (\sqrt{m}\psi_{m-1,n}^{\text{HG}} - \sqrt{m+1}\psi_{m+1,n}^{\text{HG}}), \quad (\text{E.1b})$$

$$\partial_y \psi_{m,n}^{\text{HG}} = \frac{1}{w_0} (\sqrt{n}\psi_{m,n-1}^{\text{HG}} - \sqrt{n+1}\psi_{m,n+1}^{\text{HG}}). \quad (\text{E.1c})$$

The remaining terms can in Eq. (5.19) be calculated using the above expressions, together with

$$x\psi_{m,n}^{\text{HG}} = \frac{1}{2kw_0} \left[\sqrt{m} (w_0^2k + i\sqrt{2}v) \psi_{m-1,n}^{\text{HG}} + \sqrt{m+1} (w_0^2k - i\sqrt{2}v) \psi_{m+1,n}^{\text{HG}} \right], \quad (\text{E.2a})$$

$$y\psi_{m,n}^{\text{HG}} = \frac{1}{2kw_0} \left[\sqrt{n} (w_0^2k + i\sqrt{2}v) \psi_{m,n-1}^{\text{HG}} + \sqrt{n+1} (w_0^2k - i\sqrt{2}v) \psi_{m,n+1}^{\text{HG}} \right]. \quad (\text{E.2b})$$

Using these equations, together with Eq. (5.19), we can easily determine the side modes excited by different components of the memory tensors when the ingoing beam before the gravitational wave is $\partial_v \psi_{m,n}^{\text{HG}}$. The excited side modes are summarized in Fig. 11.

2. Counter-propagating LG beams

For counter-propagating LG beams $\psi_{l,p}^{\text{LG}}$ defined in Eq. (5.31b), the relevant partial derivatives for calculating the scattered beam are

$$\partial_v \psi_{l,p}^{\text{LG}} = \frac{i}{\sqrt{2}kw_0^2} \left[\sqrt{p(p+|l|)}\psi_{l,p-1}^{\text{LG}} + (2p+|l|+1)\psi_{l,p}^{\text{LG}} + \sqrt{(p+1)(p+|l|+1)}\psi_{l,p+1}^{\text{LG}} \right], \quad (\text{E.3a})$$

$$\partial_x \psi_{l,p}^{\text{LG}} = \left[\frac{e^{+i\theta}}{2} \left(\partial_r + \frac{i}{r} \partial_\theta \right) + \frac{e^{-i\theta}}{2} \left(\partial_r - \frac{i}{r} \partial_\theta \right) \right] \psi_{l,p}^{\text{LG}}, \quad (\text{E.3b})$$

$$\partial_y \psi_{l,p}^{\text{LG}} = \left[\frac{e^{+i\theta}}{2i} \left(\partial_r + \frac{i}{r} \partial_\theta \right) - \frac{e^{-i\theta}}{2i} \left(\partial_r - \frac{i}{r} \partial_\theta \right) \right] \psi_{l,p}^{\text{LG}}, \quad (\text{E.3c})$$

where

$$\frac{e^{+i\theta}}{2} \left(\partial_r + \frac{i}{r} \partial_\theta \right) \psi_{l,p}^{\text{LG}} = \frac{1}{\sqrt{2}w_0} \begin{cases} -\sqrt{p+|l|+1}\psi_{l-1,p}^{\text{LG}} - \sqrt{p}\psi_{l-1,p-1}^{\text{LG}} & l \leq 0, \\ +\sqrt{p+|l|}\psi_{l-1,p}^{\text{LG}} + \sqrt{p+1}\psi_{l-1,p+1}^{\text{LG}} & l > 0. \end{cases} \quad (\text{E.4a})$$

$$\frac{e^{-i\theta}}{2} \left(\partial_r - \frac{i}{r} \partial_\theta \right) \psi_{l,p}^{\text{LG}} = \frac{1}{\sqrt{2}w_0} \begin{cases} +\sqrt{p+|l|}\psi_{l+1,p}^{\text{LG}} + \sqrt{p+1}\psi_{l+1,p+1}^{\text{LG}} & l < 0, \\ -\sqrt{p+|l|+1}\psi_{l+1,p}^{\text{LG}} - \sqrt{p}\psi_{l+1,p-1}^{\text{LG}} & l \geq 0. \end{cases} \quad (\text{E.4b})$$

The remaining type of terms that appear in Eq. (5.19) are

$$x\psi_{l,p}^{\text{LG}} = r \cos \theta \psi_{l,p}^{\text{LG}} = r \frac{e^{+i\theta} + e^{-i\theta}}{2} \psi_{l,p}^{\text{LG}}, \quad (\text{E.5a})$$

$$y\psi_{l,p}^{\text{LG}} = r \sin \theta \psi_{l,p}^{\text{LG}} = r \frac{e^{+i\theta} - e^{-i\theta}}{2i} \psi_{l,p}^{\text{LG}}, \quad (\text{E.5b})$$

where

$$re^{+i\theta} \psi_{l,p}^{\text{LG}} = \frac{1}{\sqrt{2}kw_0} \begin{cases} \sqrt{p+|l|+1} (kw_0^2 - i\sqrt{2}v) \psi_{l-1,p}^{\text{LG}} - \sqrt{p} (kw_0^2 + i\sqrt{2}v) \psi_{l-1,p-1}^{\text{LG}} & l \leq 0, \\ \sqrt{p+|l|} (kw_0^2 + i\sqrt{2}v) \psi_{l-1,p}^{\text{LG}} - \sqrt{p+1} (kw_0^2 - i\sqrt{2}v) \psi_{l-1,p+1}^{\text{LG}} & l > 0. \end{cases} \quad (\text{E.6a})$$

$$re^{-i\theta} \psi_{l,p}^{\text{LG}} = \frac{1}{\sqrt{2}kw_0} \begin{cases} \sqrt{p+|l|} (kw_0^2 + i\sqrt{2}v) \psi_{l+1,p}^{\text{LG}} - \sqrt{p+1} (kw_0^2 - i\sqrt{2}v) \psi_{l+1,p+1}^{\text{LG}} & l < 0, \\ \sqrt{p+|l|+1} (kw_0^2 - i\sqrt{2}v) \psi_{l+1,p}^{\text{LG}} - \sqrt{p} (kw_0^2 + i\sqrt{2}v) \psi_{l+1,p-1}^{\text{LG}} & l \geq 0. \end{cases} \quad (\text{E.6b})$$

Using these equations, together with Eq. (5.19), we can easily determine the side modes excited by different components of the memory tensors when the ingoing beam before the gravitational wave is $\partial_v \psi_{l,p}^{\text{LG}}$. The excited side modes are summarized in Fig. 12.

-
- [1] Y. B. Zel'dovich and A. G. Polnarev, Radiation of gravitational waves by a cluster of superdense stars, *Soviet Astronomy* **18**, 17 (1974).
- [2] E. T. Newman and R. Penrose, Note on the Bondi-Metzner-Sachs group, *Journal of Mathematical Physics* **7**, 863 (1966).
- [3] D. Christodoulou, Nonlinear nature of gravitation and gravitational-wave experiments, *Physical Review Letters* **67**, 1486 (1991).
- [4] D. Christodoulou and S. Klainerman, The global nonlinear stability of the Minkowski space, *Séminaire Équations aux dérivées partielles (Polytechnique) dit aussi "Séminaire Goulaouic-Schwartz"*, 1 (1989-1990), talk:13.
- [5] D. Christodoulou and S. Klainerman, *The Global Nonlinear Stability of the Minkowski Space (PMS-41)* (Princeton University Press, Princeton, 1994).
- [6] A. G. Wiseman and C. M. Will, Christodoulou's nonlinear gravitational-wave memory: Evaluation in the quadrupole approximation, *Physical Review D* **44**, R2945 (1991).
- [7] K. S. Thorne, Gravitational-wave bursts with memory: The Christodoulou effect, *Physical Review D* **45**, 520 (1992).
- [8] V. B. Braginsky and K. S. Thorne, Gravitational-wave bursts with memory and experimental prospects, *Nature (London)* **327**, 123 (1987).
- [9] P. D. Lasky, E. Thrane, Y. Levin, J. Blackman, and Y. Chen, Detecting gravitational-wave memory with LIGO: Implications of GW150914, *Physical Review Letters* **117**, 061102 (2016).
- [10] O. M. Boersma, D. A. Nichols, and P. Schmidt, Forecasts for detecting the gravitational-wave memory effect with Advanced LIGO and Virgo, *Physical Review D* **101**, 083026 (2020).
- [11] A. Tolish, L. Bieri, D. Garfinkle, and R. M. Wald, Examination of a simple example of gravitational wave memory, *Physical Review D* **90**, 044060 (2014).
- [12] D. Garfinkle, Gravitational wave memory and the wave equation, *Classical and Quantum Gravity* **39**, 135010 (2022).
- [13] L. Bieri and A. Polnarev, Gravitational Wave Displacement and Velocity Memory Effects, [arXiv:2402.02594](https://arxiv.org/abs/2402.02594) (2024).
- [14] L. Blanchet and T. Damour, Tail-transported temporal correlations in the dynamics of a gravitating system, *Physical Review D* **37**, 1410 (1988).
- [15] L. Blanchet and T. Damour, Hereditary effects in gravitational radiation, *Physical Review D* **46**, 4304 (1992).
- [16] M. Favata, The gravitational-wave memory effect, *Classical and Quantum Gravity* **27**, 084036 (2010).
- [17] D. A. Nichols, Spin memory effect for compact binaries in the post-Newtonian approximation, *Physical Review D* **95**, 084048 (2017).
- [18] S. Pasterski, A. Strominger, and A. Zhiboedov, New gravitational memories, *Journal of High Energy Physics* **2016**, 53 (2016).
- [19] É. É. Flanagan and D. A. Nichols, Conserved charges of the extended Bondi-Metzner-Sachs algebra, *Physical Review D* **95**, 044002 (2017).
- [20] G. Satishchandran and R. M. Wald, Asymptotic behavior of massless fields and the memory effect, *Physical Review D* **99**, 084007 (2019).
- [21] D. A. Nichols, Center-of-mass angular momentum and memory effect in asymptotically flat spacetimes, *Physical Review D* **98**, 064032 (2018).
- [22] L. Bieri, New effects in gravitational waves and memory, *Physical Review D* **103**, 024043 (2021).
- [23] J. Frauendiener, Note on the memory effect, *Classical and Quantum Gravity* **9**, 1639 (1992).
- [24] L. Donnay, G. Giribet, H. A. González, and A. Puhm, Black hole memory effect, *Physical Review D* **98**, 124016 (2018).
- [25] A. A. Rahman and R. M. Wald, Black hole memory, *Physical Review D* **101**, 124010 (2020).
- [26] A. I. Harte, Strong lensing, plane gravitational waves and transient flashes, *Classical and Quantum Gravity* **30**, 075011 (2013).
- [27] A. I. Harte, Optics in a nonlinear gravitational plane wave, *Classical and Quantum Gravity* **32**, 175017 (2015).

- [28] E. E. Flanagan, A. M. Grant, A. I. Harte, and D. A. Nichols, Persistent gravitational wave observables: General framework, *Physical Review D* **99**, 084044 (2019).
- [29] E. E. Flanagan, A. M. Grant, A. I. Harte, and D. A. Nichols, Persistent gravitational wave observables: Non-linear plane wave spacetimes, *Physical Review D* **101**, 104033 (2020).
- [30] A. M. Grant and D. A. Nichols, Persistent gravitational wave observables: Curve deviation in asymptotically flat spacetimes, *Physical Review D* **105**, 024056 (2022).
- [31] A. M. Grant, Persistent gravitational wave observables: Nonlinearities in (non-)geodesic deviation, [arXiv:2401.00047](https://arxiv.org/abs/2401.00047) (2024).
- [32] J. Ehlers and W. Kundt, Exact solutions of the gravitational field equations, in *Gravitation: An Introduction to Current Research*, edited by L. Witten (J. Wiley & Sons, 1962) p. 49.
- [33] G. S. Hall, *Symmetries and Curvature Structure in General Relativity* (World Scientific, 2004).
- [34] C. Roche, A. B. Aazami, and C. Cederbaum, Exact parallel waves in general relativity, *General Relativity and Gravitation* **55**, 40 (2023).
- [35] J. B. Griffiths and J. Podolský, *Exact Space-Times in Einstein's General Relativity*, Cambridge Monographs on Mathematical Physics (Cambridge University Press, 2009).
- [36] R. Penrose, A remarkable property of plane waves in general relativity, *Reviews of Modern Physics* **37**, 215–220 (1965).
- [37] R. Penrose, Any space-time has a plane wave as a limit, in *Differential Geometry and Relativity: A Volume in Honour of André Lichnerowicz on His 60th Birthday*, edited by M. Cahen and M. Flato (Springer Netherlands, Dordrecht, 1976) pp. 271–275.
- [38] M. Blau, D. Frank, and S. Weiss, Fermi coordinates and Penrose limits, *Classical and Quantum Gravity* **23**, 3993 (2006).
- [39] M. Blau, Plane waves and penrose limits, *Lecture Notes for the ICTP School on Mathematics in String and Field Theory (2-13 June 2003)* (2011).
- [40] P.-M. Zhang, C. Duval, G. Gibbons, and P. Horvathy, The memory effect for plane gravitational waves, *Physics Letters B* **772**, 743 (2017).
- [41] P.-M. Zhang, C. Duval, G. Gibbons, and P. Horvathy, Velocity memory effect for polarized gravitational waves, *Journal of Cosmology and Astroparticle Physics* **2018** (05), 030.
- [42] P.-M. Zhang, C. Duval, and P. A. Horvathy, Memory effect for impulsive gravitational waves, *Classical and Quantum Gravity* **35**, 065011 (2018).
- [43] R. Steinbauer, Comment on ‘Memory effect for impulsive gravitational waves’, *Classical and Quantum Gravity* **36**, 098001 (2019).
- [44] P. M. Zhang, M. Elbistan, G. W. Gibbons, and P. A. Horvathy, Sturm–Liouville and Carroll: at the heart of the memory effect, *General Relativity and Gravitation* **50**, 107 (2018).
- [45] P.-M. Zhang, M. Cariglia, C. Duval, M. Elbistan, G. W. Gibbons, and P. A. Horvathy, Ion traps and the memory effect for periodic gravitational waves, *Physical Review D* **98**, 044037 (2018).
- [46] P.-M. Zhang, C. Duval, G. W. Gibbons, and P. A. Horvathy, Soft gravitons and the memory effect for plane gravitational waves, *Physical Review D* **96**, 064013 (2017).
- [47] M. Elbistan, P.-M. Zhang, and P. Horvathy, Memory effect & Carroll symmetry, 50 years later, *Annals of Physics* **459**, 169535 (2023).
- [48] I. Chakraborty and S. Kar, Geodesic congruences in exact plane wave spacetimes and the memory effect, *Physical Review D* **101**, 064022 (2020).
- [49] P.-M. Zhang and P. Horvathy, Displacement within velocity effect in gravitational wave memory, [arXiv:2405.12928](https://arxiv.org/abs/2405.12928) (2024).
- [50] J. B. Achour and J.-P. Uzan, Displacement versus velocity memory effects from a gravitational plane wave, [arXiv:2406.07106](https://arxiv.org/abs/2406.07106) (2024).
- [51] T. Adamo, E. Casali, L. Mason, and S. Nekovar, Scattering on plane waves and the double copy, *Classical and Quantum Gravity* **35**, 015004 (2017).
- [52] L. Andersson and M. A. Oancea, Spin Hall effects in the sky, *Classical and Quantum Gravity* **40**, 154002 (2023).
- [53] A. I. Harte and M. A. Oancea, Spin Hall effects and the localization of massless spinning particles, *Physical Review D* **105**, 104061 (2022).
- [54] W. G. Dixon, Dynamics of Extended Bodies in General Relativity. I. Momentum and Angular Momentum, *Proceedings of the Royal Society A: Mathematical, Physical and Engineering Sciences* **314**, 499 (1970).
- [55] M. A. Oancea, J. Joudioux, I. Y. Dodin, D. E. Ruiz, C. F. Paganini, and L. Andersson, Gravitational spin Hall effect of light, *Physical Review D* **102**, 024075 (2020).
- [56] V. P. Frolov, Maxwell equations in a curved spacetime: Spin optics approximation, *Physical Review D* **102**, 084013 (2020).
- [57] P. Gosselin, A. Bérard, and H. Mohrbach, Spin Hall effect of photons in a static gravitational field, *Physical Review D* **75**, 084035 (2007).
- [58] M. A. Oancea and T. Harko, Weyl geometric effects on the propagation of light in gravitational fields, *Physical Review D* **109**, 064020 (2024).
- [59] V. P. Frolov, Spinoptics in a curved spacetime, [arXiv:2405.01777](https://arxiv.org/abs/2405.01777) (2024).
- [60] L. Andersson, J. Joudioux, M. A. Oancea, and A. Raj, Propagation of polarized gravitational waves, *Physical Review D* **103**, 044053 (2021).
- [61] N. Yamamoto, Spin Hall effect of gravitational waves, *Physical Review D* **98**, 061701(R) (2018).
- [62] M. A. Oancea, R. Stiskalek, and M. Zumalacárregui, Frequency- and polarization-dependent lensing of gravitational waves in strong gravitational fields, *Physical Review D* **109**, 124045 (2024).
- [63] M. A. Oancea, R. Stiskalek, and M. Zumalacárregui, Probing general relativistic spin-orbit coupling with gravitational waves from hierarchical triple systems, [arXiv:2307.01903](https://arxiv.org/abs/2307.01903) (2023).
- [64] V. P. Frolov and A. A. Shoom, Gravitational spinoptics in a curved space-time, [arXiv:2406.17905](https://arxiv.org/abs/2406.17905) (2024).
- [65] M. A. Oancea and A. Kumar, Semiclassical analysis of Dirac fields on curved spacetime, *Physical Review D* **107**, 044029 (2023).
- [66] A. Seraj and B. Oblak, Precession caused by gravitational waves, *Physical Review Letters* **129**, 061101 (2022).
- [67] A. Seraj and B. Oblak, Gyroscopic gravitational memory, *Journal of High Energy Physics* **2023**, 57 (2023).
- [68] L. J. Mason, On Ward’s Integral formula for the wave equation in plane-wave space-times, *Twistor Newsletter*

- 28**, 17 (1989).
- [69] B. Araneda, Parallel spinors, pp-waves, and gravitational perturbations, *Classical and Quantum Gravity* **40**, 025006 (2022).
- [70] A. Kulitskii and E. Y. Melkumova, Newman-Penrose-Debye formalism for fields of various spins in pp-wave backgrounds, in *The Sixteenth Marcel Grossmann Meeting* (World Scientific, 2023).
- [71] Z. Tang, Test gravitational waves in sandwich wave background, *General Relativity and Gravitation* **55**, 70 (2023).
- [72] R. S. Ward, Progressing waves in flat spacetime and in plane-wave spacetimes, *Classical and Quantum Gravity* **4**, 775 (1987).
- [73] J. K. Beem, P. E. Ehrlich, and K. L. Easley, *Global Lorentzian Geometry* (Routledge, 2017).
- [74] A. I. Harte and T. D. Drivas, Caustics and wave propagation in curved spacetimes, *Physical Review D* **85**, 124039 (2012).
- [75] C. Duval, G. W. Gibbons, P. A. Horvathy, and P.-M. Zhang, Carroll symmetry of plane gravitational waves, *Classical and Quantum Gravity* **34**, 175003 (2017).
- [76] J.-M. Lévy-Leblond, Une nouvelle limite non-relativiste du groupe de Poincaré, *Annales de l'institut Henri Poincaré. Section A, Physique Théorique* **3**, 1 (1965).
- [77] H. Bondi, F. A. E. Pirani, I. Robinson, and W. H. McCrea, Gravitational waves in general relativity III. Exact plane waves, *Proceedings of the Royal Society A: Mathematical and Physical Sciences* **251**, 519 (1959).
- [78] R. Maartens and S. D. Maharaj, Conformal symmetries of pp-waves, *Classical and Quantum Gravity* **8**, 503 (1991).
- [79] A. J. Keane and B. O. J. Tupper, Killing tensors in pp-wave spacetimes, *Classical and Quantum Gravity* **27**, 245011 (2010).
- [80] G. H. Katzin and J. Levine, Geodesic first integrals with explicit path-parameter dependence in Riemannian space-times, *Journal of Mathematical Physics* **22**, 1878 (1981).
- [81] T. J. Hollowood and G. M. Shore, The causal structure of QED in curved spacetime: analyticity and the refractive index, *Journal of High Energy Physics* **2008**, 091 (2008).
- [82] A. I. Harte, Tails of plane wave spacetimes: Wave-wave scattering in general relativity, *Physical Review D* **88**, 084059 (2013).
- [83] W. G. Dixon, Dynamics of Extended Bodies in General Relativity. III. Equations of Motion, *Philosophical Transactions of the Royal Society A: Mathematical, Physical and Engineering Sciences* **277**, 59 (1974).
- [84] A. I. Harte, Motion in classical field theories and the foundations of the self-force problem, in *Equations of motion in relativistic gravity*, Fundamental Theories of Physics, Vol. 179, edited by D. Puetzfeld, C. Lämmerzahl, and B. Schutz (Springer, Cham, 2015) pp. 327–398.
- [85] A. I. Harte, Approximate spacetime symmetries and conservation laws, *Classical and Quantum Gravity* **25**, 205008 (2008).
- [86] M. Grasso, M. Korzyński, and J. Serbenta, Geometric optics in general relativity using bilocal operators, *Physical Review D* **99**, 064038 (2019).
- [87] M. Korzyński and E. Villa, Geometric optics in relativistic cosmology: New formulation and a new observable, *Physical Review D* **101**, 063506 (2020).
- [88] M. Korzyński, J. Miśkiewicz, and J. Serbenta, Weighing the spacetime along the line of sight using times of arrival of electromagnetic signals, *Physical Review D* **104**, 024026 (2021).
- [89] J. Serbenta and M. Korzyński, Bilocal geodesic operators in static spherically-symmetric spacetimes, *Classical and Quantum Gravity* **39**, 155002 (2022).
- [90] N. Uzun, Reduced phase space optics for general relativity: symplectic ray bundle transfer, *Classical and Quantum Gravity* **37**, 045002 (2020).
- [91] S. Seitz, P. Schneider, and J. Ehlers, Light propagation in arbitrary spacetimes and the gravitational lens approximation, *Classical and Quantum Gravity* **11**, 2345 (1994).
- [92] M. Korzyński and N. Uzun, Algebraic symmetries of the observables on the sky: Variable emitters and observers, *arXiv:2405.05105* (2024).
- [93] I. M. H. Etherington, Republication of: LX. On the definition of distance in general relativity, *General Relativity and Gravitation* **39**, 1055 (2007).
- [94] V. Perlick, *Ray optics, Fermat's principle, and applications to general relativity*, Vol. 61 (Springer Science & Business Media, 2000).
- [95] L. P. Grishchuk and A. G. Polnarev, Gravitational wave pulses with “velocity coded memory”, *Journal of Experimental and Theoretical Physics* **69**, 653 (1989).
- [96] A. Seraj, Gravitational breathing memory and dual symmetries, *Journal of High Energy Physics* **2021**, 283 (2021).
- [97] A. K. Divakarla and B. F. Whiting, First-order velocity memory effect from compact binary coalescing sources, *Physical Review D* **104**, 064001 (2021).
- [98] R. M. Wald, *General Relativity* (University of Chicago Press, 1984).
- [99] G. W. Gibbons and S. W. Hawking, Theory of the detection of short bursts of gravitational radiation, *Physical Review D* **4**, 2191 (1971).
- [100] P.-M. Zhang, M. Cariglia, C. Duval, M. Elbistan, G. W. Gibbons, and P. A. Horvathy, Ion traps and the memory effect for periodic gravitational waves, *Physical Review D* **98**, 044037 (2018).
- [101] A. Gerrard and J. M. Burch, *Introduction to matrix methods in optics* (Courier Corporation, 1994).
- [102] A. Torre, *Linear Ray and Wave Optics in Phase Space* (Elsevier Science, Amsterdam, 2005).
- [103] R. van Haasteren and Y. Levin, Gravitational-wave memory and pulsar timing arrays, *Monthly Notices of the Royal Astronomical Society* **401**, 2372–2378 (2010).
- [104] D. R. Madison, Persistent astrometric deflections from gravitational-wave memory, *Physical Review Letters* **125**, 041101 (2020).
- [105] J. L. Synge, *Relativity: The General Theory* (North-Holland Publishing Company, Amsterdam, 1960).
- [106] E. Poisson, A. Pound, and I. Vega, The motion of point particles in curved spacetime, *Living Reviews in Relativity* **14**, 7 (2011).
- [107] E. Corinaldesi and A. Papapetrou, Spinning test-particles in general relativity. II, *Proceedings of the Royal Society A: Mathematical, Physical and Engineering Sciences* **209**, 259 (1951).
- [108] L. F. O. Costa and J. Natário, Center of mass, spin supplementary conditions, and the momentum of spinning particles, in *Equations of Motion in Relativistic Gravity*, edited by D. Puetzfeld, C. Lämmerzahl, and B. Schutz

- (Springer, Cham, 2015) pp. 215–258.
- [109] R. Penrose and W. Rindler, *Spinors and Space-Time*, Vol. 2 (Cambridge University Press, 1988).
- [110] K. Y. Bliokh and F. Nori, Spatiotemporal vortex beams and angular momentum, *Physical Review A* **86**, 033824 (2012).
- [111] K. Y. Bliokh, Spatiotemporal vortex pulses: Angular momenta and spin-orbit interaction, *Physical Review Letters* **126**, 243601 (2021).
- [112] D. L. Andrews and M. Babiker, *The Angular Momentum of Light* (Cambridge University Press, 2012).
- [113] K. Y. Bliokh and F. Nori, Transverse and longitudinal angular momenta of light, *Physics Reports* **592**, 1 (2015).
- [114] P. Günther, Ein beispiel einer nichttrivialen Huygensschen differentialgleichung mit vier unabhängigen variablen, *Archive for Rational Mechanics and Analysis* **18**, 103–106 (1965).
- [115] T. Adamo, E. Casali, L. Mason, and S. Nekovar, Amplitudes on plane waves from ambitwistor strings, *Journal of High Energy Physics* **2017**, 160 (2017).
- [116] T. Adamo and A. Ilderton, Classical and quantum double copy of back-reaction, *Journal of High Energy Physics* **2020**, 200 (2020).
- [117] A. I. Harte, Gravitational lensing beyond geometric optics: II. Metric independence, *General Relativity and Gravitation* **51**, 160 (2019).
- [118] G. Hobbs *et al.*, The International Pulsar Timing Array project: using pulsars as a gravitational wave detector, *Classical and Quantum Gravity* **27**, 084013 (2010).
- [119] S. Detweiler, Pulsar timing measurements and the search for gravitational waves, *The Astrophysical Journal* **234**, 1100 (1979).
- [120] A. P. Kiselev, Localized light waves: Paraxial and exact solutions of the wave equation (a review), *Optics and Spectroscopy* **102**, 603 (2007).
- [121] A. E. Siegman, *Lasers* (University Science Books, 1986).
- [122] R. J. Ducharme, Constrained Bateman-Hillion solutions for Hermite-Gaussian beams, *arXiv:1412.1928* (2014).
- [123] Q. Exirifard, E. Culf, and E. Karimi, Towards communication in a curved spacetime geometry, *Communications Physics* **4**, 171 (2021).
- [124] Wolfram Research, Inc., *Mathematica*, Version 13.0.0 (2021), Champaign, US-IL, 2021.
- [125] I. Chakraborty and S. Kar, A simple analytic example of the gravitational wave memory effect, *The European Physical Journal Plus* **137**, 418 (2022).
- [126] F. G. Friedlander, *The wave equation on a curved spacetime* (Cambridge University Press, 1976).
- [127] F. G. Friedlander, Simple progressive solutions of the wave equation, *Mathematical Proceedings of the Cambridge Philosophical Society* **43**, 360–373 (1947).
- [128] E. T. Whittaker, On the partial differential equations of mathematical physics, *Mathematische Annalen* **57**, 333 (1903).
- [129] L. Bieri and D. Garfinkle, An electromagnetic analogue of gravitational wave memory, *Classical and Quantum Gravity* **30**, 195009 (2013).
- [130] A. Herdegen, There is no ‘velocity kick’ memory in electrodynamics, *Acta Physica Polonica B* **55**, 3 (2024).
- [131] G. E. Andrews, R. Askey, and R. Roy, *Special Functions*, Encyclopedia of Mathematics and its Applications (Cambridge University Press, 1999).